

COORDINATION OF GEOLOGICAL AND ENGINEERING RESEARCH IN SUPPORT
OF THE GULF COAST CO-PRODUCTION PROGRAM

ANNUAL REPORT
(June 1986 - May 1987)

Prepared by
N. Tyler, M. P. R. Light, and W. A. Ambrose

Bureau of Economic Geology
W. L. Fisher, Director
and
Center for Energy Studies
The University of Texas at Austin
Austin, Texas 78713

For
GAS RESEARCH INSTITUTE
Contract No. 5084-212-0924
Scot C. Hathaway, GRI Project Manager

August 31, 1987

DISCLAIMER

LEGAL NOTICE This report was prepared by the Bureau of Economic Geology as an account of work sponsored by the Gas Research Institute (GRI). Neither GRI, members of GRI, nor any person acting on behalf of either:

- a. Makes any warranty or representation, express or implied, with respect to the accuracy, completeness, or usefulness of the information contained in this report, or that the use of any apparatus, method, or process disclosed in this report may not infringe privately owned rights; or
- b. Assumes any liability with respect to the use of, or for damages resulting from the use of, any information, apparatus, method, or process disclosed in this report.

REPORT DOCUMENTATION PAGE	1. REPORT NO. GRI-87/0147	2.	3. Recipient's Accession No.	
4. Title and Subtitle Coordination of Geological and Engineering Research in Support of the Gulf Coast Co-production Program		5. Report Date August 31, 1987		6.
7. Author(s) N. Tyler, M. P. R. Light, and W. A. Ambrose		8. Performing Organization Rept. No.		
9. Performing Organization Name and Address Bureau of Economic Geology Center for Energy Studies The University of Texas at Austin Austin, Texas 78713		10. Project/Task/Work Unit No.		11. Contract(C) or Grant(G) No. (C) 5084-212-0924 (G)
12. Sponsoring Organization Name and Address Gas Research Institute 8600 West Bryn Mawr Chicago, Illinois 60631		13. Type of Report & Period Covered Annual Report (June 1986 - May 1987)		14.
15. Supplementary Notes				
16. Abstract (Limit: 200 words) Complex and heterogeneous Hackberry reservoirs at Port Arthur field were deposited in a submarine canyon/fan setting. Conventional fieldwide hydrocarbon recovery efficiencies are low, but the potential for secondary gas recovery is high. Free gas remains trapped in uncontacted and untapped compartments at reservoir abandonment. The total fieldwide resource amounts to 13.9 Bcf. The probable and possible resource for a single infill well is 6.5 Bcf in four separate stringers. Three optimum brine-disposal sands and the best brine-disposal site were selected in Northeast Hitchcock field on the basis of sand-body complexity, thickness, depth, and brine-disposal capacity. The equilibrium distribution of inorganic species in different combinations in the produced waters at surface and formation temperatures and pH were estimated from chemical analyses. SOLMNEQ computations suggest carbonate scaling may occur in surface equipment of Miocene disposal sandstones unless inhibitors are used. At Northeast Hitchcock field, well-sorted sandstones of shallow-marine origin compose the major reservoir sands and act as preferential conduits for fluid migration. Dislodged, abundant authigenic kaolinite in these sands can plug pores during production, suggesting a maximum rate of production will need to be determined to avoid reservoir damage.				
17. Document Analysis a. Descriptors southeast Texas, Frio Formation, Hackberry Formation, submarine fan reservoirs, Port Arthur field, Northeast Hitchcock field, water chemistry, brine-disposal sands b. Identifiers/Open-Ended Terms gas resources, geological characterization of gas reservoirs and disposal sands, chemistry of formation waters c. COSATI Field/Group				
18. Availability Statement Release unlimited		19. Security Class (This Report) unclassified	21. No. of Pages 216	
		20. Security Class (This Page) unclassified	22. Price	

RESEARCH SUMMARY

Title Coordination of Geological and Engineering Research in Support of the Gulf Coast Co-Production Program

Contractor Bureau of Economic Geology and Center for Energy Studies, The University of Texas at Austin, GRI Contract No. 5084-212-0924

Principal Investigators R. J. Finley/D. W. Koppenaal/M. H. Dorfman/H. F. Dunlap

Report Period June 1, 1986 - May 31, 1987

Objectives

To detect and investigate the potential resource base in untapped free-gas-bearing stringers in the Port Arthur (Hackberry) field and to delineate the most prospective location for a strategic infill well to tap these stringers.

To investigate the likelihood of scale formation in production tubing, surface equipment, and Miocene disposal sandstones at Port Arthur and Northeast Hitchcock fields.

To investigate in detail the control of depositional environment and diagenetic history on porosity and permeability preservation in the Frio 'A' sandstones.

To select six Miocene sands in Northeast Hitchcock field for disposal of brines from the Frio 1-A sand on the basis of evaluation of potential aquifer volumes and heterogeneities through analysis and interpretation of net-sand and log facies maps.

To document known brine-disposal potential of Miocene sands in Northeast Hitchcock field and nearby fields where significant brine disposal has occurred in analagous and correlative Miocene sands using data from the Railroad Commission of Texas.

To select sites for brine disposal in Northeast Hitchcock field by noting the common occurrence of the thickest and most laterally continuous portions of potential brine-disposal Miocene sands.

To evaluate the effect of certain trace and rare earth elements with high neutron-capture cross sections (particularly boron) on neutron logs.

To evaluate the short-term variations in mud and mud filtrate resistivity and their effect on logging calculations.

Technical
Perspective

Technical coordination and liaison with the Department of Energy in those parts of the geopressured-geothermal project that are of mutual benefit to the Gas Research Institute.

Hackberry reservoirs at Port Arthur were deposited in a submarine canyon/submarine fan depositional setting. These reservoirs are inherently complex and highly heterogeneous. Hydrocarbon recovery efficiencies are low, but the potential for secondary gas recovery is high. Free gas remains trapped in uncontacted and untapped compartments at reservoir abandonment. In this era of depressed gas prices these untapped zones could provide additional financial returns and incentive for initiation of more co-production projects.

Ten Miocene formation-water analyses, five from Cameron Parish, Louisiana, and five from Galveston County, Texas, were averaged and compared with Hackberry and Frio 'A' formation-water analyses from the co-production wells in the Port Arthur and Northeast Hitchcock fields, respectively. The equilibrium distribution of inorganic aqueous species in Frio 'A,' Miocene, and different combinations of these waters at surface (separator) and formation temperature and pH values were estimated from chemical analyses.

Detailed work has been completed on the core cut in the Frio 'A' sandstone at the Delee No. 1 well, Northeast Hitchcock field, Galveston County. This work has resulted in the identification of a number of trace fossils and sedimentary structures that include the "*Skolithos* assemblage" in the coarse glauconitic sandstones and planolites burrows in the more shaly sediments.

The three most optimum Miocene brine-disposal sands were selected by consideration of their sand-body complexity, thickness, depth, and previously documented brine-disposal capacity. Brine-injection histories from 43 brine-disposal wells in the nearby Hastings West field in Brazoria County were analyzed in order to determine the brine-disposal capacity of Miocene sands analogous to those in Northeast Hitchcock field, which contained only scarce brine-disposal data.

The best brine-disposal site in Northeast Hitchcock field was selected by noting the common occurrence of the thickest and most laterally continuous portions of the three primary brine-disposal Miocene sands. Potential pore volumes available for brine disposal in these sands were calculated from net-sand maps of each of the primary brine-disposal sands. Porosity values for these sands were derived from previous studies of the shallow Miocene in the Texas Gulf Coast.

Results

A total of 11 sand stringers are considered prospective in the Port Arthur (Hackberry) field. On the basis of water saturations these sand stringers are divided into probable pay zones (water saturations of 72 to 79 percent) and possible pay zones (water saturation greater than 79 percent). Some of these heterogeneous sands contain more than one untapped compartment; in all, 14 zones are considered prospective. The total resource base amounts to 13.9 Bcf. More than half of this resource (7.9 Bcf) is in the probable category. The probable and possible resource for a single well on the crest of the structure is 6.5 Bcf in four separate sand stringers.

At the Northeast Hitchcock field the presence of the "*Skolithos* assemblage" and other structures has substantiated the shallow-marine, tidal, distributary-mouth-bar, and channel depositional environment for most of the major reservoir sands. Several shaly horizons show the characteristics of interdistributary bays while the Frio 'A' is capped by a thin sequence of crevasse splays and washover sands, which represent the initiation of the transgression that overlapped the Frio in Anahuac times.

The high-energy depositional environment of reworked on distributary-mouth-bar sandstones is the major control of the high porosity (± 30 percent) and permeability ($\pm 1,000$ md, $0.99 \mu\text{m}^2$) shown by the Frio 'A' at the Northeast Hitchcock field. Although porosity and permeability were subsequently modified by diagenetic reactions, carbonate cementation prior to leaching has not been the mechanism through which primary porosity was preserved in the Frio 'A' reservoirs. Hydration of potassium feldspar to kaolinite by migrating acid waters prior to the introduction of hydrocarbons has resulted in a porosity increase of up to 3.5 percent in the well-sorted distributary mouth bar Frio 'A' sandstones. Because the conversion of K-feldspar to kaolinite results in a decrease in volume of about 50 percent, the percentage concentration of kaolinite is a rough estimate of the volume of secondary porosity produced by this process.

Well-sorted sandstones having high porosities and permeabilities contain the most abundant authigenic kaolinite and have acted as preferential conduits for migrating acid waters and for major fluid flow during co-production. Authigenic kaolinite can create fluid production problems because of its delicate structure. Dislodged clay and chlorite flakes will obstruct pore throats at high production rates. A maximum safe rate of fluid production will need to be determined for co-produced wells. Experimental flow tests conducted at different flow rates on kaolinite-rich sandstones and measurement of resulting changes in permeability will assist in determining this safe upper flow rate.

Three lower Miocene sands, the 3780 ft., 4240 ft., and 5460 ft., should be capable of receiving 7,500 barrels of brine per day from a three-well disposal site centered around the Phillips Thompson No. 1 well in Northeast Hitchcock field. Each of these sands are 70 to 90 ft thick and sheetlike in the brine-disposal area, and should constitute excellent aquifers for brine disposal.

SOLMNEQ computations suggest that some carbonate scaling should occur in surface equipment or in Miocene disposal sandstones unless inhibitors are used in Hackberry and Frio 'A' formation waters.

Technical
Approach

Formation waters from the Port Arthur and Northeast Hitchcock fields were collected by IGT staff, and analyses were conducted at the Bureau of Economic Geology (BEG) using standard procedures. The BEG'S SOLMNEQ computer program (Kharaka and Barnes, 1973) was used to perform 50 equilibrium (saturation index) computations with measured and published formation-water analyses. Twenty-nine water-composition diagrams have been constructed from water-composition data for the Hackberry, Frio 'A,' and Miocene formation fluids in the Port Arthur and Northeast Hitchcock areas.

A detailed lithological description was made of the core cut in the Frio 'A' sandstone at the Delee No. 1 well, Northeast Hitchcock field. Relationships were sought between depositional and diagenetic structures and sequence and high porosity and permeability. Sandstone petrography and porosity measurements were carried out by point counting 18 rock sections from the Frio 'A' sandstone core, Delee No. 1 well. Relationships between diagenetic minerals were studied in detail.

CONTENTS

Reexploration of Submarine Canyon and Fan Reservoirs at Port Arthur (Hackberry) Field, Jefferson County, Texas

by Noel Tyler, assisted by James Reistroffer

Introduction.....	1
Setting of Hackberry reservoirs.....	2
Hackberry stratigraphy ^o at Port Arthur.....	5
Reservoir architecture and the potential for untapped compartments.....	8
Prospective units.....	12
Sand distribution.....	22
Facies architecture.....	22
Net pay.....	23
Remaining resource.....	24
Brine disposal.....	29
Conclusions.....	29

Compatibility of Hackberry and Miocene Formation Waters, Port Arthur Field, Texas

by M. P. R. Light

Introduction.....	31
Thermodynamic calculations.....	35
Computational uncertainties.....	43
SOLMNEQ computations.....	46
Diagenetic sequence.....	51
Conclusions.....	52

Depositional Environment and Diagenetic History of Upper Frio Sandstones and Their Effect on Porosity and Permeability Preservation in the Northeast Hitchcock Field, Galveston County, Texas

by M. P. R. Light

Introduction.....	53
Deep Frio sandstones and shales.....	53
Frio 'A' reservoir sandstones.....	54
Frio 'A2' unit.....	54
Frio 'A1' unit.....	67
Trace fossils in the Frio 'A' reservoir.....	86
General depositional environment of the Frio 'A' reservoir.....	91
Anahuac Formation.....	96
Diagenetic history.....	104
Anahuac Formation.....	104
Frio 'A' sandstones.....	106
Porosity types in the Frio 'A' reservoir.....	109
Macroporosity.....	109
Primary intergranular porosity.....	109
Secondary porosity.....	109
Microporosity.....	110
Mineralogy of Frio 'A' sandstones.....	110
Depositional and diagenetic sequence.....	112
Initial diagenesis and leaching of feldspars.....	113
Feldspar overgrowth formation.....	113
Poikilotopic calcite formation.....	113
Clay coat formation.....	114
Smectite-illite transformation and formation of quartz overgrowths.....	114
Leaching and secondary porosity formation.....	117

Continued transformation of smectite to illite and formation of late fibrous illite.....	117
Sparry calcite cements.....	119
Ferroan calcite and chlorite cements.....	119
Albitization of feldspars.....	123
Kaolinite cements.....	124
Dissolution of feldspars.....	126
Iron chlorite.....	127
Conclusions	128

**Fluid-Injection Potential of Proposed Miocene Brine-Disposal Sands
in the Northeast Hitchcock and Alta Loma Fields,
Galveston County, Texas**

by William A. Ambrose

Introduction	131
Objectives.....	131
Study area, data base, and methods.....	132
Miocene depositional systems in the Texas Gulf Coast.....	141
Regional Miocene depositional systems.....	141
Miocene depositional systems, Northeast Hitchcock and Alta Loma fields.....	142
Proposed brine-disposal sands, Northeast Hitchcock and Alta Loma fields.....	142
Factors considered in selection of the brine-disposal sands.....	142
Sand-body complexity.....	144
Thickness of the brine-disposal sand.....	145
Previously documented brine-disposal capacity.....	146
Northeast Hitchcock and Alta Loma fields.....	146
Hastings West field (Brazoria County).....	146

Depth of the brine-disposal sand.....	148
Lower Miocene brine-disposal sands, Northeast Hitchcock and Alta Loma fields.....	148
Primary brine-disposal sands.....	148
Alternate brine-disposal sands.....	149
Upper Miocene brine-disposal sands, Northeast Hitchcock and Alta Loma fields.....	149
Potential sites for brine disposal, Northeast Hitchcock field.....	161
Potential pore volumes available in proposed brine-disposal sands, Northeast Hitchcock and Alta Loma fields.....	165
Conclusions	170
 Compatibility of Frio 'A' and Miocene Formation Waters, Northeast Hitchcock Field, Galveston County	
by M. P. R. Light	173
ACKNOWLEDGMENTS.....	180
REFERENCES	183

Figures

1. Frio stratigraphic relations and diagnostic foraminifers, Jefferson County area.....	3
2. Regional distribution of sand-bearing lower Hackberry channels.....	4
3. Depositional model of Hackberry reservoirs, Port Arthur field.....	6
4. Typical log from the Port Arthur field (Port Arthur No. 14).....	7
5. Evolution of Hackberry reservoirs from canyon fill to submarine fan sands.....	9
6. Facies cross section of the C sand illustrating rapid and multiple facies changes in this submarine fan reservoir.....	11
7. Net-sand map of the B-2 No. 7 stringer.....	13
8. Log facies map of the B-2 No. 7 stringer and log facies cross section showing zones favorable for perforation.....	14
9. Net-pay map of the B-2 No. 7 stringer.....	15

10.	Net-sand map of the C-4 stringer.....	16
11.	Log facies map of the C-4 stringer.....	17
12.	Net-pay map of the C-4 stringer.....	18
13.	Net-sand map of the E-6 stringer.....	19
14.	Log facies map of the E-6 stringer.....	20
15.	Net-pay map of the E-6 stringer.....	21
16.	Areas of untapped gas-saturated sand.....	25
17.	Cross section showing potential location for a strategic infill well and existing and potential completion intervals.....	27
18.	Sodium versus chloride for the Hackberry formation waters in Port Arthur field, Texas, and Miocene formation waters, Cameron Parish, Louisiana.....	34
19.	Piper diagram showing compositions of Hackberry and Miocene formation waters.....	36
20.	Comparison of major inorganic components of Hackberry and Miocene formation fluids.....	37
21.	Chloride/bromide ratio versus total dissolved solids for Frio formation waters from the Texas Gulf Coast compared with Miocene formation fluids from Cameron Parish, Louisiana.....	38
22.	Calcium, potassium, strontium, magnesium, barium, boron, and bicarbonate versus chloride and sodium versus bicarbonate for the Hackberry formation waters in Port Arthur field, Texas, and Miocene formation waters, Cameron Parish, Louisiana.....	39
23a.	Variation of pressure, temperature, oil, gas, brine, gas/brine ratio, and oil/gas ratio of formation waters versus time for the 1-6 well, Port Arthur field, Jefferson County, Texas.....	40
23b.	Variation of inorganic components of formation waters versus time for the 1-6 well, Port Arthur field, Jefferson County, Texas.....	40
24.	Gibbs free energy difference of carbonates versus pH in Hackberry formation waters from the 1-6 well, Port Arthur field, at formation temperature.....	45
25.	Gibbs free energy difference of silica, clays, and carbonates versus temperature at measured pH in Hackberry formation waters from the 1-6 well, Port Arthur field.....	47
26.	Gibbs free energy difference of silica, clays, and carbonates versus pH at separator temperature in Hackberry formation waters from the 1-6 well, Port Arthur field.....	48

27.	Saturation index of carbonates and barite versus different mixes of Hackberry and Miocene formation waters, Port Arthur field.....	49
28.	Core log for the Frio 'A' sandstone Delee No. 1 well, Northeast Hitchcock field, Galveston County.....	55
29.	Environmental distribution of selected trace fossils.....	59
30.	Rippled shale break at 9.191 ft (2.801 m) in the Frio 'A2' sandstone, Northeast Hitchcock field.....	61
31.	Calcareous shale break at 9.184.6 ft (2.799.5 m) in the Frio 'A2' sandstone, Northeast Hitchcock field.....	62
32.	Burrowed calcareous shale break at 9.183.6 ft (2.799 m) in the Frio 'A2' sandstone, Northeast Hitchcock field.....	63
33.	Plane bedded unit at 9.184 ft (2.799 m) near the base of the Frio 'A2' sandstone, indicating rapid deposition in high-energy upper flow regime conditions.....	64
34.	Spotty kaolinite-cemented Frio 'A1' sandstone above planolites burrowed mud at 9.178.3 ft (2.797.6 m).....	66
35.	Closely laminated Frio 'A1' sandstone with horizontal planolites burrows between 9.158 and 9.159 ft (2.791.4 m and 2.791.7 m).....	69
36.	Indurated calcareous Frio 'A1' sandstone overlying an erosional break at 9.155.1 ft (2.790.5 m).....	70
37.	Horizontally laminated Frio 'A1' sandstones and shales at 9.136.7 ft (2.785 m) crosscut by horizontal planolites burrows.....	74
38.	Inclined lined ophiomorpha burrow with horizontal grazing structures at 9.130.6 ft (2.783 m).....	77
39.	Tidal Frio 'A1' sandstones containing an arenicolites burrow at 9.124.1 ft (2.781 m).....	78
40.	Frio 'A1' sandstone with subvertical lined skolithos burrow at 9.121 ft (2.780 m).....	79
41.	Distributary-mouth-bar Frio 'A1' sandstone containing a steeply inclined carbonized twig erosively overlain by shell hash at 9.105.5 ft (2.775.4 m).....	81
42.	Upper crevasse splay Frio 'A1' sandstone at 9.102 ft (2.774.3 m), which contains gregarious, overlapping horizontal planolites burrows.....	83
43.	Horizontal view of a planolites burrow in a carbonaceous Frio 'A1' sandstone at 9.102.5 ft (2.774.5 m).....	85

44.	Depositional model of the Lower Frio Formation, Upper Texas Gulf Coast.....	95
45.	(a) Echinoid spines with ribbed margin and ornate center in basal lag deposit of the Anahuac Formation at 9,100.6 ft (2,773.9 m). (b) End view of spine showing ribbed margin and ornate center.....	98
46.	Close-up view of ornate center of echinoid spines in a basal lag deposit of the Anahuac Formation at 9,100.6 ft (2,773.9 m).....	99
47.	Rounded quartz grains, blocky feldspars, and organic spines in basal Anahuac lag deposit directly above the T2 marker horizon at 9,100.6 ft (2,773.9 m).....	100
48.	Shell fragment in basal Anahuac lag deposit directly above the T2 marker horizon at 9,100.6 ft (2,773.9 m).....	101
49.	Anahuac basal shale lag erosively overlying the Upper Frio at 9,100.6 ft (2,773.9 m).....	102
50.	Corroded dolomite rhombohedron in the Anahuac shales at 9,092 ft (2,771 m) with fibrous illite overgrowths.....	103
51.	Mold after pelecypod in Anahuac shales at 9,099.8 ft (2,773.7 m).....	105
52.	Sandstone compositions of Northeast Hitchcock samples compared with distribution of sandstone compositions from Pleasant Bayou samples.....	108
53.	Concentration of quartz overgrowths, kaolinite cement, and volcanic rock fragments/chlorite clasts versus primary porosity in the Frio 'A' sandstones, Northeast Hitchcock field.....	116
54.	Concentration of quartz, quartz and feldspar overgrowths, and secondary porosity versus primary porosity, Frio 'A' sandstone, Northeast Hitchcock field.....	118
55.	Concentration of carbonate, kaolinite, and chlorite cements and secondary porosity versus primary porosity, Frio 'A' sandstones, Northeast Hitchcock field.....	121
56.	Concentration of plagioclase, potassium feldspar, feldspar overgrowths, kaolinite cement, and secondary porosity versus primary porosity, Frio 'A' sandstones, Northeast Hitchcock field.....	122
57.	Location of Northeast Hitchcock field.....	133
58.	Structure map of Northeast Hitchcock and Alta Loma fields, contoured on the top of the 4,240-ft sand.....	135

59.	South end of structural dip section B-B' through Northeast Hitchcock and Hitchcock fields.....	140
60.	Type log from Northeast Hitchcock field.....	143
61.	Type log in Hastings West field.....	147
62.	Net-sand and depositional facies map of the 3,780-ft sand (lower Miocene).....	151
63.	Net-sand and depositional facies map of the 4,240-ft sand (lower Miocene).....	153
64.	Net-sand and depositional facies map of the 5,460-ft sand (lower Miocene).....	155
65.	Net-sand and depositional facies map of the 5,750-ft sand (lower Miocene).....	157
66.	Net-sand map of the 6,150-ft sand (lower Miocene).....	159
67.	SP log facies map of the 6,150-ft sand.....	160
68.	Net-sand map of the 2,800-ft sand.....	163
69.	SP log facies of the 2,800-ft sand (upper Miocene).....	164
70.	Net-sand map of the 2,030-ft sand (upper Miocene).....	167
71.	SP log facies map of the 2,030-ft sand.....	168
72.	Saturation indices of silica and carbonates in Frio 'A' formation waters, Delee No. 1 well, versus pH at formation temperature (101.7°C, 215°F) and separator temperature (82.2°C, 180°F).....	177
73.	Saturation indices of silica and carbonates in Frio 'A' formation waters, Delee No. 1 well, versus temperature at measured pH (7.51).....	178
74.	Saturation indices of calcite versus pH at Miocene formation temperatures of 48°C (118.4°F) and 63.5°C (146.3°F).....	179
75.	Saturation indices of various mixes of Frio 'A' and Miocene waters at a Miocene formation temperature of 48°C (118.4°F) and measured pH of 6.4.....	181
76.	Saturation indices of of various mixes of Frio 'A' and Miocene waters at a Miocene formation temperature of 63.5°C (146.3°F) and measured pH of 6.25.....	182

Tables

1. Gas-in-place in unperforated zones, Port Arthur (Hackberry) field.....	26
2. Probable and possible resources for a single well (or recompletion) in general location of well 31.....	28
3. Analyses of oil field brines from Upper Miocene sands, Cameron Parish, Louisiana.....	32
4. Analyses of co-production brines from the unit 1-6 well Port Arthur field, Jefferson County, Texas.....	33
5. Scale of approximate saturation index values.....	42
6. Saturation indices of combinations of Hackberry and Miocene formation waters, Port Arthur field.....	50
7. Frio 'A' Sandstone components as percentages, Delee No. 1 well.....	107
8. Well logs used in brine-disposal study of Northeast Hitchcock and Alta Loma fields.....	136
9. Volumes available for brine disposal into sand greater than 40 ft thick.....	169
10. Analyses of Miocene formation waters from Galveston County.....	174
11. Analyses of Frio 'A' formation waters from the Delee No. 1 well, Northeast Hitchcock field, Galveston County.....	175
12. Temperature, pH, and concentration of aqueous species in combinations of Frio 'A' and Miocene waters, Northeast Hitchcock field.....	176
13. Assumed temperatures of Miocene waters at varying pH.....	176

REEXPLORATION OF SUBMARINE CANYON AND FAN RESERVOIRS AT PORT ARTHUR (HACKBERRY) FIELD, JEFFERSON COUNTY, TEXAS

by Noel Tyler, assisted by James Reistroffer

INTRODUCTION

Stacked and heterogeneous submarine canyon and submarine fan reservoirs in Port Arthur field, Jefferson County, produced 57 billion cubic feet (Bcf) of gas and 2.65 million barrels (bbl) of condensate in a 13-yr period prior to abandonment of the field in 1972. Port Arthur field was abandoned when increasing disposal of the formation brines from strong water-driven gas reservoirs resulted in uneconomical production. These reservoirs were considered to have been watered out.

Watered-out reservoirs contain substantial quantities of gas that can be produced by the co-production method. This technology attempts to reduce reservoir pressure through the production of large volumes of water. Free gas, bypassed in the reservoir as it was invaded by the rising gas-water interface, becomes mobilized and recoverable. Additional but minor gas dissolved in formation water is produced at the surface as pressure is reduced. The co-production potential of Port Arthur field was analyzed in detail during an ongoing project funded by the Gas Research Institute (Gregory and others, 1984) and was considered highly prospective.

Highly encouraging initial production potential was obtained from a Hackberry sand identified by The University of Texas at Austin and ResTech log analysts during detailed site characterization. On the basis of this result and in light of ongoing oil reservoir characterization studies, which have shown that substantial volumes of producible hydrocarbons remain in untapped compartments in complex reservoirs (Tyler and others, 1984; Galloway and Cheng, 1985; Tyler and Ambrose, 1985; Fisher and Finley, 1986), it was decided to reexamine the potential for additional recovery of free gas at Port Arthur.

Hackberry reservoirs at Port Arthur were deposited in a submarine canyon and fan environment (Ewing and Reed, 1984). Submarine canyon and fan reservoirs are notoriously complex and because of this heterogeneity are characterized by low hydrocarbon recovery efficiencies (Guevara, in press; Tyler and Gholston, in press). The high degree of compartmentalization of these deep-water reservoirs results from rapid lateral facies changes coupled with noncontinuous or episodic depositional events. Deep-water Hackberry reservoirs at Port Arthur field display complex internal architectures consistent with their depositional setting. The existence of additional untapped free-gas-bearing zones is thus highly likely. This report describes the methodology and results of the reexploration of framework sandstone reservoirs at Port Arthur field.

Setting of Hackberry Reservoirs

The updip Frio Formation in southeast Texas consisted of a deltaic headland adjacent to which (to the east) was an interdeltic barrier-island and strandplain complex composed of sandstones encased in shelf, lagoonal, and coastal plain mudstones (Galloway and others, 1982). Sand-body orientation in the Buna barrier/strandplain system is strike parallel. Gross sand content decreases while the total thickness of the formation increases seaward.

The Hackberry consists of a basinward-thickening wedge of muds and sands erosionally juxtaposed on the middle and lower parts of the formation (fig. 1). The thickness of the proximal Hackberry is strongly controlled by the presence or absence of canyons and thus displays rapid thickness variations. South- to southeastward-trending linear sand thicks mapped in the subsurface by Ewing and Reed (1984) were deposited in a system of dip-oriented, areally restricted canyons (fig. 2) that probably merge basinward beyond the limits of well control with a more extensively developed

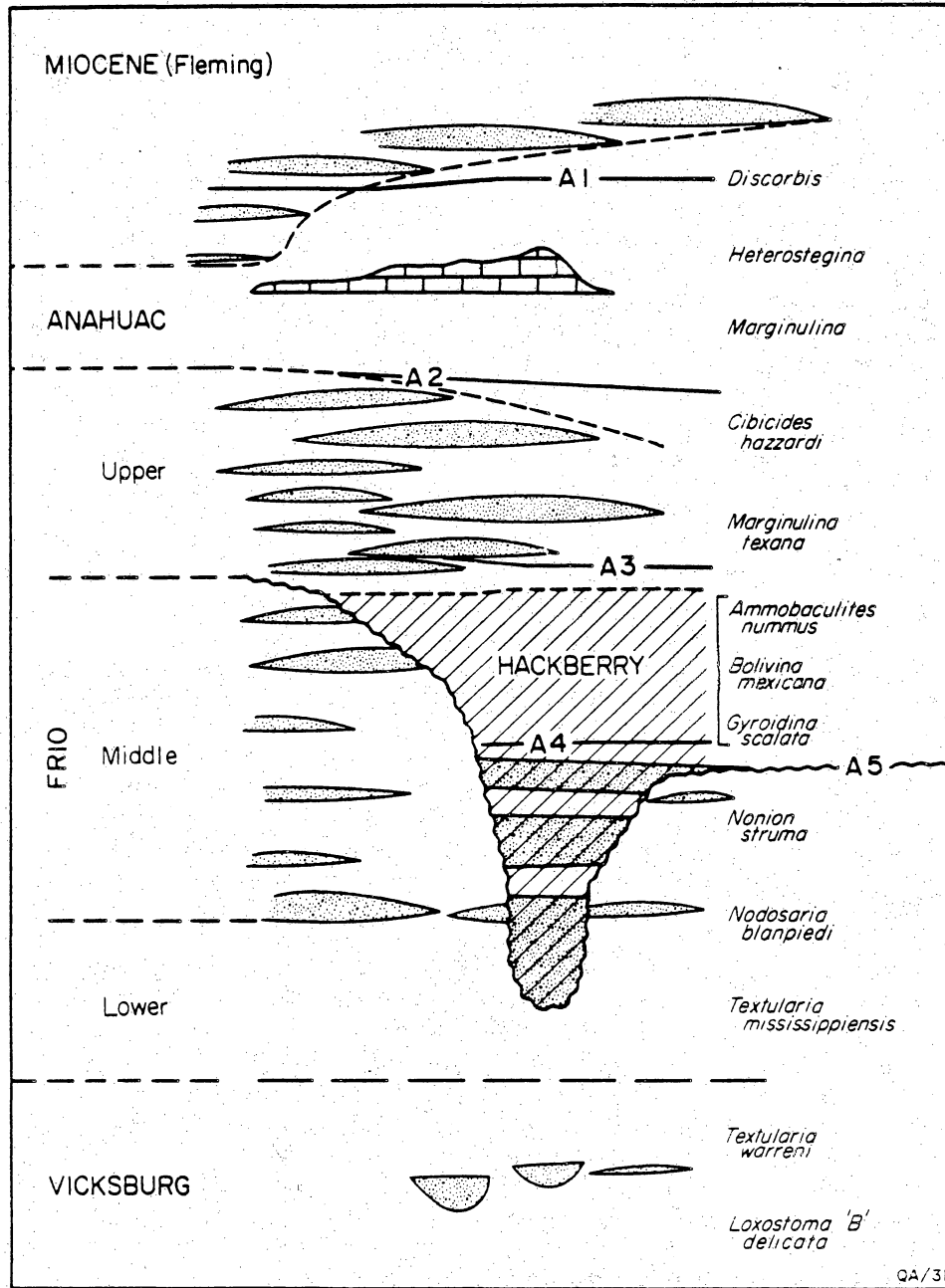


Figure 1. Frio stratigraphic relations and diagnostic foraminifera, Jefferson County area (from Ewing and Reed, 1984).

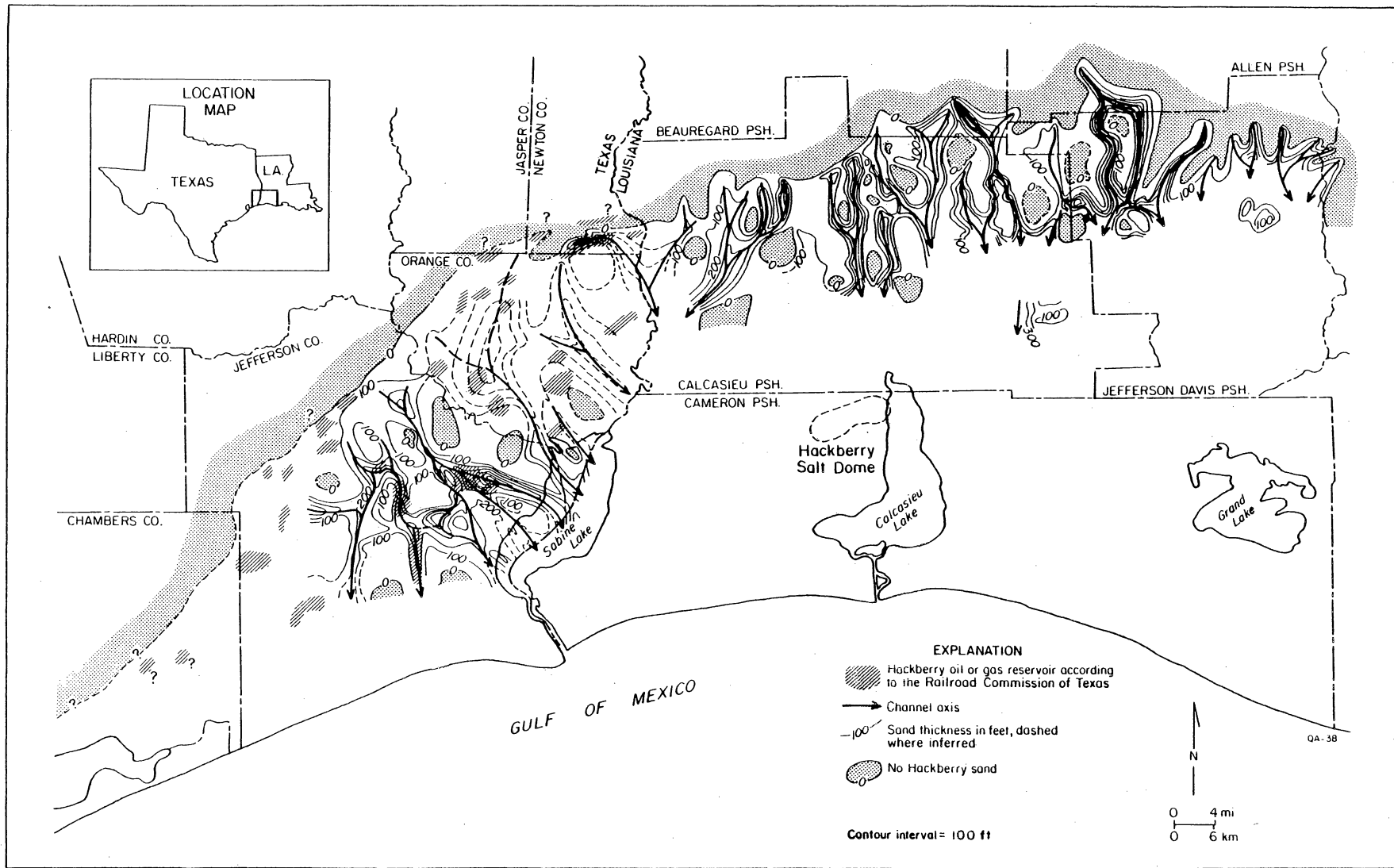


Figure 2. Regional distribution of sand-bearing lower Hackberry channels (from Ewing and Reed, 1984).

submarine fan system.

The source of sands and intervening muds in the Hackberry was the contemporaneous Houston delta system that lay west of the Buna shore zone. Sands that passed through the delta system into the receiving basin were transported alongshore by longshore drift. Much of the sediment not deposited in the Buna barriers and strandplains was captured by canyons that extended landward from the deep basin onto the shelf (fig. 3). The origin of the canyons remains enigmatic; however, they were efficient conduits for the siphoning of sediment from the shelf. Much of the sediment was deposited internally within the canyons. Depositional processes were highly complex and evolved through time. The resulting sand-body reservoirs display an evolving internal architecture from canyon-fill facies deeper in the section to an abundance of unconfined-flow submarine fan facies in the overlying younger Hackberry sediment.

Hackberry Stratigraphy at Port Arthur

Gross stratigraphic relations at Port Arthur have been described previously (Gregory and others, 1984; Ewing and Reed, 1984). More important to extended recovery of hydrocarbons is the detailed internal stratigraphy of individual reservoirs, but it is appropriate to review Hackberry stratigraphy in the field as a prelude to detailed reservoir description.

Deep in the lower Frio, barrier and strandplain sandstones encased in shelf and lagoonal mudstones are present. These sands thin upward and grade into thinner shelf sands encased in thickly developed shelf mudstones. This lower Frio interval was deposited during coastal onlap. The Hackberry rests unconformably and erosionally on the truncated shelf mudstones of the lower Frio (fig. 4). Basal Hackberry sands that have been informally named the G and H sands are thick and massive with a

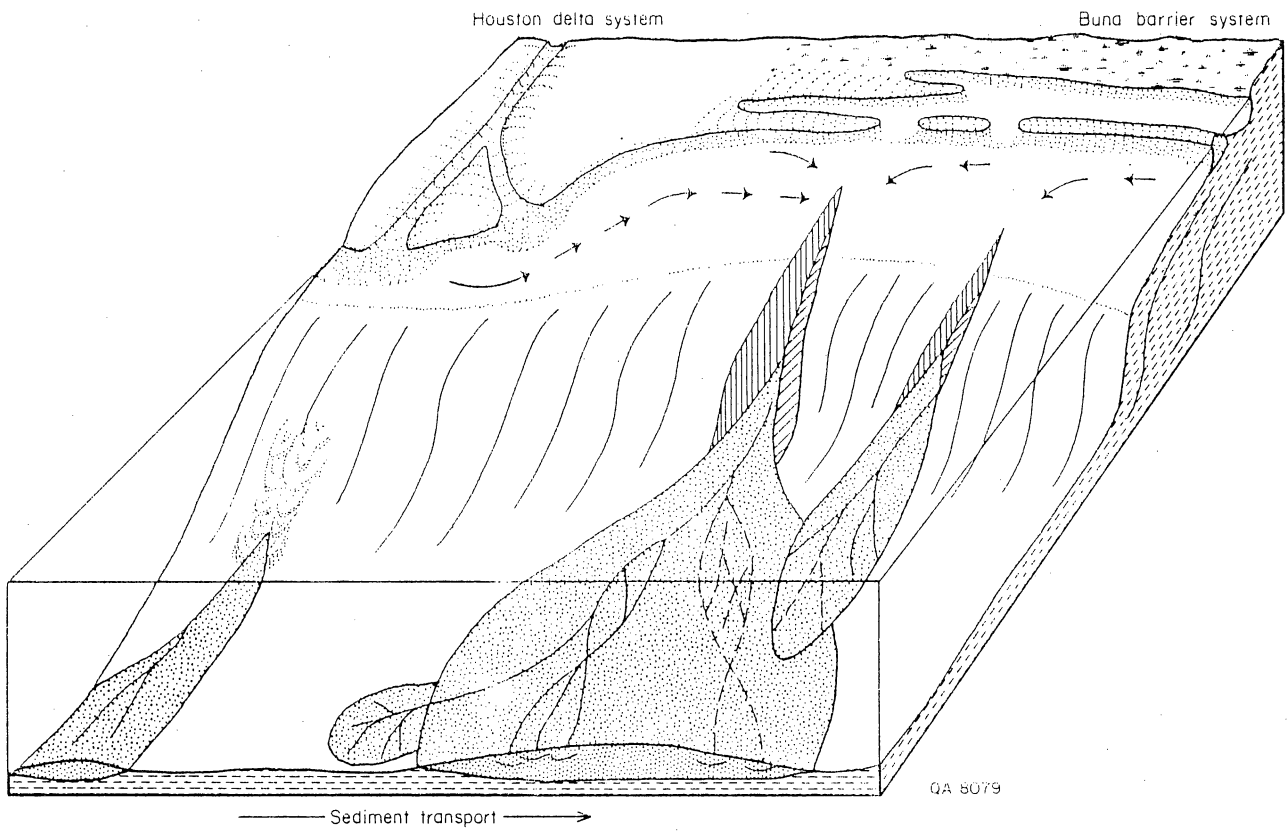
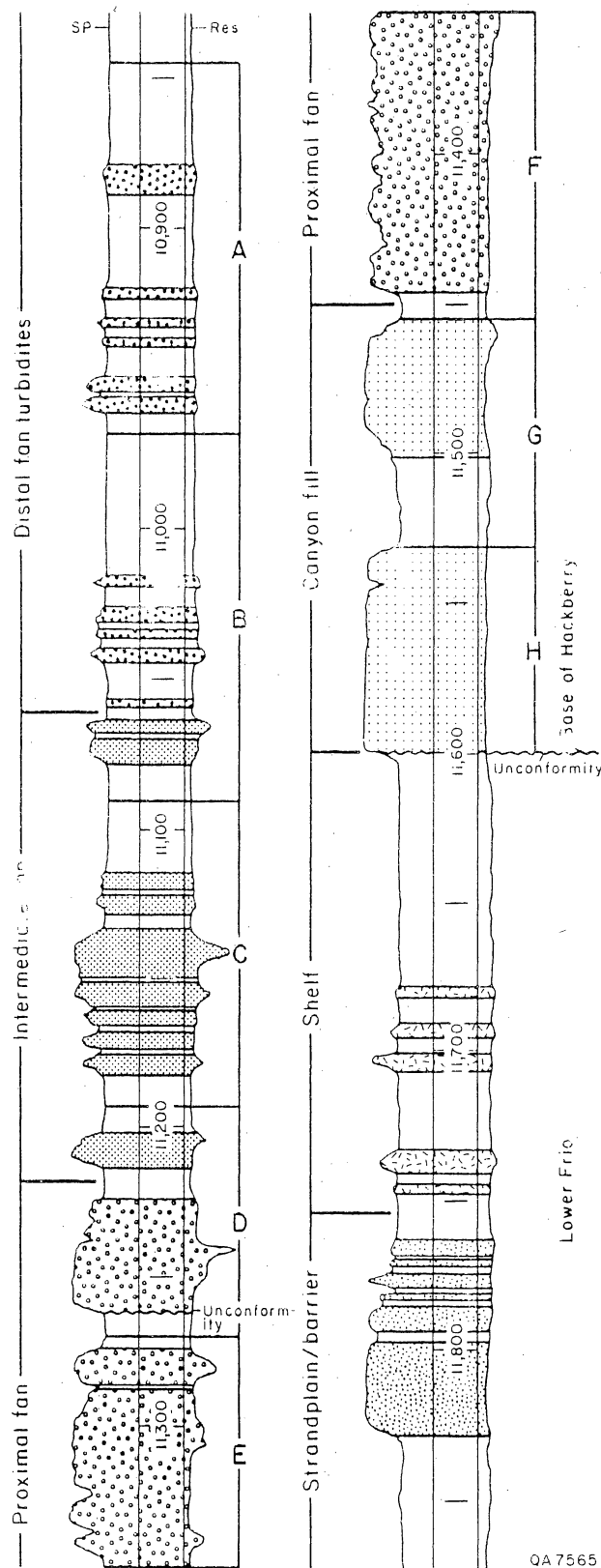


Figure 3. Depositional model of Hackberry reservoirs, Port Arthur field.



QA7565

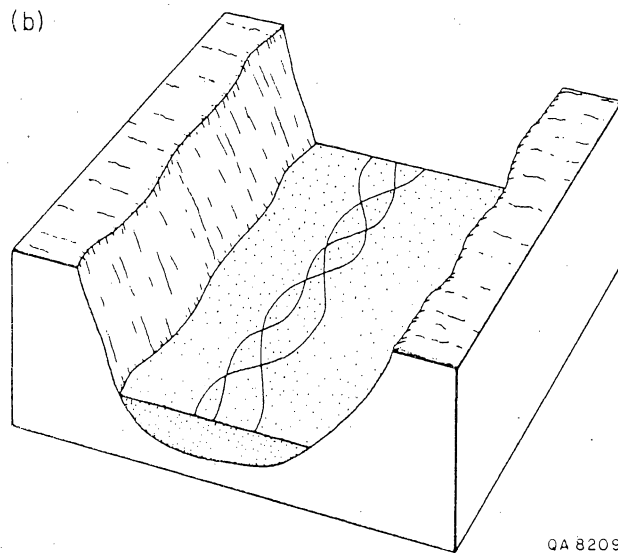
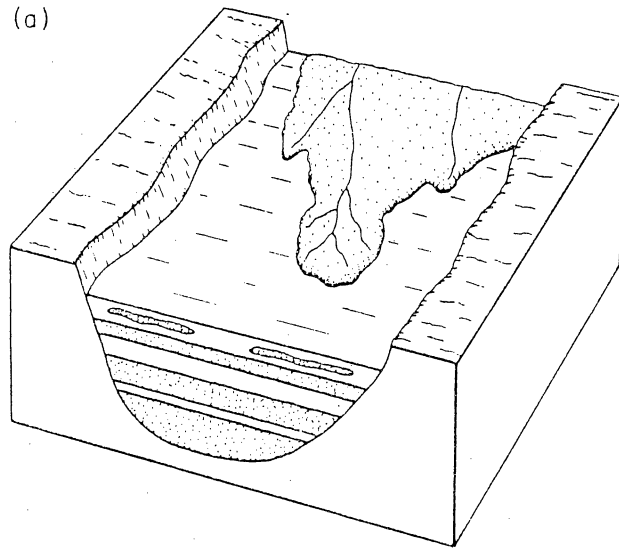
Figure 4. Typical log from the Port Arthur field (Port Arthur No. 14).

characteristic blocky spontaneous potential (SP) log motif. The D, E, and F sands also are thickly developed and strongly aggradational. In contrast to the underlying Hackberry sands, these three intervals contain numerous shale interbeds that impart a sand-rich but serrate SP log motif. The upper intervals of the Hackberry show increasing amounts of mud layers deposited between more and more thinly developed sand units. Sands of interval C are more thinly developed than those of interval D, and the upper intervals are characterized by thin sand stringers dominated by thickly developed mud layers (fig. 4).

Lower Hackberry intervals D through H were deposited during submarine fan aggradation (fig. 4). The style of sedimentation changed during the waning phases of deposition of unit D. Younger Hackberry intervals were deposited during abandonment of the submarine fan complex as successive turbidite pulses were weakened and became unable to pass through the canyon (fig. 5). Most of the gas production from Port Arthur (68 percent, or 38.6 Bcf) was from these upper, highly complex sandstone intervals.

RESERVOIR ARCHITECTURE AND THE POTENTIAL FOR UNTAPPED COMPARTMENTS

A body of evidence confirming that the internal geometric arrangement of depositional facies, that is, the internal architecture of the reservoir, is critical in controlling reservoir recovery characteristics is emerging. Although well spacing and drive mechanism are undeniably important, an additional fundamental control on production character is reservoir genesis. Certain classes of reservoirs (a small minority) contain laterally continuous pay intervals. Far more typical are those reservoirs that are heterogeneous and internally compartmentalized. Submarine fan reservoirs are the most complex and internally variable and consequently display the lowest recovery efficiencies of all terrigenous clastic reservoirs (Tyler and others, 1984).



QA 8209

Figure 5. Evolution of Hackberry reservoirs from canyon-fill to submarine fan sands.

Internal compartmentalization, both lateral and vertical, prevents mobile hydrocarbons from migrating to the well. This is certainly true in oil reservoirs, and sparse reports in the literature (Seal and Gilreath 1975) suggest that similar behavior may be present in gas reservoirs. Thus by utilizing a detailed understanding of the internal architecture of the reservoir, additional uncontacted gas may be recovered.

Interval C, deposited at the inception of abandonment of the Hackberry fan complex, exemplifies the complexity of submarine fan reservoirs. Originally mapped by Gregory and others (1984) as a braided-fan channel-fill deposit, detailed reexamination of the interval shows that it consists of a mosaic of channel, overbank and levee, sand-rich distal fan, and mud-rich distal fan facies (fig. 6). Channel facies characterized by blocky SP response form the framework around which associated facies are arranged. Channels were erosive, as is shown by truncation of preexisting deposits. Immediately adjacent to the channel are levee and overbank facies that display variable grain-size and bed-thickness trends and consequently variable SP log motifs. These two facies rest on an upward-coarsening and upward-thickening distal fan (perhaps fan lobe) facies that in turn rests on distal fan to basinal muds (fig. 6). Channel facies are the most porous (31 percent average porosity); associated sand-rich but nonchannel facies have much lower porosities (26 percent average porosity).

In addition to well-developed lateral heterogeneity, interval C is also highly stratified. Hemipelagic muds deposited during episodes of submarine fan quiescence divide the reservoir into discrete layers. Each layer is composed of the facies elements described above and, in particular, a core of channel deposits enveloped by levee and overbank facies. Submarine fan reservoirs are clearly highly compartmentalized both laterally and vertically. It is this compartmentalization that

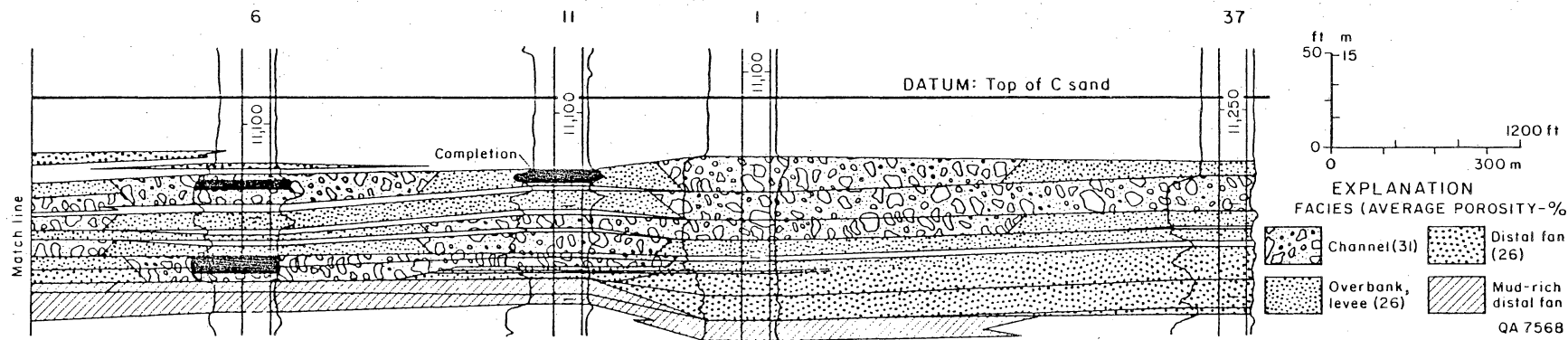
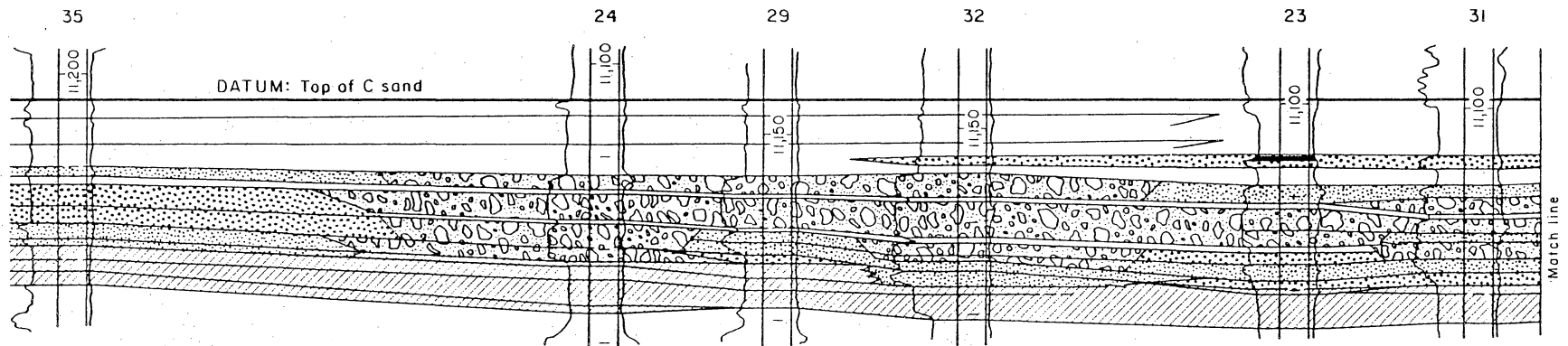


Figure 6. Facies cross section of the C sand illustrating rapid and multiple facies changes in this submarine fan reservoir.

inhibits efficient drainage of the reservoir at typical well spacings.

Conversely, highly compartmentalized reservoirs have the greatest potential for additional hydrocarbon recovery. Although interval C was the most prolific of the Port Arthur Hackberry sands, having produced 19.6 Bcf of gas and 863,000 bbl of condensate, undrained compartments still existed in this reservoir at abandonment. Recompletion of an abandoned well in an abandoned field (lower completion in well 6, fig. 6) displayed an initial potential of 5.5 MMcf of gas and 300 bbl of condensate at a flowing tubing pressure of 6,300 lb over a 24-hr test.

Considerable potential exists for the detection and production of additional uncontacted gas-bearing reservoir intervals. This report describes the reservoir development geology of three such zones and provides an estimate of remaining conventionally producible gas in the field.

Prospective Units

Sands that were isolated from sub- and superjacent sands by continuous hemipelagic muds, that exhibited gas-saturation characteristics on well logs, and that had not been perforated were selected for detailed mapping. A total of 11 sands are considered prospective, each of which was mapped. For the sake of brevity, only three are presented in this report; the remaining maps are on open file at the Bureau of Economic Geology.

Depositional elements demonstrated in figure 6 are present in each of the sands mapped. Similar depositional trends are repeated in each of the sands mapped but with differing orientations (figs. 7 through 15).

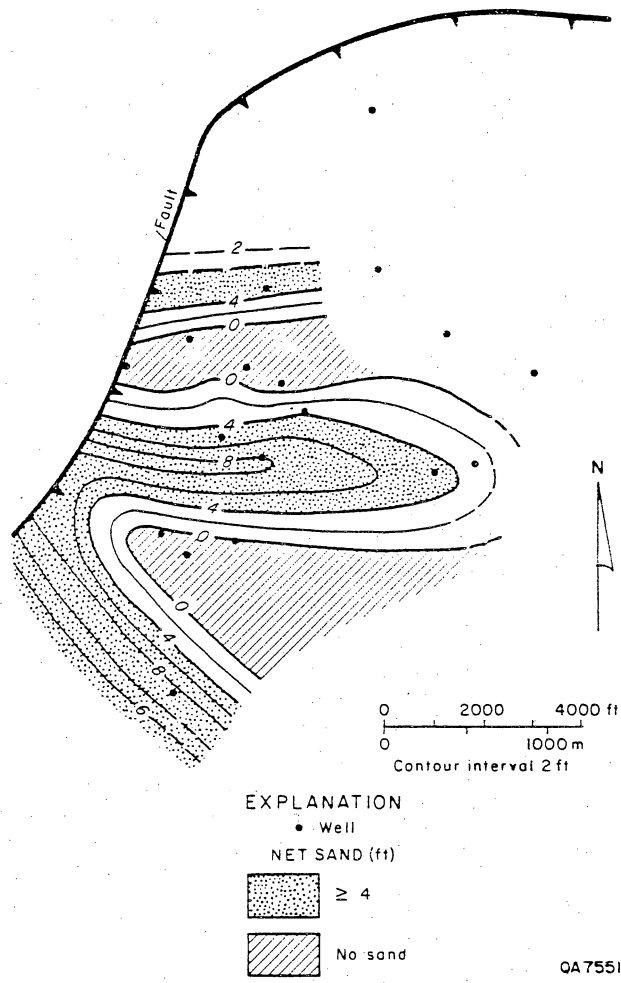
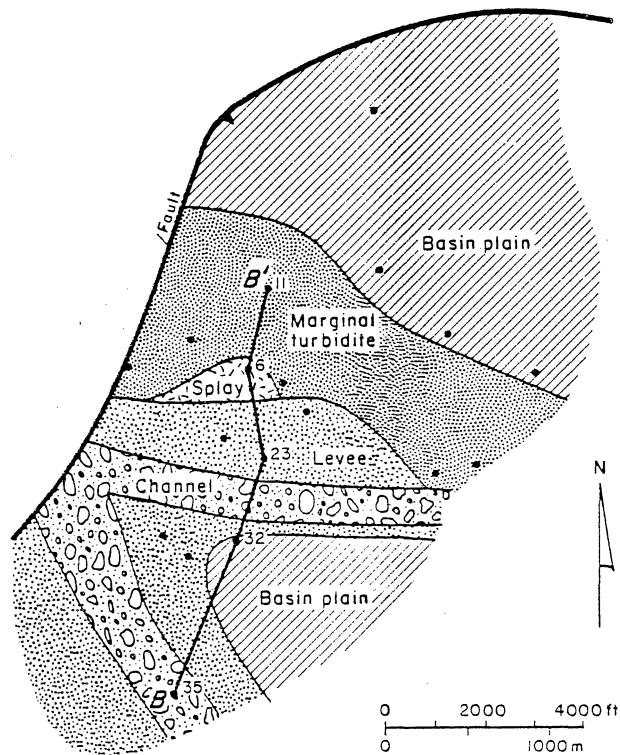


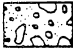

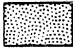


Figure 7. Net-sand map of the B-2 No. 7 stringer.



EXPLANATION

• Well

MOTIF / INTERPRETATION

	Blocky		Spike
	Upward fining		No sand
	Upward coarsening-upward fining		

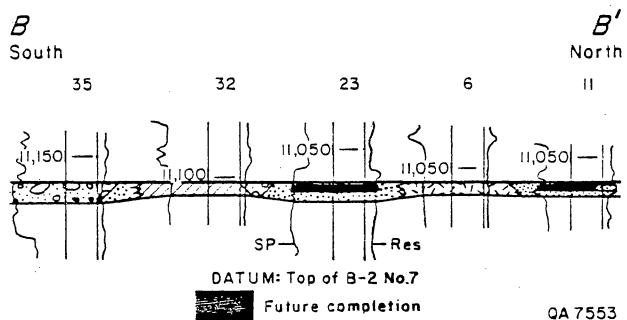
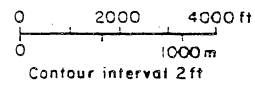
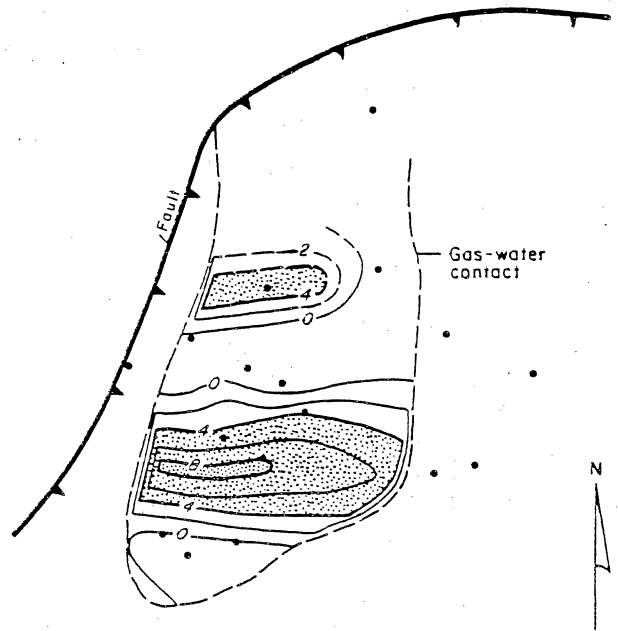




Figure 8. Log facies map of the B-2 No. 7 stringer and log facies cross section showing zones favorable for perforation.



EXPLANATION

- Well
- NET PAY (ft)
-  ≥ 8
-  ≥ 4

QA 7549

Figure 9. Net-pay map of the B-2 No. 7 stringer.

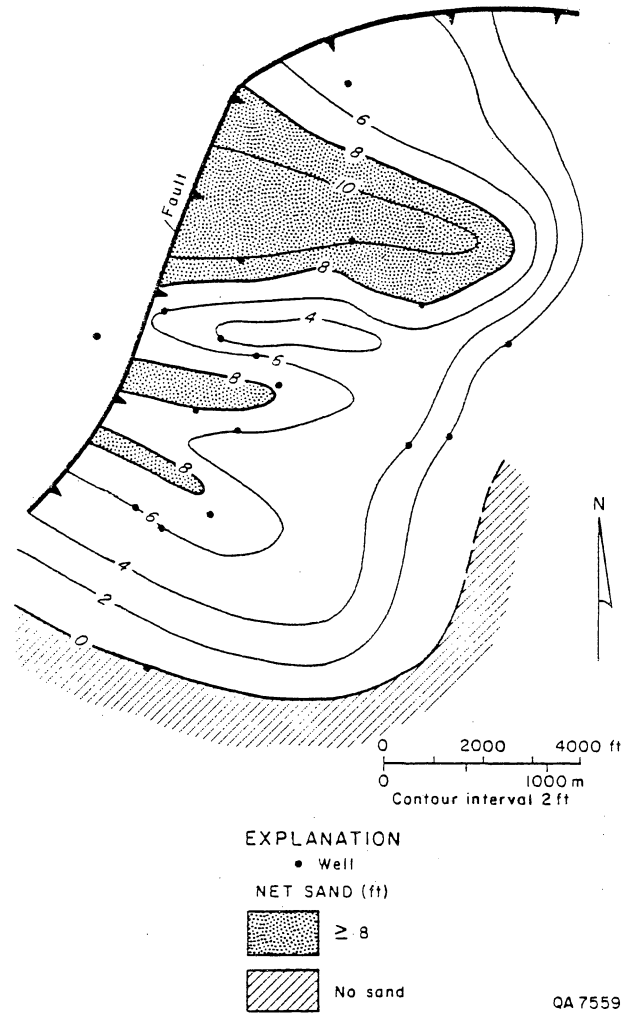
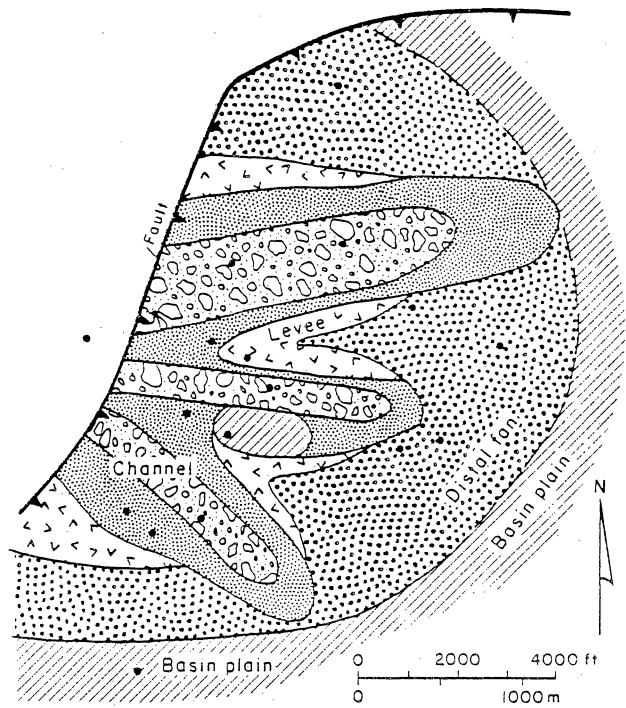


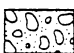
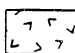


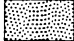
Figure 10. Net-sand map of the C-4 stringer.



EXPLANATION

• Well

MOTIF/INTERPRETATION

	Blocky		Serrate
	Upward coarsening		No sand
	Upward fining		

QA 7545

Figure 11. Log facies map of the C-4 stringer.

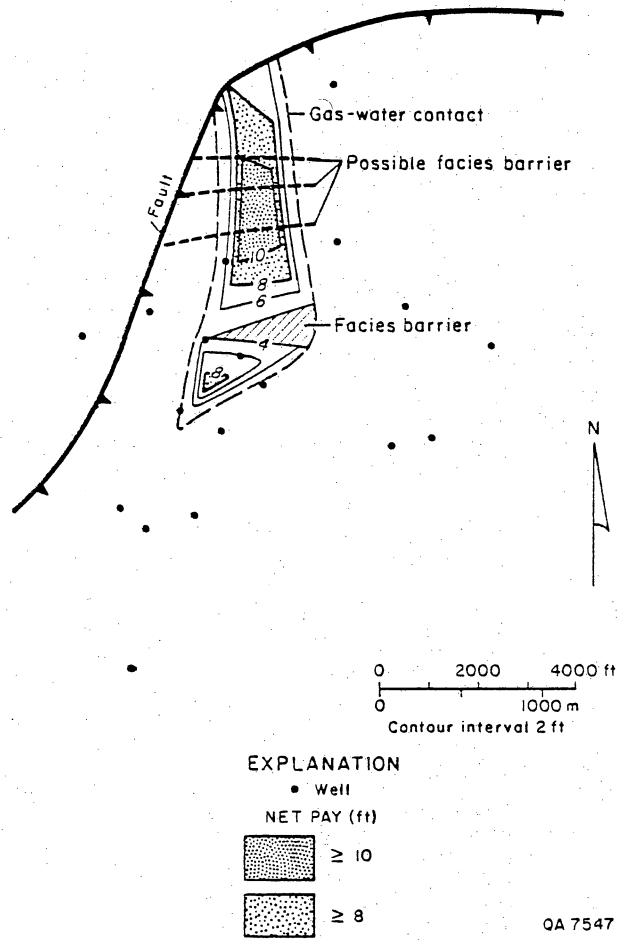


Figure 12. Net-pay map of the C-4 stringer.

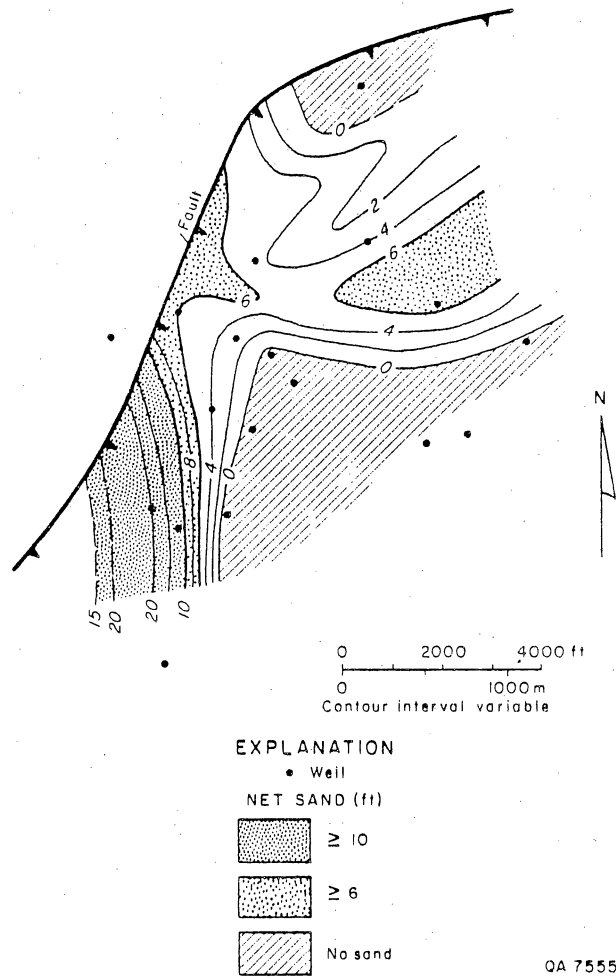
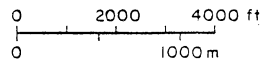
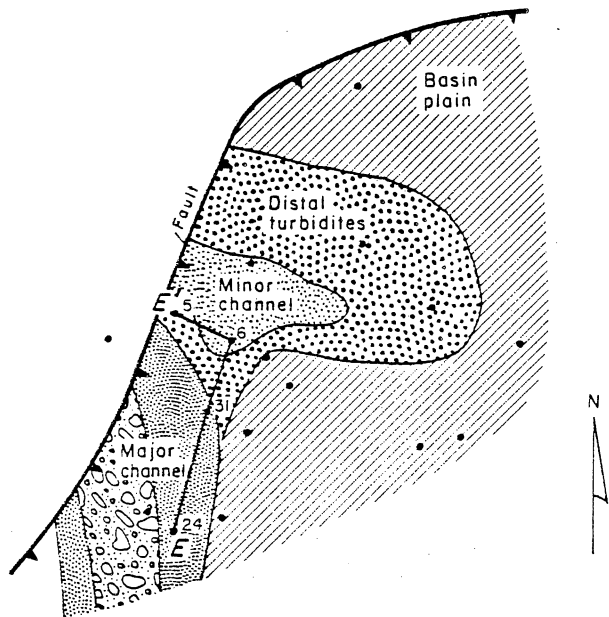




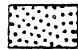


Figure 13. Net-sand map of the E-6 stringer.

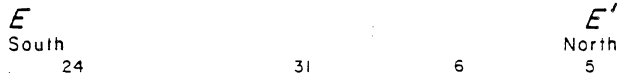




EXPLANATION

• Well

MOTIF/INTERPRETATION

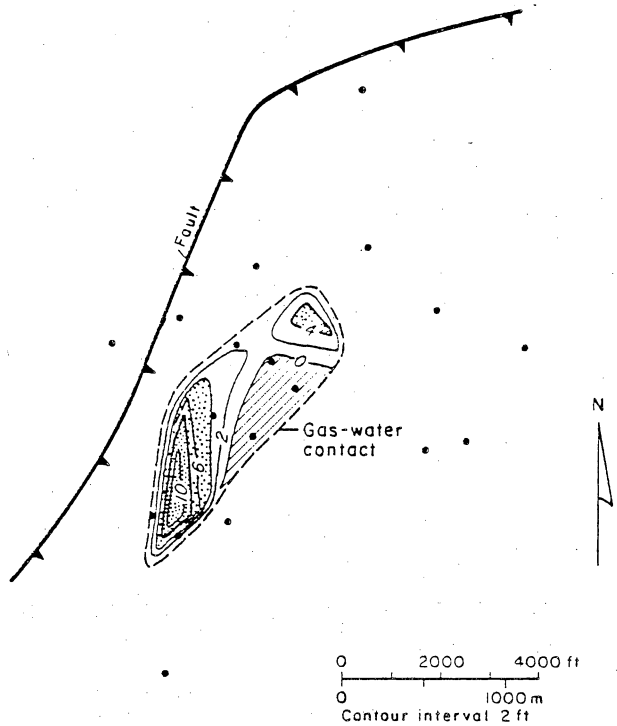
	Blocky		Upward coarsening/ upward fining
	Upward coarsening		No sand
	Upward fining		





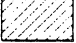
 Future completion
 Existing completion

QA 7557

Figure 14. Log facies map of the E-6 stringer.



EXPLANATION

- Well
- NET PAY (ft)
-  ≥ 8
-  ≥ 4
-  No sand

QA 7543

Figure 15. Net-pay map of the E-6 stringer.

Sand Distribution

A recurring characteristic in many of the sand stringers is the presence of sand thicks that show a bifurcating pattern. Sand thicks are oriented toward the east, southeast, and south. Adjacent to the zones of greater sand development, sands thin abruptly (fig. 10) or pinch out completely (figs. 7 and 13).

Facies Architecture

Depositional elements as shown by net-sand mapping are repeated on log facies maps. Log facies maps, which are based on the shape of the SP curve, show the lateral variation in vertical grain-size trends across the field area. Thus in the B-2 No. 7 stringer (fig. 8) a cone (also called Christmas tree) motif on the SP log represents an upward-fining sand; symmetrical motifs suggest early progradation (upward-coarsening sands) overlain by aggradational deposits (upward-fining sands); and blocky motifs indicate no vertical grain-size trends. Blocky motifs form the core of the complex and correspond to the sand thicks. As such these sands were deposited in submarine channels.

Flanking the channels are a variety of log facies that are variable in log response, which suggests variability in the processes responsible for their origin. The most common facies association is a trend of blocky to upward-fining to serrate to upward-coarsening motifs as is displayed by the C-4 stringer (fig. 11). This facies association represents a gradation from channels (blocky and upward-fining motifs), to levee (serrate motif), to unconfined flow facies on the distal fan or fan lobe (upward-coarsening motif). In the B-2 No. 7 stringer, channel-flanking deposits are inferred from upward-fining sands superimposed on distal progradational deposits.

Cross sections transverse to the local depositional fabric of the Hackberry illustrate the profound influence of facies architecture on reservoir continuity (figs. 8 and 14). Coupled with the bifurcating geometry of the channels, shale out of reservoir facies into basin plain mudstone provides a first-order magnitude facies change. Equally important are the changes from channel to levee to splay and marginal turbidite as these variations and the accompanying changes in petrophysical attributes at the interface between facies result in the intrareservoir entrapment of gas.

Net Pay

The distribution of pay in individual stringers is a unique function of three parameters: structure, sand distribution, and facies architecture. The trapping structure at Port Arthur is a linear north-south-trending anticline downdip (east) of a bounding fault. Structure determines the position of the gas-water contact within each of the individual stringers. Sand distribution and architecture of the reservoir sands determines the spatial variability of hydrocarbons. In most of the reservoirs at Port Arthur, sand pinch-out results in discontinuous pods of pay within the confines of the gas-water contact (figs. 9, 12, and 15). The orientation of the pods is directly related to the depositional fabric of the reservoir sand. Channel and channel-fringe facies compose the principal pay elements; boundaries between these two facies probably create partial to complete barriers to reservoir drainage (fig. 12). Discontinuous pods and lenses of pay typify the remaining undrained reservoirs at Port Arthur.

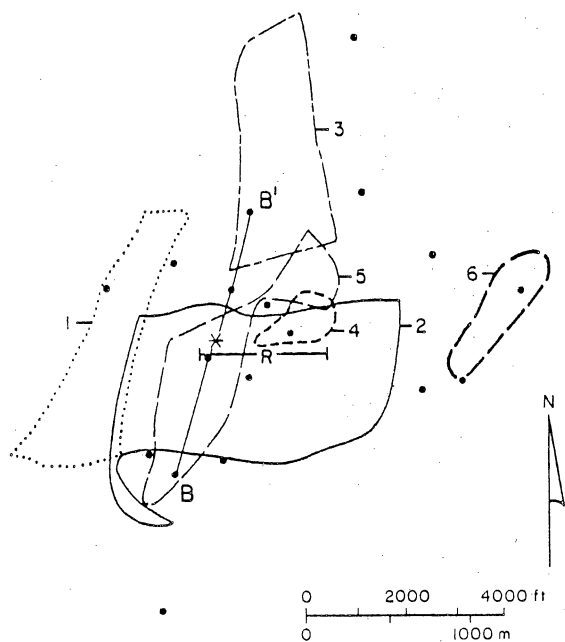
Remaining Resource

Primary gas production at Port Arthur emphasized the high-permeability, highly gas-saturated sands. Those sands having strong resistivity deflections were perforated; sands with lower saturations were left untapped. Water saturations in the primary production zones ranged from 35 to 84 percent. To determine the remaining resource base in the field, water saturations and, from these data, gas saturations in the untapped zones were calculated using the few available porosity logs and, in wells without porosity logs, using the resistivity curve coupled with available sidewall core porosities. Sidewall core porosities were further characterized according to environment of deposition. Channel facies consistently display higher porosities and lower saturations (averages of 31 percent and 61 percent, respectively) compared with non-channel facies (26.5 percent and 64 percent, respectively).

Gas-bearing untapped zones were ranked into two classes on the basis of calculated water saturations. Those zones having water saturations of between 70 and 79 percent were classified probable pay, those zones with saturations greater than 79 percent were classified possible pay.

Facies-based untapped compartments are unevenly distributed throughout the field area (fig. 16). The 11 untapped zones in the Port Arthur field contain a total gas resource of 13.9 Bcf. Calculations show that 7.9 Bcf gas remain in the probable pay zone category; the remaining 6 Bcf is located in those zones of higher water saturation (table 1).

Strategic location of a single infill well on the crest of the structure (fig. 16) and completions in probable pay zones E-6 and B-2 No. 7 and possible pay zones B-1 No. 2 and B-1 No. 5 would tap a total resource base of 6.5 Bcf gas, that is, the equivalent of greater than 1.0 MMbbl of oil (fig. 17, table 2). Many of the untapped compartments are present in existing wells, and selective recompletion of existing



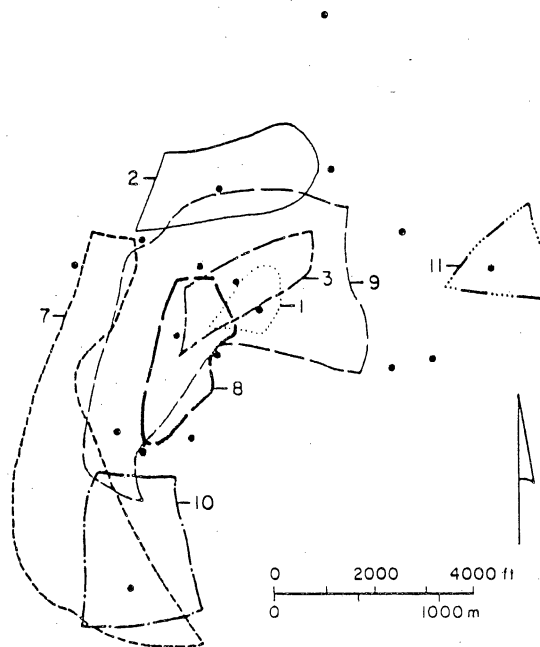
EXPLANATION

- Well * Strategic infill well
- Outline of probable pay areas
- R- Theoretical radius of drainage on 640 acre spacing

PROBABLE PAYS

1	A-2 "10,950 SD"	1.99 Bcf
2	B-2 No.7	2.66 Bcf
3	C-4	1.7 Bcf
4	E-5	0.17 Bcf
5	E-6	0.93 Bcf
6	F-6	0.47 Bcf

QA 7563



EXPLANATION

- Well
- Outline of possible pay areas

POSSIBLE PAYS

1	A-2 "10,950 SD"	0.2 Bcf
2	B-2 No.7	0.3 Bcf
3	C-4	0.3 Bcf
7	B No.0	1.8 Bcf
8	B-1 No.2	0.3 Bcf
9	B-1 No.5	2.3 Bcf
10	B-1 No.5.5	0.6 Bcf
11	D-8	0.2 Bcf

QA7561

Figure 16. Areas of untapped gas-saturated sand: (a) Probable pay (water saturation between 70 and 79 percent) and (b) possible pay (water saturation greater than 79 percent).

Table 1. Gas-in-place in unperforated zones.
Port Arthur (Hackberry) field.

Sand	Probable Bcf	Possible Bcf
A-2 (10,950')	2.0	0.2
B-0		1.8
B-1 No. 2		0.3
B-1 No. 5		2.3
B-1 No. 5.5		0.6
B-2 No. 7	2.6	0.3
C-4	1.7	0.3
D-8		0.2
E-5	0.2	
E-6	0.9	
F-6	0.5	
Totals	<hr/> 7.9	<hr/> 6.0

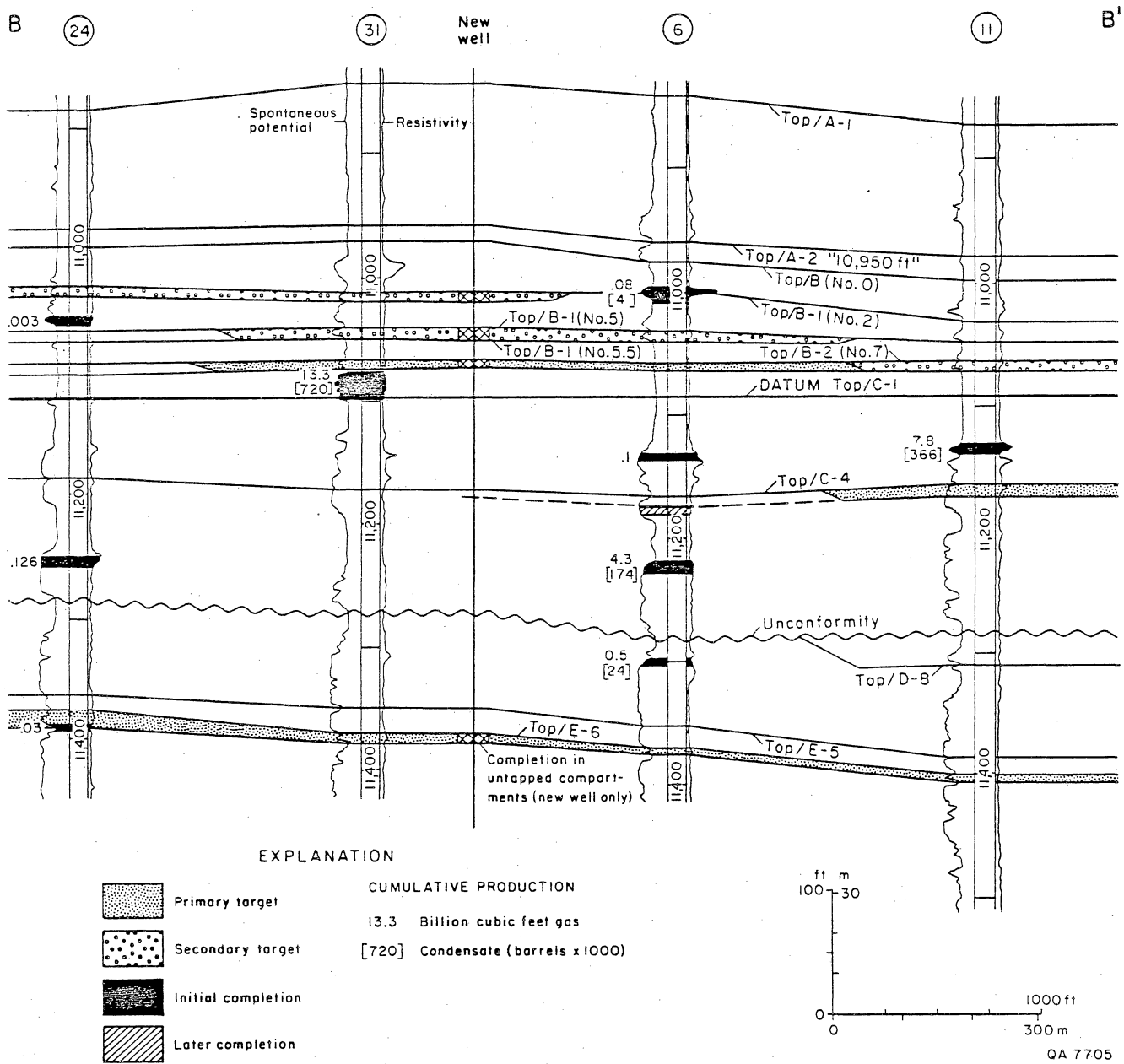


Figure 17. Cross section showing potential location for a strategic infill well and existing and potential completion intervals.

**Table 2. Probable and possible resources
for a single well (or recompletion)
in general location of well 31.**

Probable Resource	Possible Resource
3.6 Bcf	2.9 Bcf
Total Resource 6.5 Bcf or >1.0 million BOE	

(although abandoned) wells provides an alternative secondary gas recovery strategy.

Brine Disposal

As part of this analysis the disposal potential of Miocene sands at Port Arthur was examined. At least four sands in the Miocene section display sufficient lateral continuity and minimal internal heterogeneity to be considered favorable repositories for produced brines. These Miocene sands are of wave-dominated delta or strandplain origin and as such compose excellent candidates for disposal. In a subsequent section of this report the disposal geology of similar disposal sands at Northeast Hitchcock field are described in detail. Of more concern is the potential for incompatibility between the disposal fluids and the indigenous aquifer fluids. These considerations are examined in the following section of this report.

CONCLUSIONS

Port Arthur (Hackberry) reservoirs were deposited in a submarine canyon/submarine fan canyon-fill depositional setting. The lower sands in the Hackberry are thick, aggradational canyon-fill deposits; upper sands were deposited during submarine fan abandonment. It is in these upper, highly discontinuous, internally heterogeneous reservoirs that the best potential for reserve growth through strategic infill drilling, or alternatively, selective recompletion of existing wells, exists.

A recurrent characteristic of the untapped stringers is the development of thicker, more porous and permeable channel sands that form the axes around which thinner and poorer reservoir-quality nonchannel sands are arranged. Bifurcating channel

morphologies result in discontinuous and podlike belts of more favorable pay characteristics separated by poorer pay or nonpay areas. A total resource base of 13.9 Bcf of gas exists in these untapped compartments, approximately half of which could be contacted by four completions in a single strategically sited well located on structure.

COMPATIBILITY OF HACKBERRY AND MIOCENE FORMATION WATERS PORT ARTHUR FIELD, TEXAS

by M. P. R. Light

INTRODUCTION

The likelihood of scale formation in production tubing, surface equipment, and Miocene disposal sandstones at the Port Arthur field, Texas, has been investigated with regard to the disposal of Hackberry formation waters co-produced from the 1-6 well. Tomson and O'Day (1987) indicate that the formation of calcium carbonate with a few percent iron-carbonate scale in Gulf Coast systems is initiated by a drop in pressure that causes carbon dioxide to exsolve from formation waters, thereby increasing the pH. Carbonate scaling in production tubing occurs at temperatures in excess of 212°F (100°C) and less than 140°F (60°C), whereas the intervening temperature range is characterized by corrosion (Tomson and O'Day, 1987).

Disposal of Hackberry fluids into Miocene aquifers requires a knowledge of the average compositions and hence compatibility of Miocene and Hackberry formation waters. No published data are available on Miocene formation waters in the Port Arthur area, so five Miocene formation-water analyses from Cameron Parish, Louisiana (table 3; Collins, 1970), adjacent to Port Arthur, were averaged and compared with two Hackberry formation-water analyses from the co-production 1-6 well in the Port Arthur field (table 4). The Hackberry waters were collected by Institute of Gas Technology (IGT) staff, and analyses were conducted at the Bureau of Economic Geology (BEG) using standard procedures, including the use of an inductively coupled plasma atomic emission spectrometer. Both the Miocene and Hackberry waters are sodium chloride brines and plot close to the pure halite dissolution line (fig. 18). Low-salinity waters have probably been diluted with pure water because they lie along the NaCl dissolution line. Condensation of pure water from gas has apparently reduced the salinities of these waters by three orders of magnitude.

Table 3. Analyses of oil field brines from Upper-Miocene sands, Cameron Parish, Louisiana (Collins, 1970).

No.	S12 T12S R10W	S28 T12S R10W	S28 T12S R10W	S12 T13S R08W	S12 T13S R08W
Depth	5,978 ft	3,297 ft	2,925 ft	4,575 ft	5,824 ft
pH	6.6	5.6	5.99	6.1	6.0
S.G.	1.088	1.088	1.090	1.085	1.089
T.D.S.	124,378	126,457	127,649	126,631	121,867
K	195	168	187	ND	ND
Na	44,607	46,011	46,485	46,798	44,025
Ca	2,473	2,097	2,073	1,803	2,015
Mg	747	646	646	506	993
Sr	143	130	188	185	95
Ba	90	48	50	80	88
Li	2	2	4	ND	ND
B	21	30	31	ND	ND
Cl	75,837	77,085	77,789	76,906	74,422
HCO ₃	157	153	167	262	140

All aqueous species expressed in mg/L.

Table 4. Analyses of co-production brines from the unit 1-6 well,
Port Arthur field, Jefferson County, Texas (BEG - 3/21/86).

No.	86-159	86-160
pH	6.27	6.84
K	292	300
Na	24,670	24,510
Ca	2,070	2,040
Mg	212	211
Fe	118	115
Sr	268	263
Ba	95	43
Li	5.8	5.0
B	45	45
Cl	41,700	41,800
HCO ₃	515	1,001

All aqueous species expressed in mg/L.

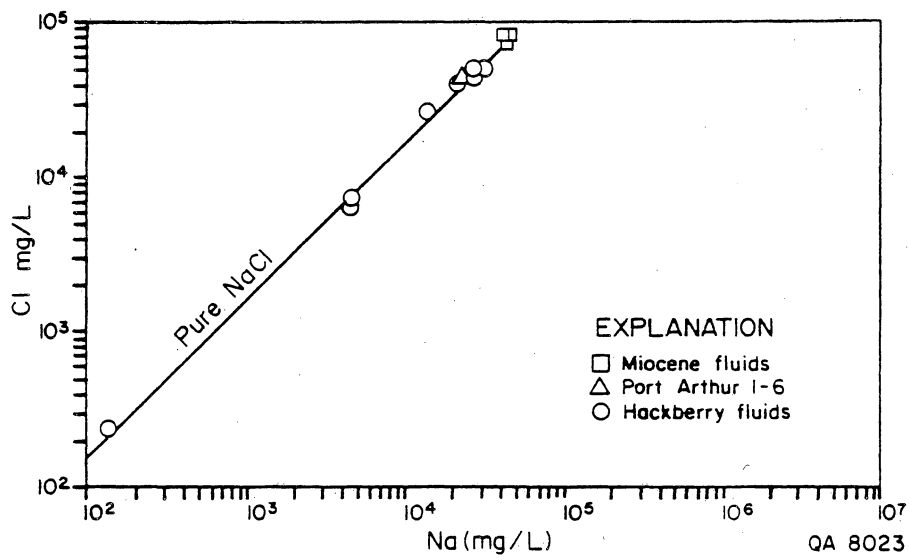


Figure 18. Sodium versus chloride for the Hackberry formation waters in Port Arthur field, Texas, and Miocene formation waters, Cameron Parish, Louisiana.

The chloride content of Miocene waters (75 000 mg/L) is much greater than that of Hackberry waters in the 1-6 well (42.000 mg/L) (figs. 19 and 20). Chloride-bromide ratios show a depletion in bromide and lie in a field between pure salt, meteoric water, and sea water, indicating that the Miocene waters have a large component derived from salt dissolution (fig. 21) (Kharaka and others, 1979), whereas the lower salinities of the Hackberry could result from the abundance of interlaminated shales in the Hackberry turbidites, a source of fresher shale waters released during production-induced pressure drawdowns. The salinity reductions, as already mentioned, could be caused equally by condensation of pure water from gas.

Twenty-four water-composition diagrams were constructed from water-composition data for the Hackberry and Miocene formation fluids in the Port Arthur area (figs. 18 and 22). Miocene fluids are enriched in most inorganic species but depleted in bicarbonate compared with Hackberry fluids (fig. 22). Slight reductions in calcium, iron, bicarbonate, barium, and sulphate in formation waters over the period of production of the 1-6 well (fig. 23) suggest that scaling may be occurring.

THERMODYNAMIC CALCULATIONS

Thermodynamic calculations can be used to study the potential for precipitation of minerals from aqueous solutions (Kharaka and others, 1979). The SOLMNEQ computer program, first published by the U.S. Geological Survey, calculates the equilibrium distribution of inorganic aqueous species of major, minor, and trace cations and anions in formation waters from reported chemical analyses at given temperature, pH, and Eh (optional) conditions over the temperature range 32 to 662°F (0 to 350°C) (Kharaka and Barnes, 1973).

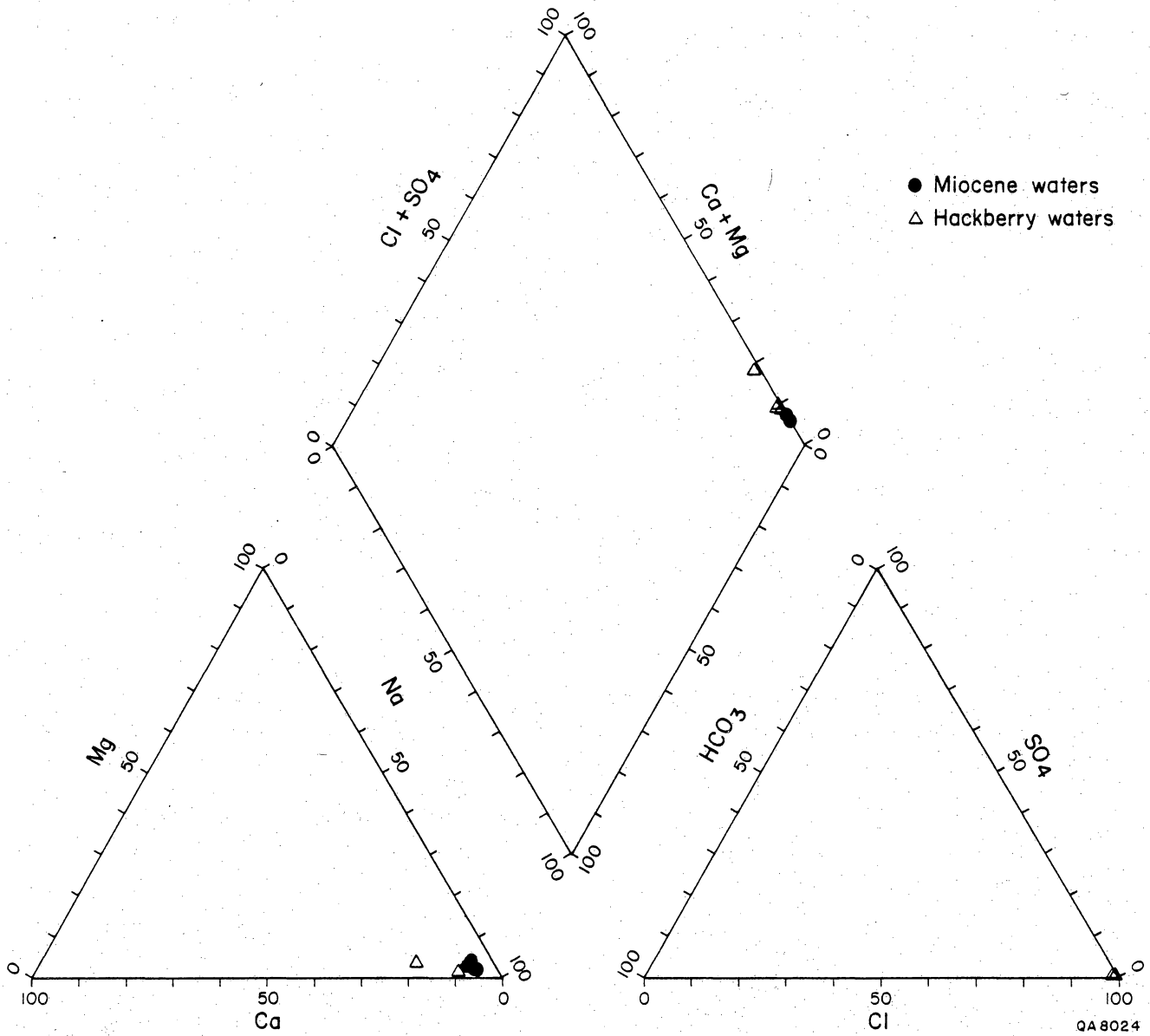


Figure 19. Piper diagram showing compositions of Hackberry and Miocene formation waters.

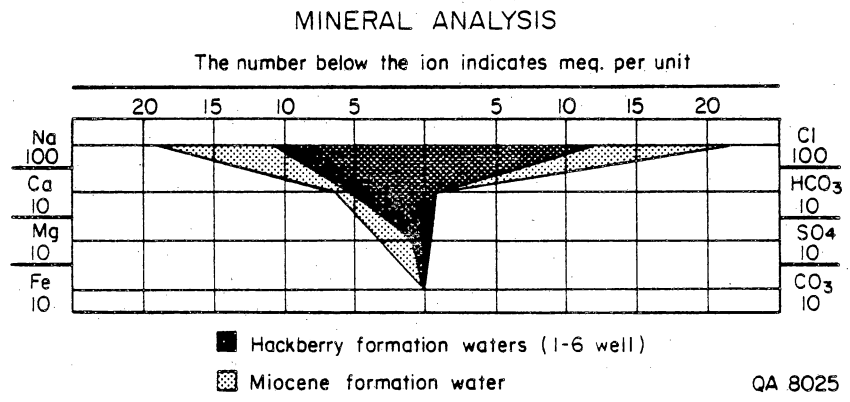


Figure 20. Comparison of major inorganic components of Hackberry and Miocene formation fluids.

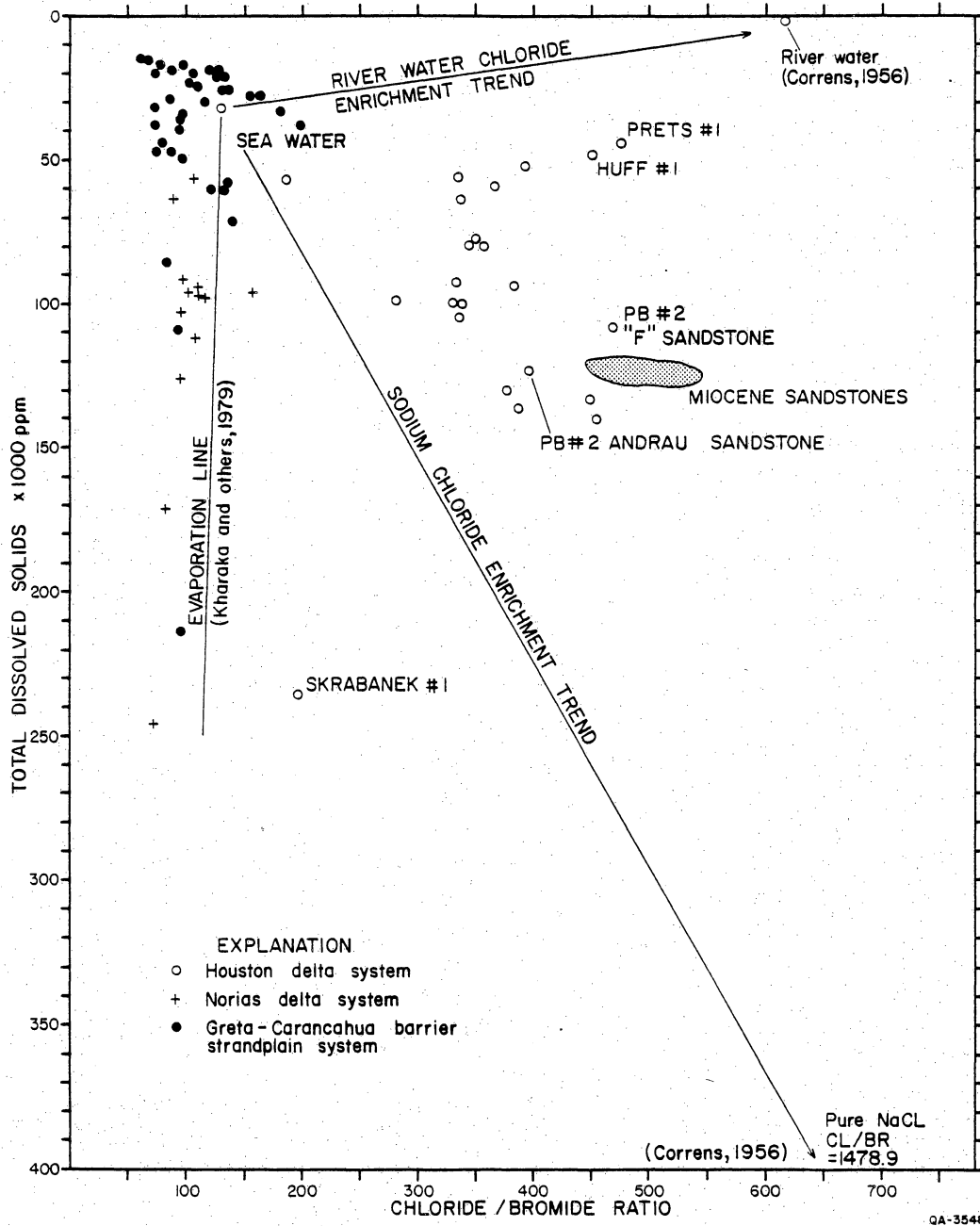


Figure 21. Chloride/bromide ratio versus total dissolved solids for Frio formation waters from the Texas Gulf Coast compared with Miocene formation fluids from Cameron Parish, Louisiana.

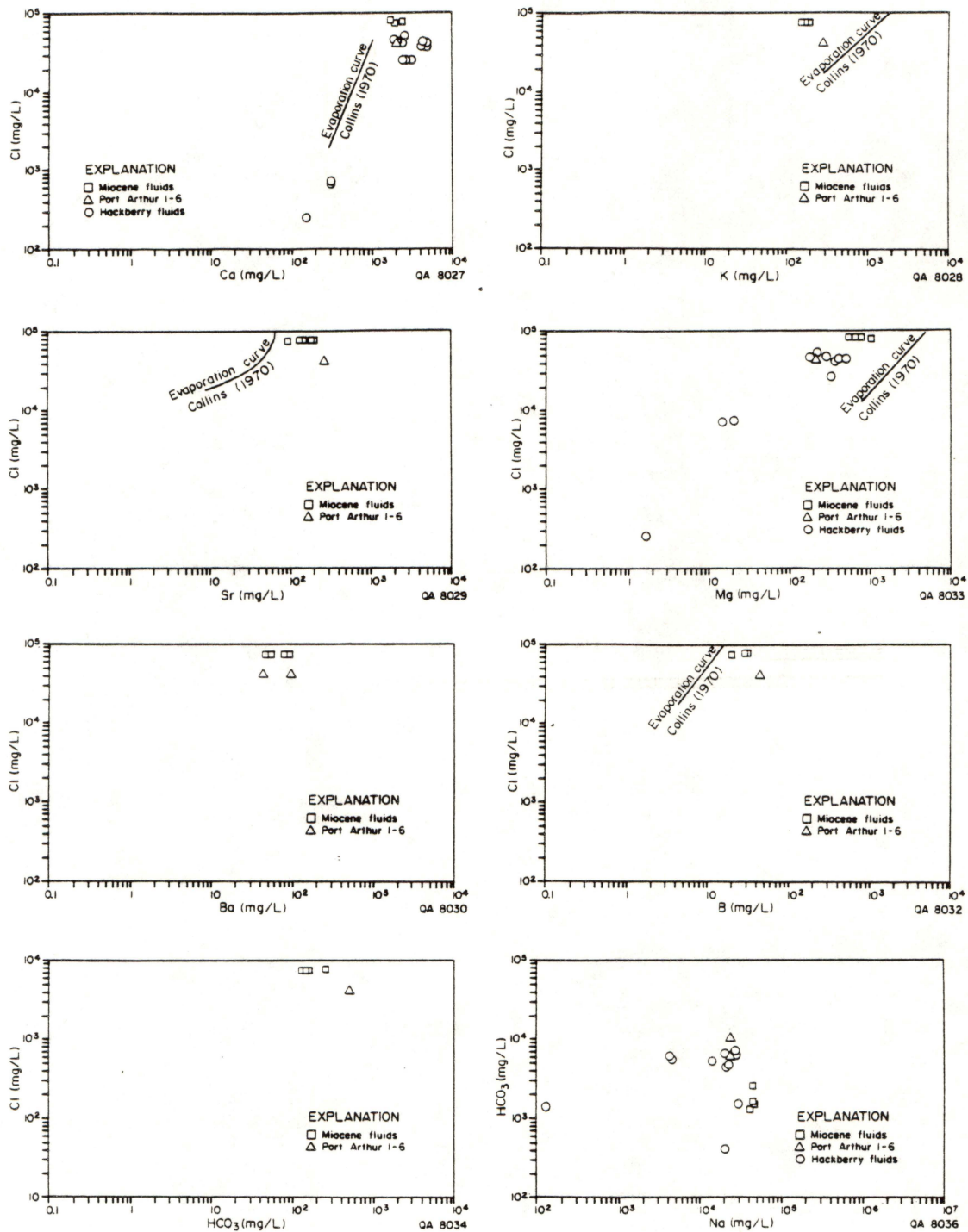


Figure 22. Calcium, potassium, strontium, magnesium, barium, boron, and bicarbonate versus chloride and sodium versus bicarbonate for the Hackberry formation waters in Port Arthur field, Texas, and Miocene formation waters, Cameron Parish, Louisiana.

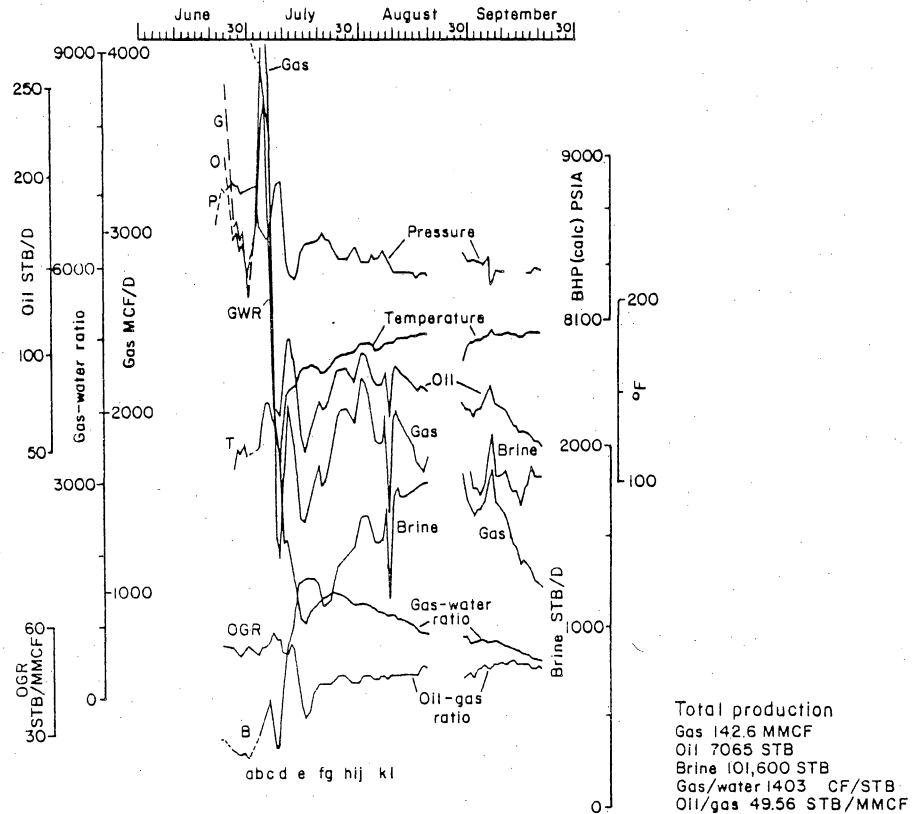


Figure 23a. Variation of pressure, temperature, oil, gas, brine, gas/brine ratio, and oil/gas ratio of formation waters versus time for the 1-6 well, Port Arthur field, Jefferson County, Texas.

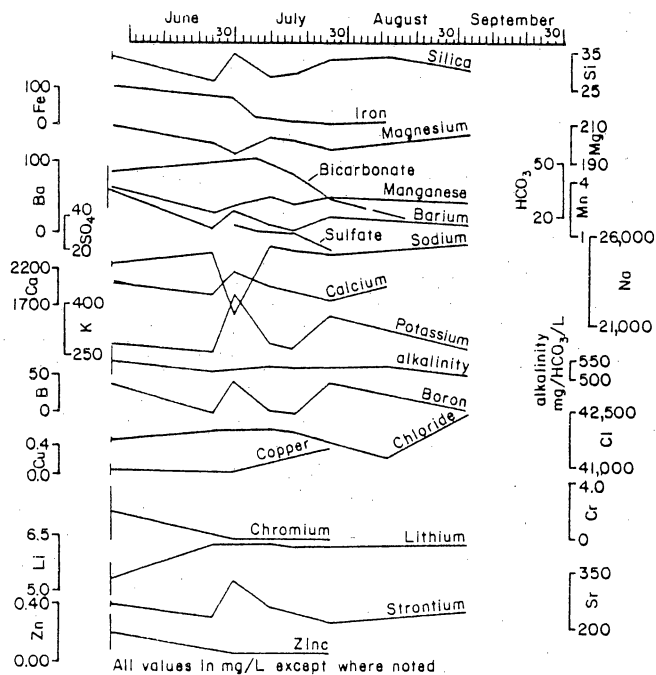


Figure 23b. Variation of inorganic components of formation waters versus time for the 1-6 well, Port Arthur field, Jefferson County, Texas.

To determine the departure from equilibrium of waters with respect to the suite of minerals, SOLMNEQ computes the Gibbs free-energy difference (δG_{diff}) between the actual and equilibrium states from the following equation (Kharaka and others, 1979):

$$\delta G_{diff}(\text{Kcal}) = RT \ln(AP/K)$$

where

- R = gas constant
- T = temperature
- AP = activity product for the dissolution of the given mineral
- K = equilibrium constant of the given mineral

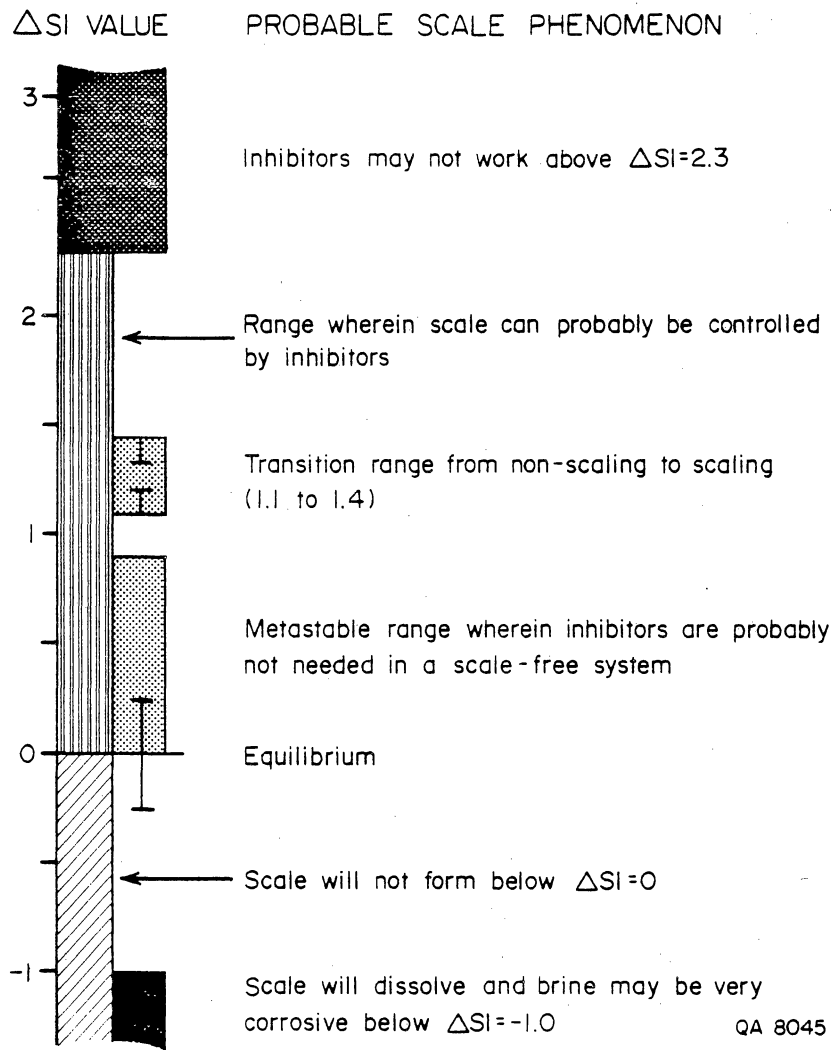
A mineral will precipitate only if the value of its δG_{diff} is greater than zero (Kharaka and others, 1979), but it is possible for a given solution to be supersaturated (unstable but permanent condition) with respect to a mineral by a number of kilocalories without precipitation (Barnes and Clarke, 1969). The amount of precipitate formed is not computed by SOLMNEQ but depends on the instantaneous concentration of solutes, which may change with precipitation and dissolution of minerals and rates of various reactions and fluxes of reactants (Kharaka and others, 1979). The δG_{diff} between actual and equilibrium states is used to demonstrate oversaturation of minerals in formation waters.

The saturation index is defined by Kharaka and Barnes (1973) as:

$$SI = \text{Log}(AP/KT)$$

The saturation indices are plotted against different temperatures and pH values for Hackberry and Miocene waters and can be compared with the SI index defined by Tomson and O'Day (1987) (table 5).

Table 5. Scale of approximate saturation index values (Tomson and O'Day, 1987).



The main difference between the BEG SOLMNEQ version and that of the U.S. Geological Survey is that an extensive compilation of borate minerals and aqueous molecules (Bassett, 1976, 1980) has been added to the BEG SOLMNEQ equation such that the mass balance and charge balance iterations include the boron species (Fisher and Ozment, 1984). In addition, log (KT) values for many minerals and ions have been revised and the acetate molecule and anion have been added (Fisher and Ozment, 1984).

The SOLMNEQ program will compute the Eh of a sample at the desired temperature, but these computations have been kept to a minimum because Barnes and Clarke (1969) showed that the measured Eh is qualitatively related only to the concentration of iron. Large changes in iron content are often unrelated to other formation-water composition changes in co-production wells (Light and D'Attilio, 1985).

Computational Uncertainties

Kharaka and Barnes (1973) outlined uncertainties involved in computations carried out by the SOLMNEQ program. Different methods of sampling, treatment, and analyses of formation waters will cause uncertainties in the final calculated equilibrium constants (Chave, 1960; Rainwater and Thatcher, 1960; White, 1965). Many chemical analyses are limited to major cations and anions (Kharaka and Barnes, 1973), as is the case with data on Miocene formation waters used in this report (Collins, 1970). BEG analytical precision for major anions and cations on the inductively coupled plasma atomic emission spectrometer is 2 percent.

The rate and reversibility of reactions control the uncertainty in thermodynamic functions, and less error is to be expected where a phase reacts more rapidly, completely, or reversibly (Kharaka and Barnes, 1973). The quality of the compilations of equilibrium constants (K) is controlled by the amount and quality of

thermodynamic and other data available in the literature, but the BEG SOLMNEQ program contains extensive revisions from recently published data (Fisher and Ozment, 1984).

A major limitation of many chemical analyses of subsurface water samples is extrapolation of determined pH to the in situ pH (Kharaka and Barnes, 1973). Precipitation of solid phases, variation of partial pressures of dissolved gases, and reactions of aqueous species produced by changes in temperature and pressure of the sample will change the pH of the sample (Kharaka and Barnes, 1973). A critical factor is the change in pH with depth, because as water is lifted to the surface, the drop in pressure results in carbon dioxide exsolving, reducing the acidity of the solution. Kharaka and others (1979) have demonstrated by modified SOLMNEQ equations and experiments adding carbon dioxide to solutions from reported gas analyses that in situ pH values computed for geopressured formation waters are greater than 2 pH units lower than measured pH values. The in situ pH at the Port Arthur field was estimated by computing the pH at which calcite would be in equilibrium with the water at formation temperature (R. S. Fisher, personal communication, 1987). The SOLMNEQ-calculated pH had to be reduced by about 1.3 units, to 5.25, before calcite was in equilibrium with the fluid (fig. 24). Activity coefficients of all neutral species are assumed equal to activity coefficients of dissolved CO_2 in NaCl solutions (Kharaka and Barnes, 1973). SOLMNEQ computes γ_{CO_2} at the temperature and ionic strength (up to 3 molal) of the solution by linear interpolation of γ_{CO_2} values as a function of temperature and ionic strength of an equivalent solution (Kharaka and Barnes, 1973). Errors due to limiting minerals to end-member compositions and from assumptions in calculating activity coefficients of aqueous species are minor compared with those given above (Kharaka and Barnes, 1973).

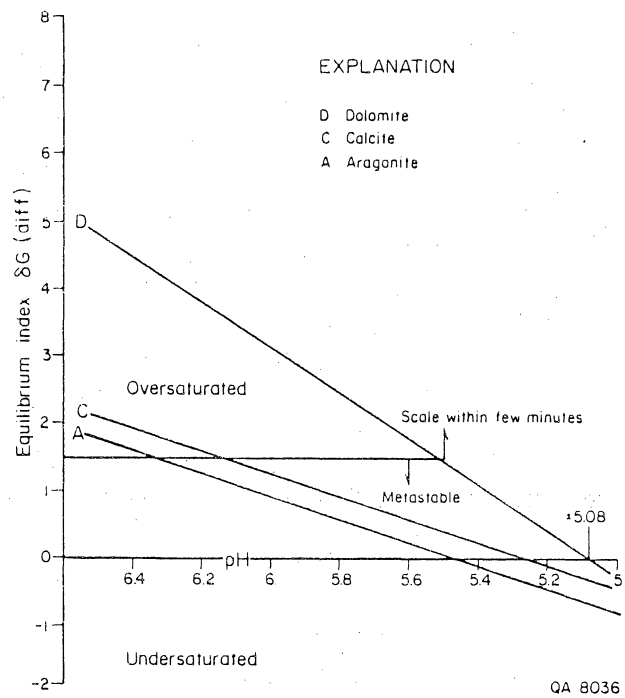


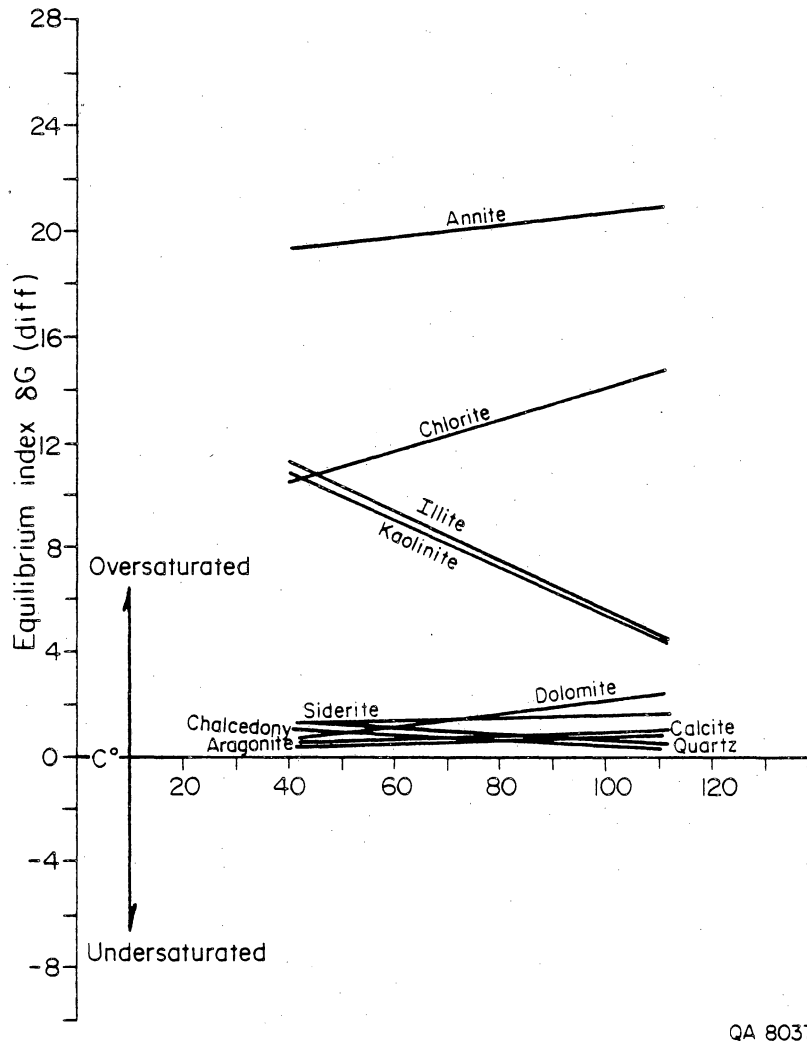
Figure 24. Gibbs free energy difference (δG_{diff}) of carbonates versus pH in Hackberry formation waters from the 1-6 well, Port Arthur field, at formation temperature (110.6°C , 231°F).

SOLMNEQ Computations

Using formation-water analyses, 25 SOLMNEQ solution-mineral equilibrium programs for average Hackberry and Miocene formation waters (tables 3 and 4) were run at reservoir separator 106°F (41.1°C) and Miocene disposal sand 144°F (62.2°C) temperatures, at measured pH (6.55), and at an estimated minimum pH (5.07) at which dolomite is in equilibrium with the fluid (fig. 24). Carbonates, barite, silica (as quartz), and clays are all oversaturated at measured pH (6.55) over a wide temperature range (fig. 25) and at separator temperature 106°F (41.1°C) over a wide pH range in the Hackberry formation waters (fig. 26). Porosity loss in disposal sandstones due to the precipitation of aluminosilicates is probably insignificant because it is a very slow process controlled by kinetic factors (Rimstidt and Barnes, 1978). At separator temperatures 106°F (41.1°C), carbonates (including siderite) become undersaturated at pH values less than 5.3 but are oversaturated at the measured pH (fig. 27).

Porosity loss from precipitation of minerals depends on the chemical composition of the water at the time of injection and the amount of mixing between the injected and formation waters (Kharaka and others, 1979). Miocene formation waters are depleted in bicarbonate compared with Hackberry fluids (fig. 22), and this difference results in decreased oversaturation of carbonates with increased addition of Hackberry waters to Miocene waters.

The result of mixing of varying proportions of Hackberry formation waters at separator temperature 106°F (41.1°C) with Miocene formation water at disposal reservoir temperature 144°F (62.2°C) was investigated (table 6). Under most circumstances the fluids are oversaturated in carbonates, especially siderite and barite, and lie within the metastable field (Tomson, 1983), except when Miocene fluids exceed 90 percent of the total (fig. 27). This indicates that scaling from Hackberry formation fluids may be a problem in the disposal sand if inhibitors are not used, but



QA 8037

Figure 25. Gibbs free energy difference (δG_{diff}) of silica, clays, and carbonates versus temperature at measured pH (6.55) in Hackberry formation waters from the 1-6 well, Port Arthur field.

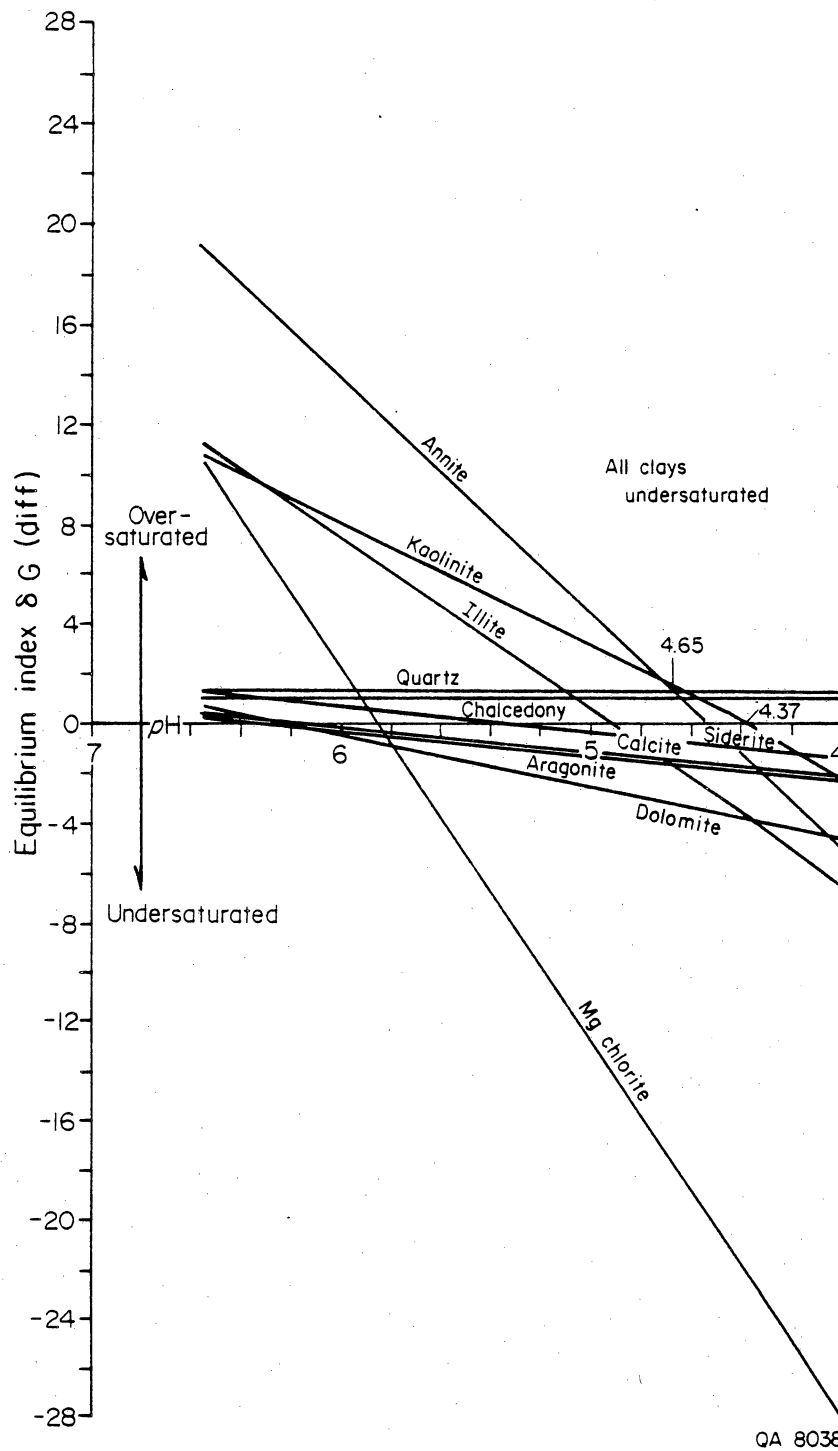


Figure 26. Gibbs free energy difference (δG_{diff}) of silica, clays, and carbonates versus pH at separator temperature (41.1°C, 106°F) in Hackberry formation waters from the 1-6 well, Port Arthur field.

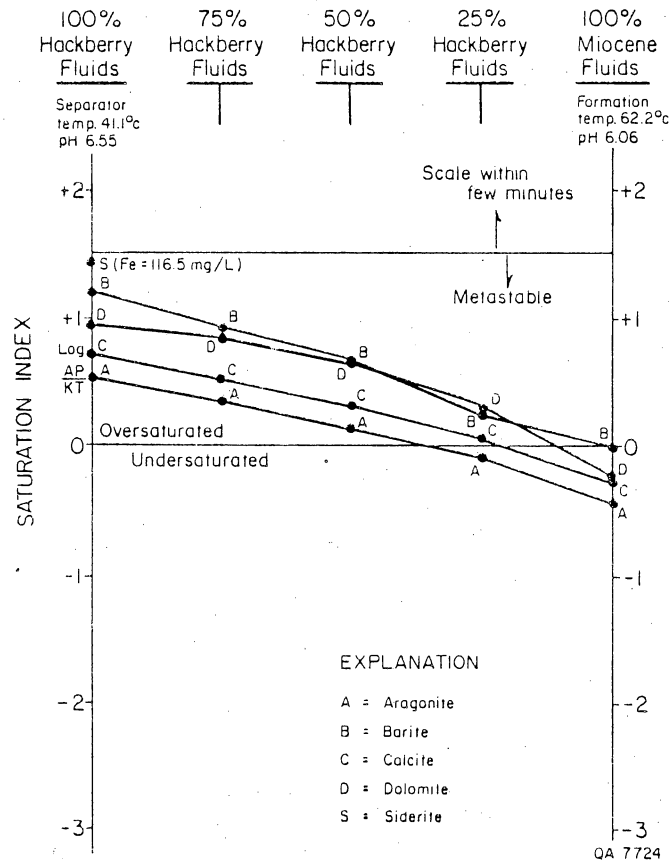


Figure 27. Saturation index of carbonates and barite versus different mixes of Hackberry and Miocene formation waters, Port Arthur field.

Table 6. Saturation indices of combinations of Hackberry and Miocene formation waters, Port Arthur field.

	Test 7 100% Hackberry	Test 14 75% Hackberry	Test 15 50% Hackberry	Test 16 25% Hackberry	Test 10 100% Miocene
Temp. (sep.)	41.1°C	46.38°C	51.65°C	56.925°C	62.2°C
pH	6.55	6.4275	6.305	6.1825	6.06
Den.	1.05	1.06	1.07	1.08	1.09
Aragonite	0.5297	0.3502	0.1493	-0.0898	-0.4299
Barite	1.1967	0.9398	0.6530	0.2562	0
Calcite	0.7094	0.5302	0.3290	0.0889	-0.02518
Dolomite	0.9388	0.8482	0.6416	0.3108	-0.2445
Siderite	1.4193				

much of the range covered by the saturation indices lies within that in which inhibitors are probably not needed in a scale-free system (table 5) (Tomson and O'Day, 1987). Barite remains oversaturated under all conditions tested but has not been seen in scale present in surface equipment at the 1-6 well (M. Tomson, personal communication, 1987). The high concentration of barite in the produced waters may result from contamination by drilling fluids trapped behind casing, although the low barium concentrations in the Northeast Hitchcock field indicate that this has not occurred there. Barite may be scaling in the formation or in the tubing near the perforations where a large pressure decline would lead to its precipitation. Barite was found to be supersaturated in geopressured waters at surface temperatures (77°F, 25°C) at the Pleasant Bayou test wells in Brazoria County (Kharaka and others, 1979).

SOLMNEQ data suggests that barite and carbonates are oversaturated in the Hackberry formation waters, and these computations are consistent with the interpretation that the declines in iron, bicarbonate, barium, and sulphate during production of the 1-6 well are a result of minor scaling.

DIAGENETIC SEQUENCE

Gold (1984, 1987) studied the diagenesis of Miocene sandstones in Louisiana. He states that detrital quartz has not substantially reacted with pore fluids at depths shallower than 20,100 ft (6,090 m) (302°F, 150°C), although some minor pressure solution has occurred.

Above 10,000 ft (3,050 m) in Miocene sandstones, feldspar concentrations are fairly constant, but potassium feldspars disappear below 15,750 ft (4,800 m) at (257°F, 125°C) and plagioclase dissolves between 11,800 ft and 16,400 ft (3,600 and 5,000 m) at temperatures in excess of (266°F, 130°C) (Gold, 1987). Major albitization

of plagioclase occurs between 11.800 ft and 16.400 ft (3.600 and 5.000 m) but continues to the limit of sample control at 19.700 ft (6.000 m) (Gold, 1987).

Below 10.000 ft (3.050 m) major pore cements in Miocene sandstones are quartz, calcite, and kaolinite, and there are small amounts of chlorite, albite and K-feldspar overgrowths, dolomite, and ankerite (Gold, 1984). Only small amounts of calcite and kaolinite cement are to be expected in Miocene sandstones above 10.000 ft (3.050 m) (Gold, 1984), so they should pose little problem to the disposal of fluids at these and shallower levels.

CONCLUSIONS

SOLMNEQ data suggest that barite and carbonates are oversaturated in the Hackberry formation waters, and these computations are consistent with the interpretation that the declines in iron, bicarbonate, barium, and sulphate during production of the 1-6 well are a result of minor scaling. Little diagenetic cement is expected above 10.000 ft (3.050 m) in Miocene sandstones and will not affect disposal of fluids into shallower aquifers.

DEPOSITIONAL ENVIRONMENT AND DIAGENETIC HISTORY OF UPPER FRIO SANDSTONES AND THEIR EFFECT ON POROSITY AND PERMEABILITY PRESERVATION IN THE NORTHEAST HITCHCOCK FIELD, GALVESTON COUNTY, TEXAS

by M. P. R. Light

INTRODUCTION

Detailed work has been completed on the core cut in the Frio 'A' sandstone at the Secondary Gas Recovery Delee No. 1 well, Northeast Hitchcock field, Galveston County, Texas. This work has resulted in the identification of a number of trace fossils and sedimentary structures, including the "*Skolithos* assemblage" in the coarse glauconitic sandstones and planolites burrows in the more shaly sediments. The presence of the *Skolithos* assemblage and other structures has substantiated the shallow-marine, tidal, distributary-mouth-bar, and distributary- and tidal-channel depositional environment for most of the major reservoir sands. Several shaly horizons show the characteristics of interdistributary bays, whereas the Frio 'A' is capped by a thin sequence of crevasse splays and washover sands filling a bay formed at the initiation of the transgression that overlapped the Frio in Anahuac times.

Deep Frio Sandstones and Shales

The Oligocene-age Frio Formation has been investigated to a depth of 9,402 ft (2,866 m) in the Delee No. 1 well. Three gas-bearing sandstones were intersected below 9,392 ft (2,863 m), 9,366 ft (2,855 m) and 9,322 ft (2,841 m) and were respectively 10 ft (3 m), 4 ft (1.2 m) and 28 ft (8.5 m) thick. The thin, light-gray sandstone units between 9,402 and 9,322 ft (2,866 and 2,841 m) consist of subangular grains that are well sorted and of fine to very fine grain size. Although abundant calcareous material is present, it appears to be moderately cemented. The presence of glauconite suggests a shallow-marine depositional environment (Selley,

1970). A crude upward-coarsening and increasing-porosity motif shown by the spontaneous potential (SP) logs suggests that these sands are prograding shoreface marine bars.

Dark-gray, indurated shales, which are present at 9,195 ft (2,803 m) at the base of a 100-ft (30-m) core cut in the Delee No. 1 well (fig. 28), contain abundant planolites burrows. Planolites are common in rocks ranging from the Recent to the Precambrian (Chamberlain, 1978). They are characterized by branched or sparsely branched burrows that are circular, elliptical, or lenticular in section and have unlined distinct walls and poorly defined internal structure (Chamberlain, 1978).

The planolites burrows at 9,195 ft (2,803 m) are horizontal, occur in clusters, and overlap parallel to one another consistent with an offshore shelf depositional environment (infralittoral shoreface toe to transition zone 1, fig. 29). This depositional environment extends from depths greater than 33 ft (10 m) to 590 ft (180 m) (Chamberlain, 1978).

Frio 'A' Reservoir Sandstones

Frio 'A2' unit

The Frio 'A' reservoir in the Delee No. 1 well consists of two sandstone units, a lower sand A2 (9,182 to 9,194.1 ft, 2,799 to 2,802 m depth) and an upper sand A1 (9,151 to 9,179 ft, 2,789 to 2,798 m depth) separated by a 3-ft-thick shale break. The lower sand (A2) is 12.1 ft (3.7 m) thick, whereas the upper sand (A1) is 28 ft (8.5 m) thick. The upper section of the Frio 'A' reservoir was deposited in a transgressive setting and contains three sandy depositional pulses before grading up into the Anahuac shelf shales at 9,101 ft (2,774 m).

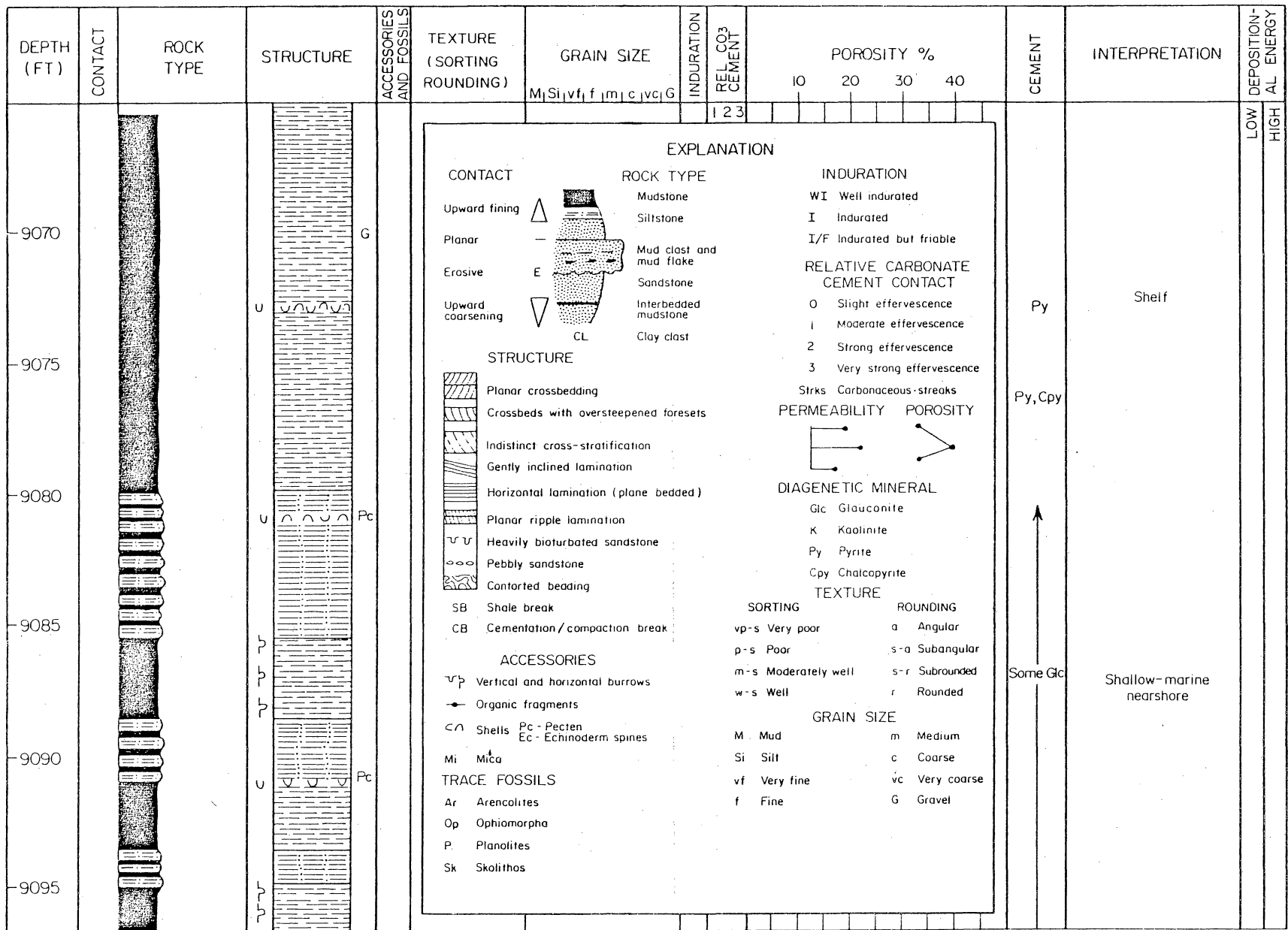


Figure 28. Core log for the Frio 'A' sandstone, Delee No. 1 well, Northeast Hitchcock field, Galveston County. After Tyler and Hahn, 1982.

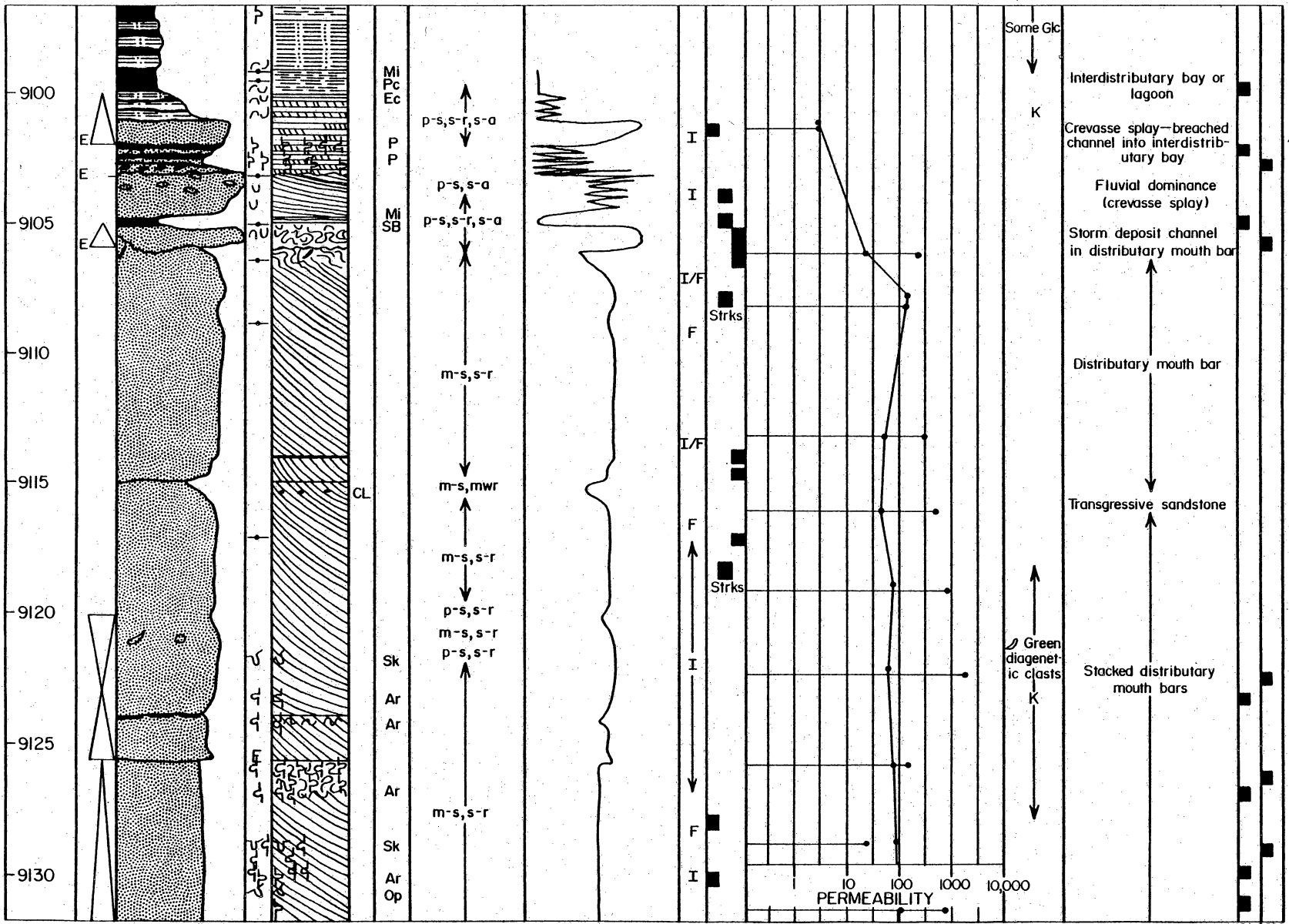
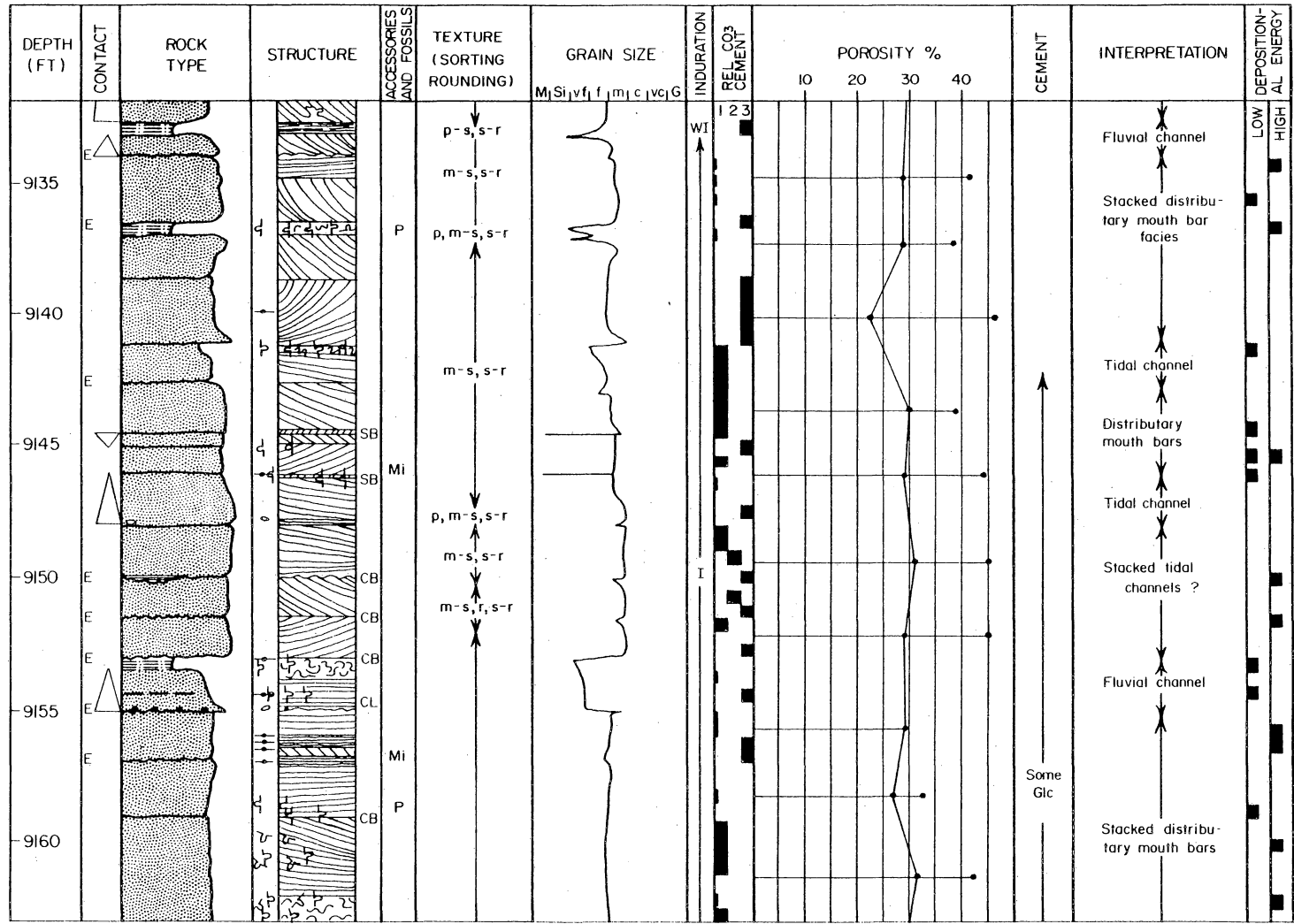


Figure 28 (cont.)



QA 8022

Figure 28 (cont.)

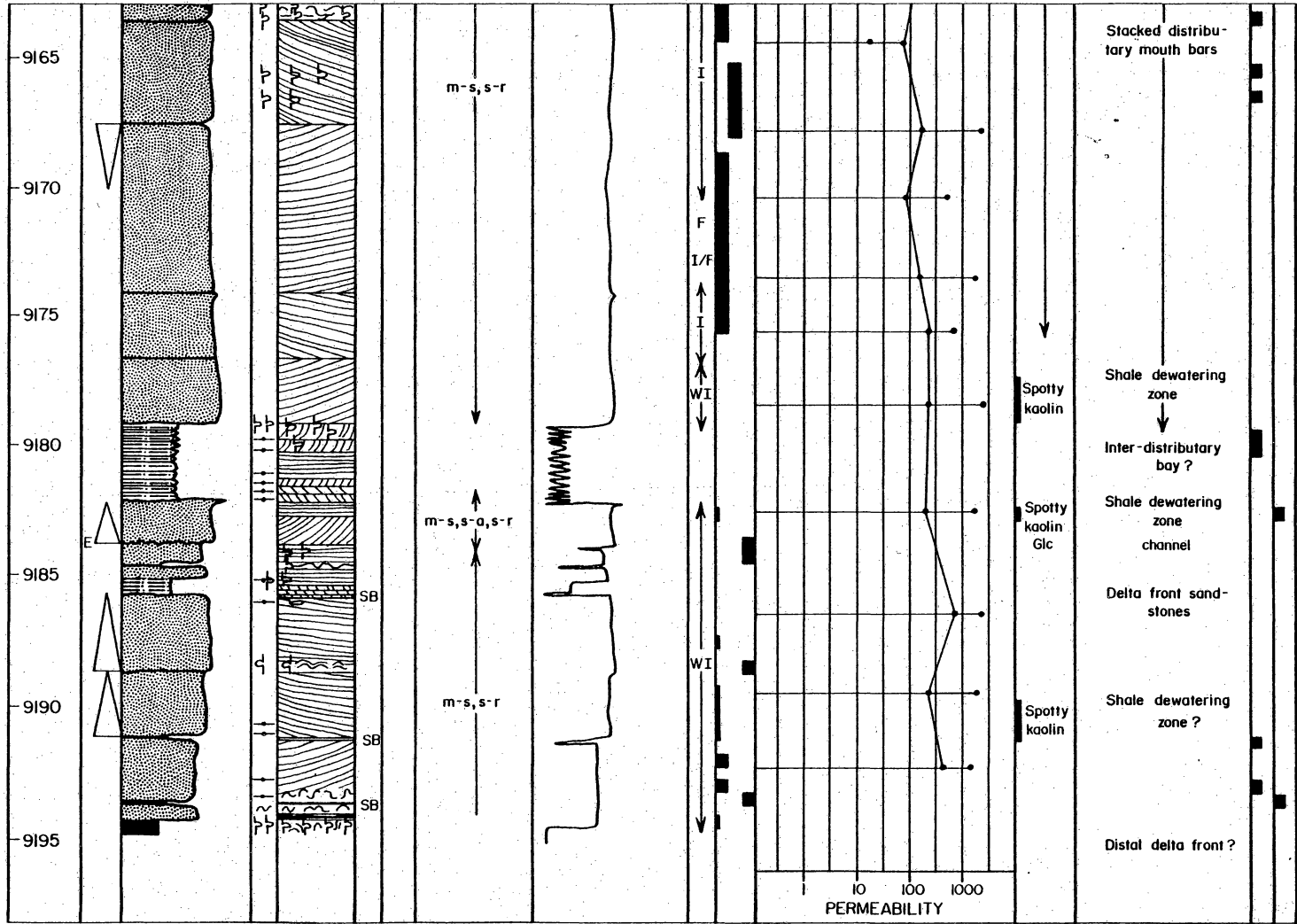
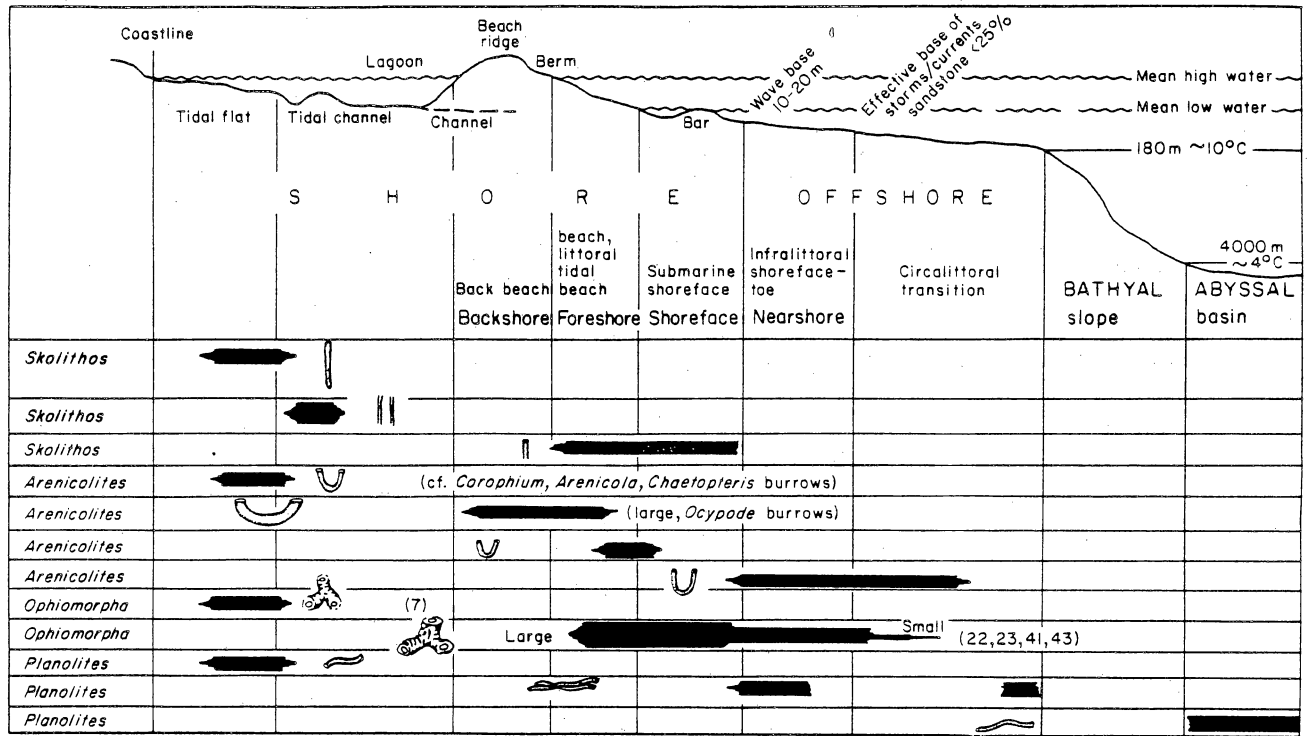


Figure 28 (cont.)



Modified from Chamberlain (1978)

QA 5940

Figure 29. Environmental distribution of selected trace fossils (modified from Chamberlain, 1978).

The lower Frio 'A2' sandstones consist of an upward-coarsening stack of crossbedded, light-gray fine- to medium-grained sandstone beds 1 to 3 ft (0.3 to 0.9 m) thick separated by thin shale breaks. The sandstones are moderately sorted and contain subrounded grains; spotty kaolinite cement occurs near the base above a rippled thin shale break at 9,191 ft (2,801 m) (fig. 30). In general the sandstones in this interval are indurated by diagenetic cementation. Other shale breaks are calcareous (9,185.05 ft, 2,799.6 m; 9184.6 ft, 2,799.5 m, fig. 31), and an erosional surface occurs at 9,183.5 ft (2,799 m) (fig. 32). Shale breaks in deltaic environments are more localized than in deep-marine sedimentation (D. Bebout, personal communication, 1985), which may explain the apparent continuity shown by the Frio 'A' sandstones during production (Anderson and others, 1984).

The Frio 'A2' sandstones tend to be tight at the base (9,194 ft, 2,802 m) but more porous in the upper parts. The Frio 'A2' reservoir has a very abrupt top at 9,182 ft (2,799 m). Thin plane-bedded sandstones near the base of the Frio 'A2' indicate rapid deposition in a high-energy environment in upper flow regime conditions (fig. 33). Flow velocities may have exceeded 2.6 ft/s (80 cm/s) (Blatt and others, 1980). Trough and planar crossbeds present in the rest of the section formed in lower flow regime conditions as dunes and sand waves with flow velocities greater than 1 ft/s (30 cm/s) (Blatt and others, 1980).

Shale breaks within the Frio 'A2' sandstones are overlain by thin carbonaceous layers, some of which are burrowed or contorted and slumped (fig. 33). The slumping occurred penecontemporaneously and is probably a result of high pore pressures that result from the rapid deposition of these sand deposits (Coleman and Prior, 1980).

Irregular layers of calcareous cement occur with increasing abundance toward the top of the Frio 'A' sandstones, where a crossbedded channel unit has cut into the underlying sandstones. Upper flow regime conditions are implied by the coarser

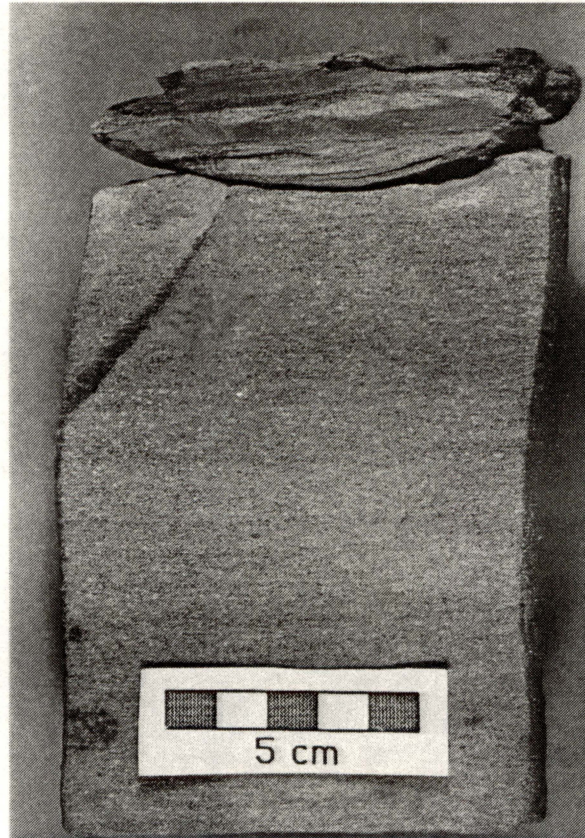


Figure 30. Rippled shale break at 9.191 ft (2.801 m) in the Frio 'A2' sandstone. Northeast Hitchcock field.

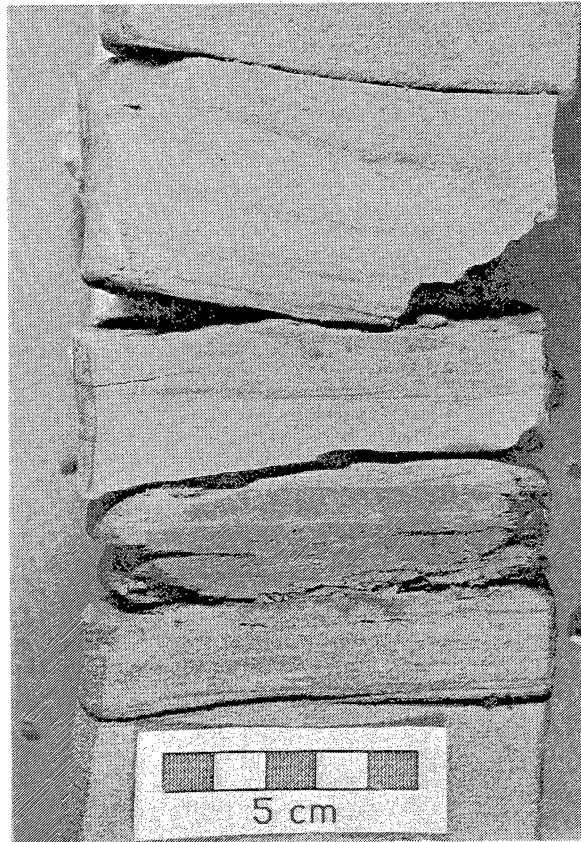


Figure 31. Calcareous shale break at 9,184.6 ft (2,799.5 m) in the Frio 'A2' sandstone, Northeast Hitchcock field.

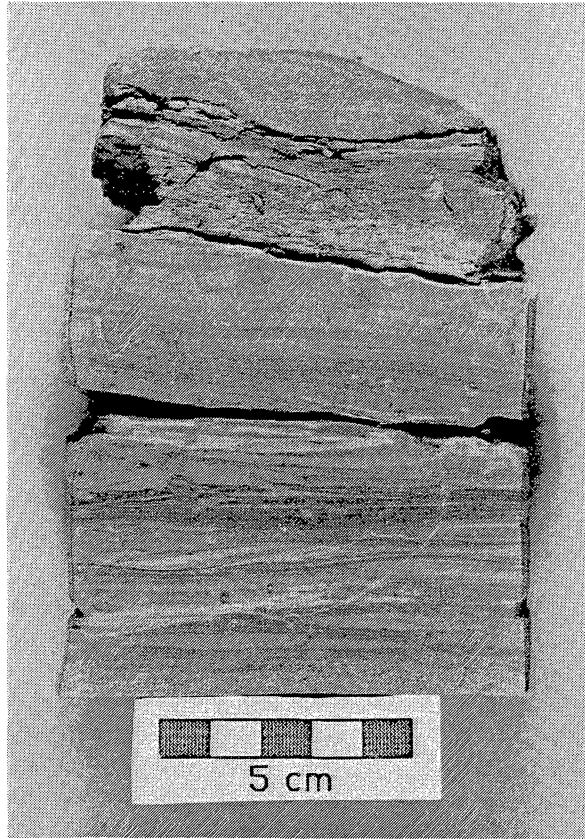


Figure 32. Burrowed calcareous shale break at 9,183.6 ft (2,799 m) in the Frio 'A2' sandstone, Northeast Hitchcock field.

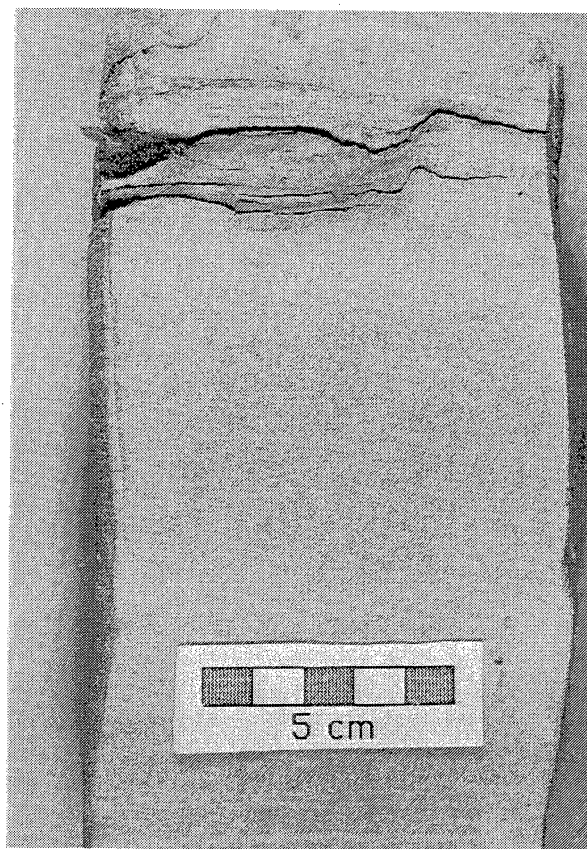


Figure 33. Plane bedded unit at 9,184 ft (2,799 m) near the base of the Frio 'A2' sandstone, indicating rapid deposition in high-energy upper flow regime conditions. Burrowed contorted carbonaceous shale laminations appear in the upper part of the core.

grained, high-energy, plane-bedded top of the channel, although in general the channel is upward fining. This channel appears to represent a distributary cut into delta-front sands because the grains within the channel are less well rounded than in the underlying upward-coarsening unit, which contains glauconite. A burrow, identified as planolites, occurs in a shale break at 9,189.6 ft (2,799.5 m).

Dark-gray calcareous mudstone with fine-grained sandstone to silty sandstone intercalations forms a 3-ft- (0.9-m-) thick layer between 9,182 and 9,179 ft (2,798 and 2,799 m) above the Frio 'A2' reservoir. Several thin, upward-coarsening units are present that grade up from clean mudstone into ripple-laminated sandstone interbedded with lenticular mudstone. Calcareous (shell) fragments are abundant near the base, whereas horizontal planolites burrows occur near the top of the 3-ft- (0.9-m-) thick layer (fig. 33). The clean nature of the mud suggests that it was deposited in a marine environment and is interbedded with upper distal delta-front sandstones (N. Tyler, personal communication, 1985), implying that the underlying distributary channel had shifted elsewhere.

The most abundant single sedimentary structure in interdistributary bay deposits consists of lenticular laminae, the product of reworking and concentration of the coarse fraction by wind-generated waves; parallel-laminated silts and silty clays are also common, as is bioturbation (Coleman and Prior, 1980). Interdistributary bay is the most likely depositional environment for the mudstones between 9,182 and 9,179 ft (2,798 and 2,799 m).

The 3-ft-thick shale layer below 9,179 ft (2,798 m) is surrounded by a zone of highly indurated sandstone that contains spotty patches of authigenic kaolinite cement. This spotty zone is approximately 20 inches (51 cm) thick above the shale (fig. 34, 9,178.3 ft, 2,797.6 m) but is only 4 inches (10 cm) thick below the shale. The development of these indurated zones is the best evidence of the introduction of fluids

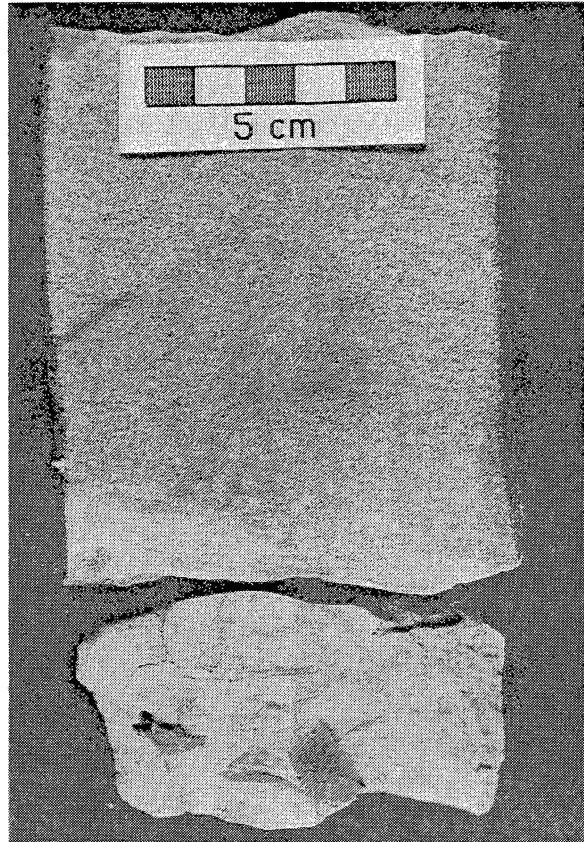


Figure 34. Spotty kaolinite cemented Frio 'A1' sandstone above planolites burrowed mud at 9.178.3 ft (2.797.6 m).

from shales into the sandstones, which resulted in the crystallization of authigenic kaolinite (Light and D'Attilio, 1985), although the induration could also result from lithologic changes. Crystallization of abundant authigenic kaolinite in the sandstones has reduced their reservoir quality (Light and D'Attilio, 1985).

Frio 'A1' Unit

A uniform, fine- to medium-grained crossbedded sandstone that is glauconitic and moderately calcareous forms a 24-ft- (7.3-m-) thick porous unit from 9,179 to 9,157 ft (2,798 to 2,791 m). It has a sharp basal contact on the underlying marine shales. These sandstones are light green or gray-green to tan, moderately to well sorted, and contain subrounded quartz grains. The rounded quartz grains appear to be coated with iron oxide, suggesting a fluvial depositional environment. The 24-ft- (7.3-m-) thick sandstone unit consists of superimposed smaller crossbedded sandstones from 2 to 6.5 ft (0.6 to 1.98 m) thick that are very indurated at the base but less indurated higher up. In the upper section (9,157 to 9,167 ft, 2,791 to 2,794 m) the sandstones are more variable in nature, more closely laminated, and are burrowed at various levels (fig. 35).

Horizontal to inclined burrows also are present in a 4-ft- (1.3-m-) thick crossbedded sandstone below 9,159 ft (2,792 m) and between 9,163.5 and 9,162.2 ft (2,793 and 2,792.6 m), where they crosscut contorted bedding that indicates highly variable energy conditions during sandstone deposition. Penecontemporaneous slumping as a result of high pore pressures developed during rapid deposition of the sand deposit is probably the reason for the contorted bedding (Coleman and Prior, 1980). The upper 1.9 ft (0.58 m) of the 4-ft- (1.3-m-) thick sandstone below 9,159 ft (2,791.7 m) is well laminated and calcareous and contains small-scale crossbeds interbedded with plane-bedded units, indicating a high-energy depositional environment.

Carbonaceous material and mica are common in this zone.

The poorly winnowed sandstones would thus appear to be the more fluviually dominated part of a distributary-mouth-bar deposit, where large amounts of transported organic debris and mica are common in the upper sections (Coleman and Prior, 1980). This is consistent with an upward decrease in permeability and porosity shown by these sandstones, a trend opposite to that normally shown by bar sandstones (Selley, 1979). The highest permeability appears to occur within the spotty kaolinite-cemented zone directly above the basal shale. The less porous and permeable zones are confined to the more laminated and burrowed upper units.

The distributary-mouth-bar sandstones are erosively overlain by medium-grained, moderately sorted sandstones (9.157 to 9.159 ft. 2.791 to 2.791.7 m) that contain subrounded grains. A zone at 9.159 ft (2.792 m) at the base of a 2.6-ft- (0.8-m-) thick sandstone is characterized by low porosity and permeability and contains horizontal planolites burrows, implying an infralittoral to transition zone 1 depositional environment (fig. 35) (Chamberlain, 1978). Horizontal burrows occur within a 4-ft- (1.2-m-) thick crossbedded unit at 9.156.6 ft (2.794 m), again suggesting a low-energy depositional environment.

The distributary-mouth-bar and marine sandstones are overlain by a 2.5-ft- (0.76-m-) thick, upper fine- to medium-grained light-green to tan sandstone. This sandstone is indurated and calcareous at the base (9.155.1 ft. 2.790.5 m) (fig. 36), where it has cut erosively into the underlying units. It grades up into fine-grained sandstones interbedded with silty shales at the top at 9.153 ft (2.790 m). A lag conglomerate consisting of green shale clasts is present near the erosive base. Poorly winnowed calcareous streaks occur within this layer, and horizontal burrows suggest low-energy conditions of deposition (Selley, 1970). Contorted bedding near the top of this deposit is a result of penecontemporaneous slumping (Coleman and Prior, 1980).

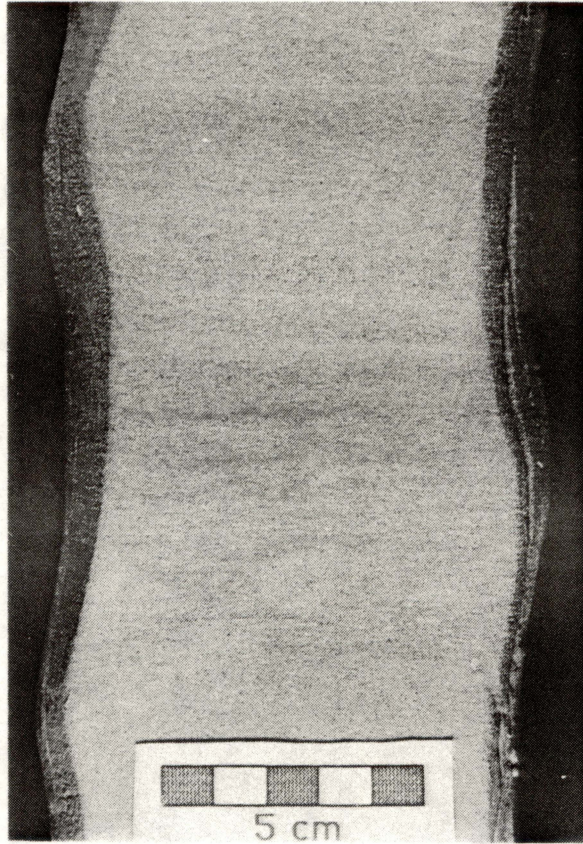


Figure 35. Closely laminated Frio 'A1' sandstone with horizontal planolites burrows between 9.158 and 9.159 ft (2.791.4 and 2.791.7 m).

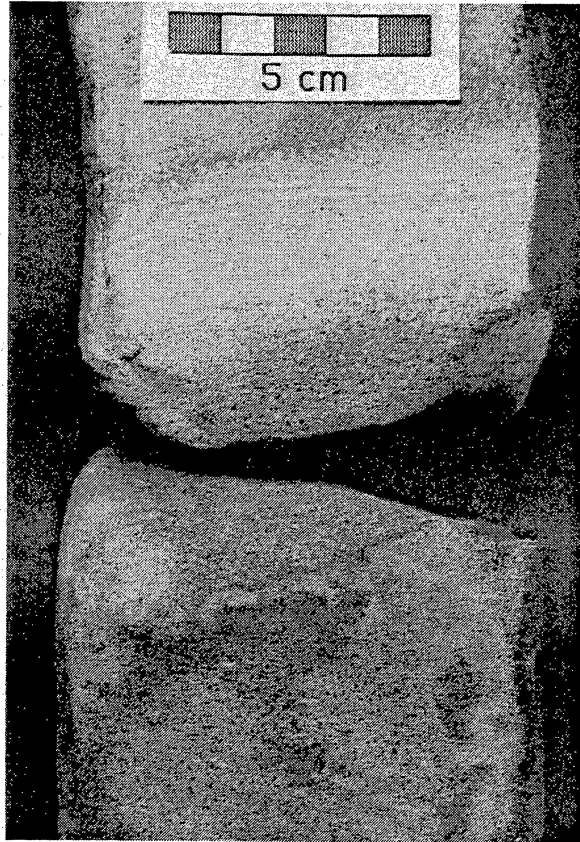


Figure 36. Indurated calcareous Frio 'A1' sandstone overlying an erosional break at 9,155.1 ft (2,790.5 m).

The subrounded grains and moderately sorted nature of these sandstones are similar to those of the underlying stacked distributary-mouth-bar sandstones. The 2.5-ft- (0.76-m-) thick erosively based unit above 9,155.1 ft. (2,790.5 m) appears to be a distributary channel that has cut through its own distributary-mouth-bar system.

Three erosively based light-green to tan porous glauconitic sandstones from 1.5 to 2 ft (0.46 to 0.6 m) thick cap the distributary-channel mouth-bar sequence between 9,153 and 9,148 ft (2,790 and 2,288 m). These indurated sandstones are upper medium grained, moderately sorted, and contain rounded to subrounded grains. The sandstones vary from calcareous to very calcareous, and shell fragments occur within coarse grained sandy clasts in the upper unit (9,148 to 9,150 ft; 2,788 to 2,789 m). Erosive contacts between these units are sandstone upon sandstone. The presence of glauconite, lack of carbonaceous material (Selley, 1979), and the more rounded nature of the grains in these sandstones compared with the underlying distributary mouth bars suggest that they are tidal channels that have cut into a distributary-mouth-bar complex. Additional reworking of the sands resulted in a higher degree of rounding, an apparent lack of burrowing, and relatively high permeabilities (fig. 28).

Light-green, weakly laminated, crossbedded, upward-fining channel sandstones lie between 9,148 and 9,146 ft (2,788.3 and 2,787.7 m) (fig. 28). These sandstones are carbonaceous and indurated at the base and are lower coarse to upper medium grained, poorly sorted, and contain elongated shale clasts. The major section of the channel is medium grained, moderately sorted, and contains subrounded grains near the top. Small grains of quartz are better rounded than the larger subangular grains and appear stained by iron oxide, suggesting a fluvial or dune source. The channel sand grades up into an irregular carbonaceous shale break .25 inch (0.63 cm) thick at 9,146 ft (2,788 m) (fig. 28). The highly calcareous nature of the channel sandstones

may have its origin in oyster development in the subtidal lagoonal environment (Embry and others, 1974), which would then be redistributed by fluvial or tidal channels.

A friable, medium-grained, moderately sorted massive to crossbedded sandstone between 9,146 and 9,144.5 ft (2,788 and 2,787 m) forms the base of a sequence of similarly stacked sandstones from 9,146 and 9,106 ft (2,787.7 and 2,775.5 m) (fig. 28). The basal sandstone contains rounded to subrounded grains and mica at the bottom. It is calcareous near the top, and horizontal sand-filled burrows occur in the central section, suggesting a poorly winnowed deltaic depositional environment (Selley, 1979). However, the presence of more rounded grains of quartz suggests marine reworking, and this sandstone is interpreted as a wave reworked distributary-mouth-bar sandstone. A thin planar laminated carbonaceous break at 9,144.5 ft (2,787 m) is overlain by small-scale trough crossbeds (fig. 28).

Indurated, moderately sorted, fine- to medium-grained trough crossbedded sandstones between 9,142.5 and 9,137 ft (2,787 and 2,786.6 m) (fig. 28) vary from calcareous near the base to very calcareous at the top. Grains tend to be subrounded, and the sandstones are porous. The base of this unit (9,142.5 to 9,141 ft; 2,786.6 to 2,786 m) (fig. 28) consists of a lower medium grained sandstone that is upward fining and has an erosive base, indicating that it is a channel. It grades up into a very fine sandstone with horizontal burrows at 9,142.5 ft (2,786.6 m) (fig. 28). Contorted bedding is present at the top, suggesting penecontemporaneous slumping consistent with a steeply dipping shoreface and reworking of the sediments (N. Tyler, personal communication, 1985).

The upward-fining channel sandstone is overlain by two similar sandstone units: the base of the lower sand is coarse (9,141 ft, 2,786 m) and contains small elongated cavities that may have formed from the dissolution of shell or other calcareous fragments. High-angle crossbeds between 9,139.8 and 9,139 ft (2,785.8 and 2,785.6 m)

(fig. 28) indicate a steeply dipping shoreface environment consistent with distributary-mouth-bar deposition (N. Tyler, personal communication, 1985). The basal upward-fining sandstone between 9,142.5 and 9,141 ft (2,786.6 to 2,786 m) may represent a tidal channel that has erosively cut into a distributary-mouth-bar and is overlain by additional distributary-mouth-bar sandstones between 9,141 and 9,137 ft (2,786 and 2,786.6 m).

The upper distributary-mouth-bar units grade up into medium-grained sandstone and are overlain by a .50-inch (1.3-cm) thick, horizontally bedded, fine-grained sandstone at 9,137 ft (2,786.6 m), which was deposited in high-energy upper flow regime conditions (Blatt and others, 1980). This sandstone at 9,137 ft (2,786.6 m) is overlain by a poorly sorted (upper coarse to lower medium grained) sandstone that contains deformed shale clasts in its upper part that suggest penecontemporaneous erosion of soft interdistributary muds during channel switching and incorporation of these materials in the distributary-mouth-bar sandstones.

A second unit of light- to dark-gray carbonaceous upper fine-grained sandstone, .75 inch (1.9 cm) thick has an erosive contact with the underlying layer and contains a basal lag conglomerate of elongated shale clasts. The upper part of this sandstone consists of horizontally laminated to cross-laminated, lower medium-grained sandstones and shales. Conditions of deposition may have ranged from high-energy upper flow regime (fig. 37) to lower flow regime crossbedded sandstones (Blatt and others, 1980). Sand-filled horizontal planolites burrows at 9,136.7 ft (2,785 m) (fig. 37) crosscut the erosive unit, suggesting that it was deposited in the infralittoral shoreface toe to transition zone (Chamberlain, 1978). These sandstones may represent interdistributary bay sediments because the lower part of a bay fill commonly consists of alternating silts and silty clays that often show silt- and sand-filled burrows (Coleman and Prior, 1980).

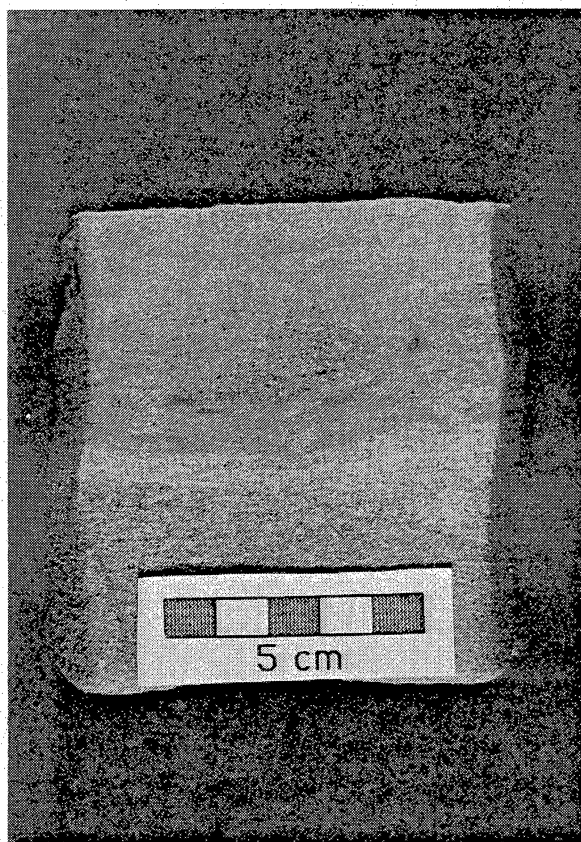


Figure 37. Horizontally laminated Frio 'A1' sandstones and shales at 9,136.7 ft (2,785 m) crosscut by horizontal planolites burrows.

A uniform, medium-grained porous glauconitic sandstone forms a 2.5-ft- (0.76-m-) thick layer between 9.136.5 and 9.134 ft (2.784.8 and 2.784 m) and is crossbedded at the base and plane bedded at the top (fig. 28). The presence of glauconite (Selley, 1978) and low- and high-energy sedimentary structures indicates a shallow-marine (littoral?) environment. This sand is overlain by a medium to very fine grained, poorly sorted, upward-fining channel sandstone that has cut erosively into the underlying unit. The upper part of the channel sandstone is well indurated and consists of a poorly sorted, subhorizontal, plane-bedded, calcareous silty shale at 9.132.7 ft (2.783.7 m) (fig. 28). The shale shows no burrowing, which suggests that it represents a mud flat developed over a fluvial channel (N. Tyler, personal communication, 1985) that has cut into its own distributary mouth bar. Sediments are better sorted in the mouth bar due to marine reworking.

A fairly continuous medium-grained sandstone sequence lies between 9.132.7 and 9.106 ft (2.783.7 and 2.775.5 m). These massive, homogeneous, glauconitic sandstones are light gray to greenish gray to tan and range from lower medium grained at the base to upper medium to coarse grained at the top. They tend to be friable, well sorted, very calcareous, weakly to moderately cemented, and to contain subrounded grains (fig. 28).

A stacked succession of thin, blocky, glauconitic sandstones from 1.5 to 9 ft (0.46 to 2.74 m) in thickness shows a number of very thin shale or carbonaceous breaks and sudden changes in grain size. A medium-grained sandstone at the base of the lower unit (9.132.3 ft, 2.783.6 m) is moderately sorted, crossbedded, and slightly calcareous, and load casts are developed above a thin (1.5 inch, 3.8 cm) silty shale layer. Load casts are produced by load deformation of the underlying hydroplastic mud and suggest very fast rates of deposition of the overlying unit (Pettijohn and Potter, 1964; Blatt and others, 1980.).

The basal sandstone at 9.132.3 ft (2.783.6 m) is indurated to friable, contains subrounded grains, and appears finer grained than the superposed units. Both horizontal and subvertical burrows which are present in the center of the sandstone layer at 9.128.5 to 9.131 ft (2.782.4 to 2.783 m) (fig. 38), are indicative of variable (high-low) depositional energy conditions (Howard, 1975). Horizontal burrows and convoluted laminations are present in the upper 1.5 ft (0.46 m) (at 9.125.5 to 9.127 ft, 2.781 to 2.782 m) (fig. 28), indicating a low-energy, subaqueous depositional environment (N. Tyler, personal communication, 1985), probably on a distal (distributary-mouth?) bar. This zone also contains abundant authigenic kaolinite.

A moderately sorted channel sandstone 1.6 ft (0.49 m) thick (at 9.125.5 to 9.123.7 ft; 2.782.5 to 2.781 m) has erosively cut into the underlying, thin, glauconitic sandstones. The base of this unit is upper coarse grained and grades up into an upper fine-grained sandstone with horizontal burrows and contorted laminations. The tidally dominated depositional environment of the channel sandstone is similar to the underlying bar sandstones, including the presence of the *Skolithos* association (fig. 39) (Seilacher, 1978), but the tidal-channel sandstone contains a larger percentage of coarse-grained material, suggesting it was sourced from less-winnowed (distributary channel?) sediments.

A homogeneous, upper medium-grained, crossbedded sandstone 9 ft (2.74 m) thick lies between 9.123.8 and 9.114.8 ft (2.781 and 2.778 m). This sandstone is moderately sorted and contains subrounded grains. Carbonaceous streaks occur at 9.118 ft (2.779 m), and horizontal to inclined burrows of the *Skolithos* association are present at the base (fig. 40), indicating a shallow-marine tidal environment (Seilacher, 1978). The sandstone grades from indurated, porous, non-calcareous, and kaolinite cemented at the base to very calcareous but friable at the top. Small rounded or

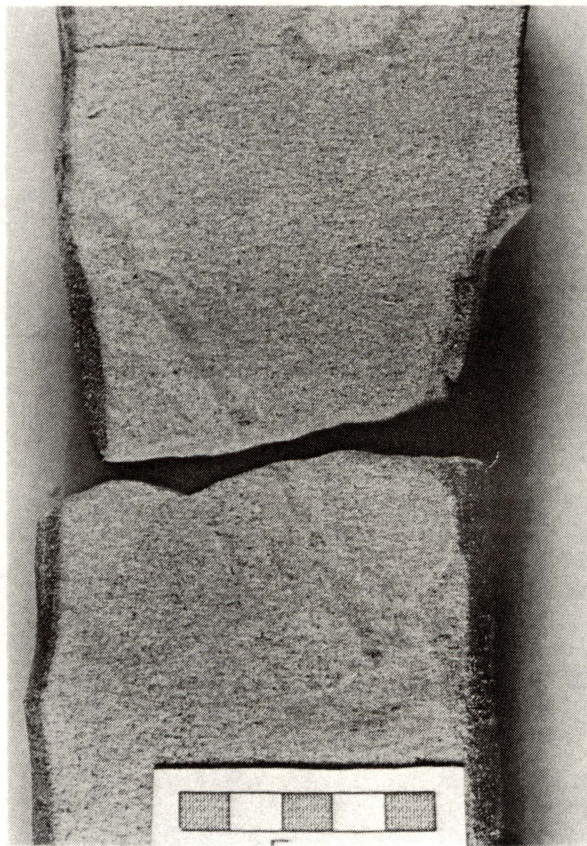


Figure 38. Inclined lined ophiomorpha burrow with horizontal grazing structures at 9,130.6 ft (2,783 m).

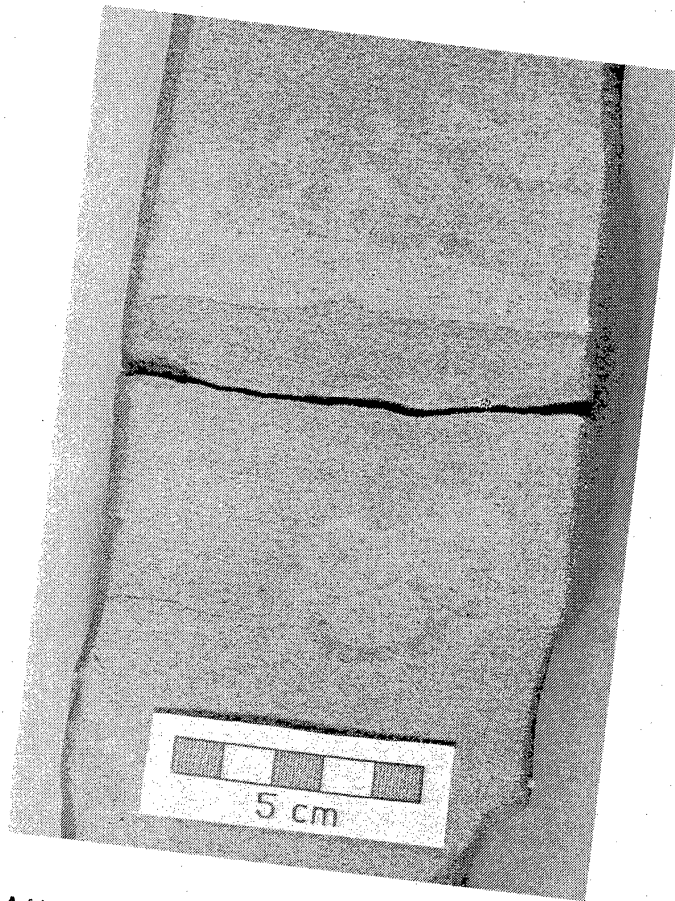


Figure 39. Tidal Frio 'A1' sandstones containing an arenicolites burrow at 9,124.1 ft (2,781 m).



Figure 40. Frio 'A1' sandstone with subvertical lined skolithos burrow at 9.121 ft (2.780 m).

irregular clay clasts are present at 9.121 ft (2.780 m), overlain by faint inclined laminations.

Poorly sorted sandstones occur at 9.120 ft (2.780 m), suggesting that the proximity of a distributary channel that fed sediment into the mouth bar. The oversteepened crossbedding at 9.115.5 ft (2.778.4 m) is probably related to shear stress exerted by aqueous currents (Allen and Banks, 1972; Blatt and others, 1980). The distributary mouth bar appears to have retreated because the top of the unit consists of an upward-fining, mud-clast-bearing, moderately well sorted transgressive sandstone. The transgressive unit grades from upper medium to fine grained at the top and contains moderately well rounded grains. Subrounded grains of the moderately sorted distributary-mouth-bar sandstones were reworked during a marine transgression (Coleman and Prior, 1980; N. Tyler, personal communication, 1985).

A similar 9-ft- (2.7-m-) thick, homogeneous, light-greenish-gray, medium-grained glauconitic sandstone occurs between 9.114.8 and 9.105.8 ft (2.778 and 2.775.5 m). Light-green, subrounded to well-rounded grains of microcline and pink orthoclase feldspar are present at 9.114 ft (2.778 m); most of the grains are subrounded. The base and top of the glauconitic sandstone is very calcareous; carbonaceous streaks occur at 9.108.8 ft (2.776.4 m) where the sandstone varies from indurated to friable. Sandstones within this unit show steeply inclined crossbeds with fine- and coarse-grained crossbedded units. The oversteepening of many of these beds and inclination of a 3-inch- (7.6-cm-) long carbonized twig at the top of the unit (fig. 41) may be related to shear stress exerted by the distributary current flow or compaction (Allen and Banks, 1972; Blatt and others, 1980).

The glauconitic sandstone between 9.114.8 and 9.105.8 ft (2.778 and 2.775.5 m) has the characteristics of a distributary-mouth-bar sandstone but has a poorly defined decrease in permeability from bottom to top. The decrease in permeability is probably



Figure 41. Distributary-mouth-bar Frio 'A1' sandstone containing a steeply inclined carbonized twig erosively overlain by shell hash at 9,105.5 ft (2,775.4 m).

a consequence of an increase in rounded, green clay clasts and scattered argillaceous detritus clearly evident at 9,108 ft (2,776 m). This sandstone represents the terminal distributary-bar sand of the delta, which was retreating at that time (R. A. Morton, personal communication, 1984).

The distributary-mouth-bar complex at 9,105.8 ft (2,775.5 m) is erosively overlain by a 1-ft- (0.3-m-) thick coarse to very coarse, poorly sorted shell hash (fig. 41), which represents a storm deposit (N. Tyler, personal communication, 1986). The hash contains subangular to angular shell fragments, is very thinly laminated (laminations are 1/10 to 1/32 of an inch; 0.08 to 0.25 cm thick), and has contorted bedding, indicating a very high energy depositional environment. The shell hash is overlain by a 2- to 3-inch- (5.1- to 7.6-cm-) thick, finely laminated, greenish-gray to dark-gray carbonaceous mudstone consisting essentially of layered smectite-illite. The mudstone probably represents deposition from storm surge waters ponded behind the distributary mouth bar (Hayes, 1980).

The storm surge complex is succeeded by two (1.6- and 1-ft-, 0.3- and 0.55-m-thick) upward-coarsening sandstones between 9,104.8 and 9,100 ft (2,775 and 2,774 m) (fig. 42). These sands are separated and overlain by laminated shales between 9,101 and 9,100 ft (2,774 and 2,773.7 m). The lower indurated sandstone unit between 9,104.8 and 9,103.2 (2,775 and 2,774.7 m) is poorly sorted, calcareous, and varies in grain size from lower coarse to fine. Clear to milky gray quartz grains, which are subrounded to angular, are arranged in gently inclined beds that contain mica at the base. Fine grained sandstone beds are interbedded with mud and carbonaceous layers and show lenticular to wavy bedding in the lower section; they are interbedded with conglomerates near the top. The poor sorting and upward-coarsening nature suggests that these are crevasse splay deposits.

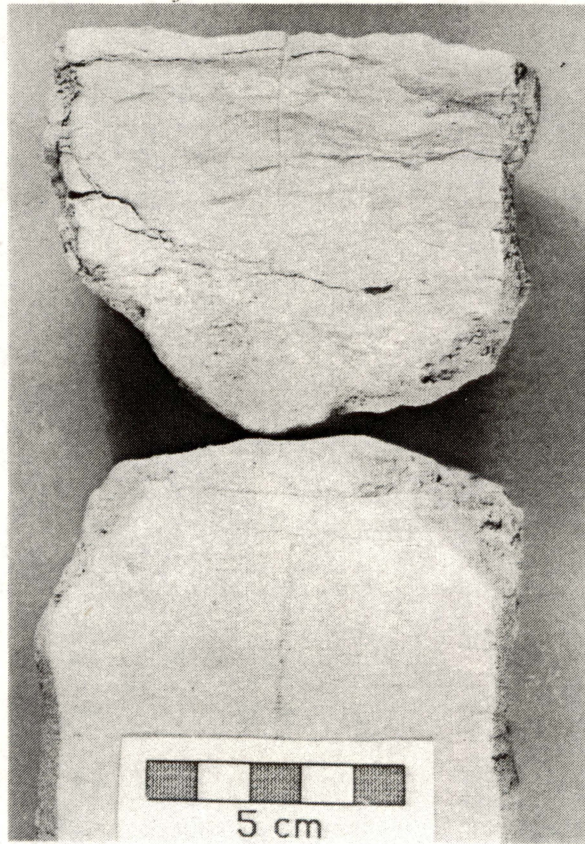


Figure 42. Upper crevasse splay Frio 'A1' sandstone at 9,102 ft (2,774.3 m), which contains gregarious, overlapping horizontal planolites burrows.

A second upward-coarsening crevasse splay sandstone between 9,103.2 and 9,101 ft (2,774.7 and 2,774 m) has erosively cut into the underlying crevasse splay deposits. The lower 1 ft (0.3 m) of this unit consists of a wavy to lenticular bedded mudstone with light-green, silty, sandy, and carbonaceous interbeds. It is highly bioturbated and contains abundant horizontal planolites burrows (fig. 43), indicating periods of very slow sedimentation. Planolites burrows are present in the finer grained deltaic sediments (N. Hyne, personal communication, 1981) and probably occur here in an interdistributary bay or lagoon. The presence of ripped up mud clasts near the base of sandy interbeds, which are often plane bedded (in other places the beds are partly rippled and burrowed), indicates variable energy depositional conditions. Deposition could have occurred by spasmodic current flow through a levee into an interdistributary bay during its early breaching. This unit is erosively overlain by a 1-ft- (0.3-m-) thick, upward-coarsening, medium to very coarse grained, poorly sorted light-gray sandstone. Sand grains are subrounded to subangular in this sandstone, which contains patchy carbonate cement. The sandstone appears to represent the upper, sand-rich distributary bar of a crevasse splay.

The crevasse splay deposits are overlain by highly stratified mudstone interlaminated with rippled, light-green siltstone and very coarse grained sandstone between 9,101 and 9,100.6 ft (2,774 and 2,773.8 m). The mudstones, which consist essentially of dark-green smectite-illite, contain clam shells, fragments of wood, and macerated organic debris. Sandstones contain patchy areas of calcite cement; kaolinized feldspars tend to be white and soft. This shelly mudstone was deposited in a saline to brackish-water swamp of an interdistributary bay or lagoon (N. Tyler, personal communication, 1985). The top of the Frio Formation in Brazoria and Galveston Counties is defined by the T2 marker horizon, which is a diachronous erosive contact.



Figure 43. Horizontal view of a planolites burrow in a carbonaceous Frio 'A1' sandstone at 9.102.5 ft (2.774.5 m).

Trace Fossils in the Frio 'A' Reservoir

Suspension feeders that live on detrital food kept in suspension by high-energy waves and currents develop unbranched vertical or steeply inclined burrows in shallow, turbulent oceanic areas (Frey, 1978; Seilacher, 1978). These shallow-water zones are exposed to storms, low-tide, and sudden changes in temperature and salinity from which the suspension feeders withdraw deeply into the buffering sediment (fig. 29, Seilacher, 1978). In quiet-water deposits, however, where large quantities of organic matter settle, shallow, horizontal, more or less ephemeral burrows and grazing traces of deposit feeders dominate (fig. 22). Gradations between these two extremes may be found in estuaries, lagoons, or shoreface sequences in shallow epeiric seas, and shelf to abyssal areas of continental margins. (Frey, 1978).

Slowly deposited beds on continental shelves are commonly completely reworked by organisms, but the high-energy shore deposits show little reworking (Howard, 1972; Chamberlain, 1978). In the latter deposits the burrows are concentrated in distinct horizons, where they may be densely crowded (Seilacher, 1978).

Spencer (1976) outlined further distinctions between these two contrasted depositional environments from associated rocks and structures. Planolites, small terebellina, and nondescript horizontal burrows characterize the siltstone, shale, and thin sandstones offshore, where bedding is discontinuous, very thin to laminar, wavy, and micro-cross-laminated. Medium-sized vertical burrows, especially arenolites and sparse ophiomorpha, characterize the porous, well-sorted, medium- to thin-bedded sandstones of the foreshore, where horizontal to low-level crossbeds are common, and current and symmetrical ripples are present in only some deposits.

A steeply inclined trace cylindrical fossil is present at 9.130.6 ft (2.783 m) (fig. 38) at the base of an indurated bioturbated zone in the sandstone interval

between 9.131 and 9.126 ft (2783.1 and 2781.6 m). This trace fossil is 0.6 to 0.8 inch (1.5 to 2 cm) wide and more than 4.3 inches (11 cm) long. It has a dark clayey protective lining rimmed by a light-colored diagenetic (kaolinite rich) halo. Unlined, overlapping, elongate, subhorizontal grazing structures (Spreiten structures, Frey, 1978) are present at the base of the trace fossil, which suggests that it is probably an immature *ophiomorpha nodosa* with a well developed basal maze (fig. 38) (Chamberlain, 1978).

Ophiomorpha occur from the Permian to the Holocene and characteristically have cylindrical pipe-shaped burrows from 1.2 to 2 inches (3 to 5 cm) in diameter with a smooth interior and pelleted exterior (Chamberlain, 1978). The center of the trace fossil is frequently left open and later filled passively; complex horizontal burrowing mazes and boxworks often form at the base (Chamberlain, 1978). Longitudinal sections display parallel bands having smooth surfaces toward one another and bumpy surfaces outside (Chamberlain, 1978).

Single, ovoid, clay-lined trace fossils, which vary from 0.8 to 1.2 inches (2 to 3 cm) in diameter, occur at several depths in the Frio 'A1' sandstones: (9.130 ft (2.782.8 m); 9.126.7 ft (2.781.9 m); 9.124.1 ft (2.781 m); and 9.123.2 ft (2.780.7 m). They have the characteristics of arenolites, which occur from the Cambrian to the Holocene (fig. 39; Chamberlain, 1978; N. Tyler, personal communication, 1985). Large arenolites may be recognized only as oval or circular tubes in cross sections, although they occur as simple vertical U-shaped tubes from 0.04 to 0.4 inch (1 to 10 mm) or more in diameter (Chamberlain, 1978).

Two vertical to steeply inclined, cylindrical to slightly curved, clay-lined burrows with tapering ends at 9.128.5 ft (2.782.4 m) and 9.121.5 ft (2.780.3 m) (fig. 40) are enclosed in an olive-green diagenetic halo 0.25 inch thick (0.64 cm). These trace fossils are 0.7 to 0.8 inch (1.8 to 2 cm) wide, have a central gallery that has been

passively filled with sand, and appear to be vertical sections through part of arenolites (U) burrows. The trace fossils present in the Delee No. 1 well represent either vertical sections through the upright parts of an arenolites U, which has the appearance of a skolithos burrow, or particularly large examples of skolithos (Chamberlain, 1978).

The large trace fossils that are present in the sandstone interval between 9.132.7 and 9.106 ft (2.783.7 and 2.775.5 m) have the characteristics of the *Skolithos* association (Seilacher, 1978; Blatt and others, 1980). According to Crimes (1975), this association is characterized by the presence of vertical to steeply inclined skolithos, arenolites, ophiomorpha, diplocraterion, and thalassinoides trace fossils (Crimes, 1975; Seilacher, 1978). However, diplocraterion had an age range that lasted from the Cambrian to the Cretaceous (Chamberlain, 1978), so the Oligocene-age Frio reservoirs should contain a more restricted *Skolithos* assemblage.

The *Skolithos* association indicates a sandy intertidal depositional environment where temperature, salinity, and light change daily, and the bottom is reworked by small waves and tidal currents (Seilacher, 1967; Rhoads, 1975; Blatt and others, 1980). This association is thus relatively restricted geographically and is commonly reworked during transgression and progradation (Chamberlain, 1978). High-energy, sand-rich shorelines have few trace fossils, but the intertidal zone is less physically active and is characterized by an abundance of U-shaped burrows and the presence of protective linings in the burrows (Blatt and others, 1980). In general, vertical and horizontal burrowing indicates high-energy and low-energy subaqueous conditions respectively (fig. 29; Howard, 1975).

The interpretation that the sandstone sequence between 9.132.7 and 9.106 ft (2.783.7 and 2.775.5 m) contains the *Skolithos* association is consistent with the presence of an ophiomorpha and few large arenolites burrows showing well-developed

protective linings. Skolithos and ophiomorpha burrows have thicker, more thickly lined, stronger retaining walls in loose sediments than in coherent sediments (Frey, 1978).

In modern sediments ophiomorpha burrows are constructed by several crustaceans, including the shrimp callianassa (Blatt and others, 1980), and these burrows may be less complex in loose sediments than in coherent sediments (Dorjes and Hertweck, 1975). Furthermore, in sandy littoral sediments, the skolithos association represents a densely crowded but low-diversity trace fossil assemblage (Seilacher, 1978), which is consistent with the low diversity shown by the *Skolithos* association fossils in the Frio 'A1' sandstones. Seilacher (1978) also notes that the mud-pelleted, lined burrows of the callianassid shrimps (ophiomorpha) in marginal facies of late Mesozoic and Cenozoic age are useful in indicating marine or brackish conditions.

The depositional ranges of the trace fossils found in the Frio 'A1' sandstones are shown in fig. 29. (Chamberlain, 1978). Large skolithos and ophiomorpha trace fossils are confined to the tidal channel and beach environments (fig. 29). However, large thick-walled arenolites only exist with the other fossils in a beach environment (fig. 29). This high-energy environment characterized by soft sand would have few trace-fossil burrows. The low-diversity burrows would have thick, strong, protectively lined walls, as is the case of the Frio 'A' sandstones (fig. 29). This zone is also marked by the presence of porous, well-sorted, medium- to thin-bedded, crossbedded sandstones containing vertical arenolites burrows and sparse ophiomorpha; the burrows tend to be concentrated in distinct horizons (Spencer, 1976).

The presence of planolites within silty and shaly horizons is clear evidence that the tidal-beach environment was transgressed on occasion by offshore sediments.

probably a result of avulsion of the fluvial system in the delta, subsidence of the delta lobe, and the formation of an interdistributary bay.

Lined ophiomorpha burrows identified at 9,130.6 ft (2,783 m) (fig. 38) occur in a 2.5-ft- (0.76-m-) thick zone that contains both horizontal and subvertical burrows, indicating highly variable (high-low) depositional energy (Seilacher, 1978). Lined burrows of the callianassid shrimps (ophiomorpha) in marginal facies are useful in indicating marine or brackish conditions (Seilacher, 1978). Brackish to marine waters fill shallow (23 to 33 ft, 7 to 10 m) interdistributary bays that form marginal to major distributary systems in a deltaic environment (Coleman and Prior, 1980). The lined ophiomorpha burrows in the Frio 'A1' sandstone may have formed in a sandy tidal beach facies adjacent to an interdistributary bay.

Certain types of organisms prefer to construct dwelling burrows in well-compacted, muddy sediment, and the presence of a stratum with many of these burrows indicates a period of nondeposition during which the necessary compaction of the sediment could take place (Blatt and others, 1980). Abundant horizontal planolites burrows occur within the silty and shaly layers of a transgressive unit between 9,100.6 and 9,101 ft (2,773.8 and 2,774 m). The planolites burrows are abundant and overlap parallel to one another. These siltstones and shales are characterized by planar ripple-lamination and contorted bedding and contain fragments of wood, macerated organic debris, and clam shells. The depositional environment of this shelly shale was a saline to brackish-water swamp of an interdistributary bay where little sediment was being deposited and compaction could take place (Blatt and others, 1980; N. Tyler, personal communication, 1985.). The planolites burrows suggest, however, water depths of 70 to 590 ft (20 to 180 m) (Chamberlain, 1978), although bay fills in the Mississippi Delta are closer to 60 ft (18.3 m) in thickness (Coleman and Prior, 1980).

General Depositional Environment of the Frio 'A' Reservoir

Coleman and Prior (1980) described the general sequence characteristic of distributary-mouth-bar deposits. The prodelta section consists of fine-grained clay and silt deposits with parallel, organically rich silt layers and distorted laminations alternating with burrowed zones. These grade up into ripple- and lenticular-laminated silts and clays representing the distal-bar deposits. Above the distal-bar deposits are distributary-mouth-bar deposits composed entirely of clean, well-sorted sands forming potential hydrocarbon reservoirs (Selley, 1970). Dip angles rarely exceed 0.5 degrees. Small-scale ripple-laminations, current ripple drift, and a variety of small-scale cross-laminae, low-angle crossbedding, and disturbed laminations are found in these deposits. Mass-movement processes such as small, localized slumps result in distorted laminae. Because of rapid deposition, pore pressures are high within these sands, and a large number of pore fluid escape structures and localized compactional structures are found in these deposits. Near the top of the sequence larger amounts of transported organic material are common within the section (calcareous fragments); mica content is high throughout the entire unit. Early diagenetic pyrite and siderite crystals are characteristically found in the marsh environment.

Extremely fast depositional rates are characteristic of a deltaic sequence. Seaward progradation rates in distributary mouth bars range from in excess of 330 ft (100 m) per year to less than (164 ft) 50 m per year in the Mississippi Delta. Sedimentation rates seaward of the river mouth are extremely high, averaging slightly less than 3 ft (1 m) per year. During high floods, however, accumulations of 10 to 13 ft (3 to 4 m) of sediment over 2 to 4 months have been documented. In adjacent interdistributary bays, accumulation rates rarely exceed 0.7 inch (a few cm) per year, and in some places bay bottoms are eroded. A normal stratigraphic section will generally show thicknesses of approximately 66 ft (20 m), but localized compaction

during deposition may increase this thickness to 230 ft (70 m) (Coleman and Prior, 1980). The Frio 'A' sandstones lie within these thickness limits.

The Frio 'A' sandstones between 9.141 and 9.106 ft (2.786 and 2.775.5 m) have the characteristics of distributary mouth bars. They are generally medium grained, moderately to well sorted, and contain angular to subrounded grains of quartz, feldspar, and volcanic rock fragments. The higher permeability sands are friable and contain thin calcareous streaks and inclined laminations that dip up to 10 degrees or steeper.

The lower permeability parts of the sand units are similar but show more variability in grain size from fine calcareous sandstones having convoluted bedding to coarse grained, erosively based pebbly sandstones. The latter are poorly sorted, have distorted or convoluted bedding, and contain carbonaceous and calcareous shell fragments, shell molds, and echinoid spines. Thin, dark-gray fissile shale layers occur between sand lobes. The tops of the sand units are faintly laminated and contain carbonaceous fragments. Mica is present in variable amounts throughout the entire mouth-bar sequence.

Distal-bar deposits are characterized by laminated siltstones, silty sandstones, and clays. Distal bars are a highly favorable environment for burrowing organisms (especially soft-bodied animals), and distal-bar deposits tend to be highly bioturbated (Coleman and Prior, 1980). Because of the proximity of these deposits to river mouths and their shallow-water nature, a wide variety of sedimentary structures can be produced by high floods on rivers or storms (Coleman and Prior, 1980). The decreasing grain size of the glauconitic sandstones between 9.132 and 9.106 ft (2.783.7 and 2.775.5 m) suggests that these sandstones represent a distributary mouth bar that was overlapped by distal-bar deposits. This interpretation is consistent with the presence of lined ophiomorpha trace fossils, which suggest brackish conditions (Seilacher, 1978). Although distal-bar deposits in most progradational sandstones grade

from finer to coarser sediments vertically (Coleman and Prior, 1980), the reversed grading seen in these sandstones may result from the distributary mouth bar retreating (R. A. Morton, personal communication, 1984).

Washover fans form on the landward side of barrier islands from storms and hurricanes (Hayes, 1980). Deposition is rapid: each upward-fining washover sand rests on a scoured contact and consists of 1 to 2 inches (2.5 to 5 cm) of shell and pebble placer at the base, grading up into mixed sand and small shells and then into relatively shell-free sand (Andrews, 1970).

The washover-fan deposits are mostly flat beds deposited under transitional to upper flow regime conditions; they can vary from 1 inch (2.4 cm) to more than 5 ft (1.5 m) in thickness (Schwartz, 1975). The shell hash at 9,105.8 ft (2775.5 m) (fig. 36), which has scoured the top of the the Frio 'A1' distributary mouth bar in the Delee No. 1 well, has contorted bedding, indicating a very high-energy depositional environment. That these sediments were deposited in a high-energy environment is supported by the presence of a long inclined twig in the underlying sediments that appears to have been dragged over by the current flow during deposition of the shell hash. The shell hash represents a storm deposit that probably fills a channel in a levee or forms a washover fan on the landward side of the distributary mouth bar that was being reworked at this time. Current oriented plant fragments are a characteristic of washover deposits (Schwartz, 1975).

The shell hash is overlain by dark-gray-green mudstone that contains coaly fragments and is much finer grained than the overlying silty Anahuac Formation. This clay may represent a pure clay layer deposited directly above the washover shell hash by storm surge waters ponded behind the distributary mouth bar (Hayes, 1980) or clay deposition under relatively quiet conditions within a lagoon developed behind bars formed by the transgressive reworking of the stacked distributary-mouth-bar system. The lack of bioturbation and close association of this mud with the washover shell

hash suggests, however, that it was deposited from ponded storm surge waters. Interdistributary bay, estuarine, tidal flat, or offshore regions below storm wave base are usually highly bioturbated (Howard, 1975; Coleman and Prior, 1980).

Coleman and Prior (1980) state that the interdistributary bays (fig. 44) into which crevasses prograde are normally open bands of brackish to marine water that are often completely surrounded by marsh or distributary channels and rarely exceed 23 to 33 ft (7 to 10 m) in depth. The lowermost part of the upward-coarsening bay fill consists of alternating silts and silty clays with organic debris, and the clays often show silt- and sand-infilled burrows. With increased sedimentation these burrows are overlain by coarser particles, silty and sandy stringers begin to intercalate with the silty clays, and burrowing is generally reduced. Finally, sands and silty sands alternate with clay laminations and graded bedding, and small-scale climbing ripple structures are the most common type of lamination. Organic debris becomes a common type of stratification.

A high content of transported organic debris and mica is common in the overlying distributary mouth bar, which progrades across the site and is capped by small overbank crevasse splays. Splay deposits contain silt, sand, and clay beds, and the silts and sands have well-developed small-scale ripple-laminations.

Complete crevasse splay sequences are represented by two sets of laminated shale, siltstone, and sandstone between 9,104.8 and 9,101 ft (2,775 and 2,774.6 m) (fig. 42) in the upper part of the Frio 'A' reservoir. The poorly sorted and conglomeratic nature indicates a fluvial dominance, and the upward-coarsening fabric suggests that they are crevasse splay deposits that have breached the fluvial channel and are being deposited directly on a washover fan developed on the bayward side of

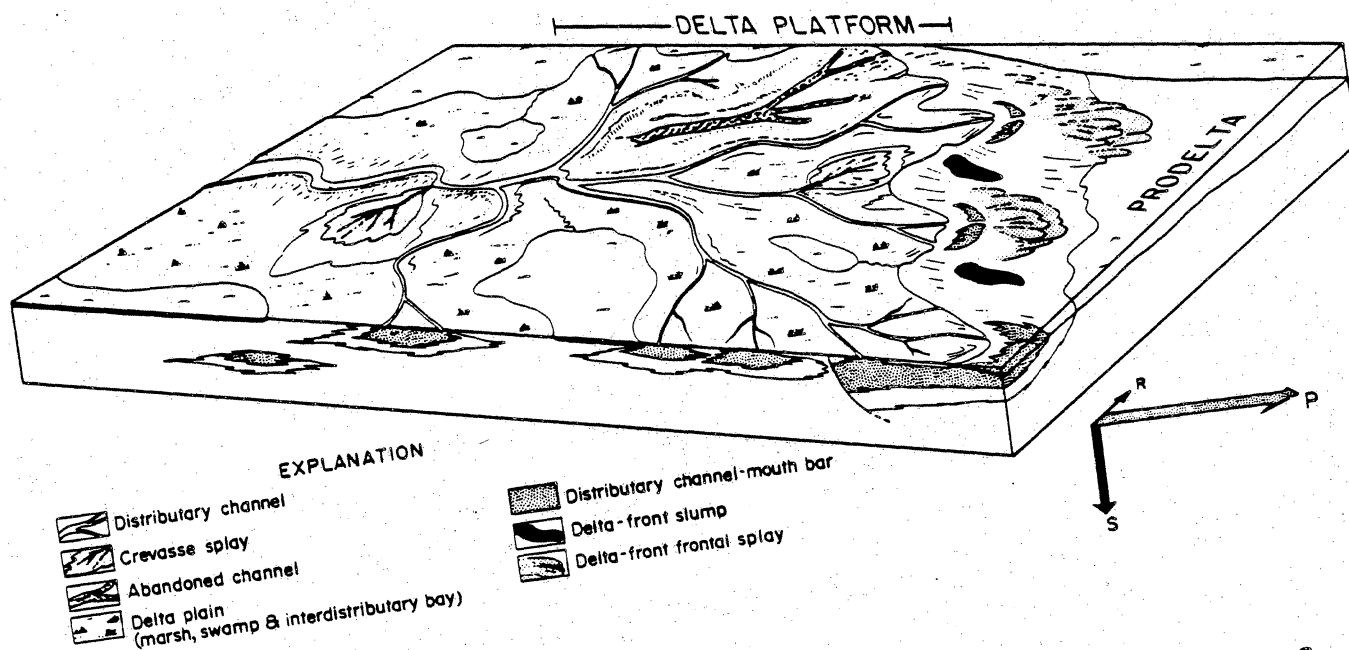


Figure 44. Depositional model of the Lower Frio Formation, Upper Texas Gulf Coast (from Tyler and Hahn, 1982).

the levee. This represents the terminal depositional event of the distributary before it was transgressed and buried by the Anahuac Formation shales.

Anahuac Formation

The transgressive Anahuac shale wedge represents a period of marine invasion of a sediment-starved shelf; it contains a neritic fauna (Galloway and others, 1982). In the Northeast Hitchcock area this unit is approximately 2,500 ft (760 m) thick and can be correlated in detail throughout the field due to its distinctive electric log signature. A core from the Delee No. 1 well, Northeast Hitchcock field (Galveston County), intersected about 35 ft (10 m) of the basal part of the Anahuac shale and entered the Upper Frio at 9,100.6 ft (2,773.8 m). The availability of this core has enabled a very detailed examination to be made of the contact relations between the transgressive Anahuac Formation and the subjacent progradational Frio Formation.

The Anahuac is a light-gray platy to blocky shale. Silty intervals tend to be very calcareous and contain pyrite. At a depth of 8,900 ft (2,713 m) during the drilling of the Delee No. 1 well, there was a sharp reduction in the rate of drilling penetration that was associated with a break in the (spontaneous potential) (SP) log and the appearance of abundant pyrite in the cuttings. The decrease in rate of penetration appears to correlate directly to the increase in pyrite. The presence of pyrite suggests conditions may have been partly euxenic during the initial deposition of the lower 200 ft (61 m) of the Anahuac Formation. Euxenic conditions are generally identified by the presence of sulphide minerals, dark color, and the absence of fauna in the sediments (Blatt and others, 1980). Sulphide minerals and the dark color of

rocks may, however, result from diagenetic changes below the sediment-water interface, and the skeletal parts may be removed totally by solution (Blatt and others, 1980).

Organic spines derived from echinoids (figs. 45 and 46), rounded quartz grains, blocky feldspars, mica, and shell fragments (figs. 47 and 48) are concentrated in carbonaceous shale directly above the top of the Frio Formation (T2 marker horizon) at 9,100.6 ft (2,773.8 m) in the Delee No. 1 well (fig. 49). This basal shale probably represents a lag deposit formed from the reworking of the top of crevasse splay deposits that breached an interdistributary bay or lagoon during the transgression of the Anahuac Formation.

Echinoids usually inhabit rocky coastlines (Crimes, 1975), although a few forms of echinoderm occur on sandy beaches living below the tide level (Komar, 1976). Flat indurated blocks of sandstone and limestone are present along the beaches of the Chandeleur Islands, which represent the reworked Saint Bernard delta lobe of the Mississippi Delta (Rankin, 1936), and beachrock forms within the intertidal zone on modern beaches (Ginsburg, 1953). Such an environment may have existed during the initial stages of the Anahuac transgression and produced conditions favorable for echinoderm proliferation.

Radiolarian tests have been identified at 9,100 ft (2,773 m) in the Anahuac shales, indicating that more open-marine (shelf) conditions prevailed shortly after the transgression. Shell fragments occur randomly or in thin layers, as do dolomite rhombohedrons that are enclosed in clay coats and fibrous illite (fig. 50). The basal 20 ft (6 m) of the Anahuac Formation is glauconitic, and there is a decreasing number of silt and shell laminae with shallowing depth, implying that the marine depositional environment was deepening.

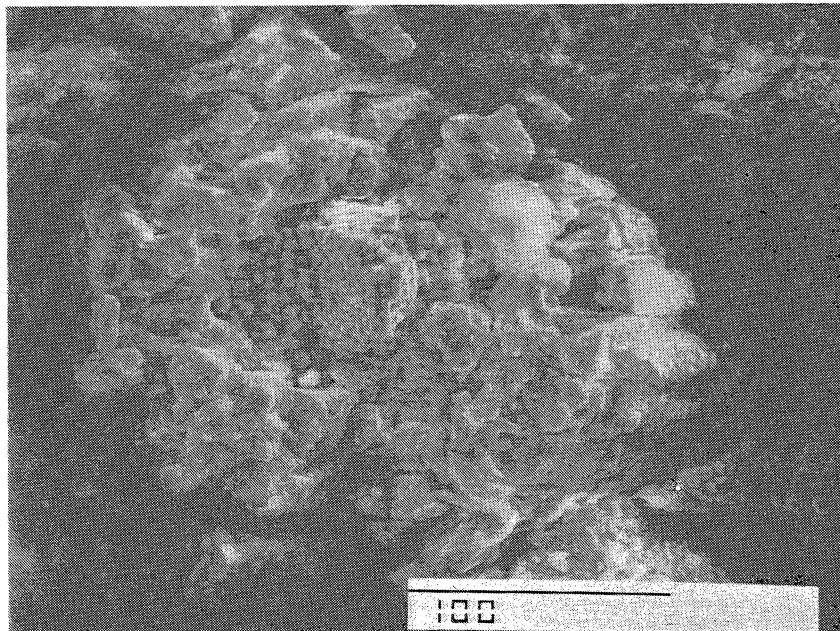
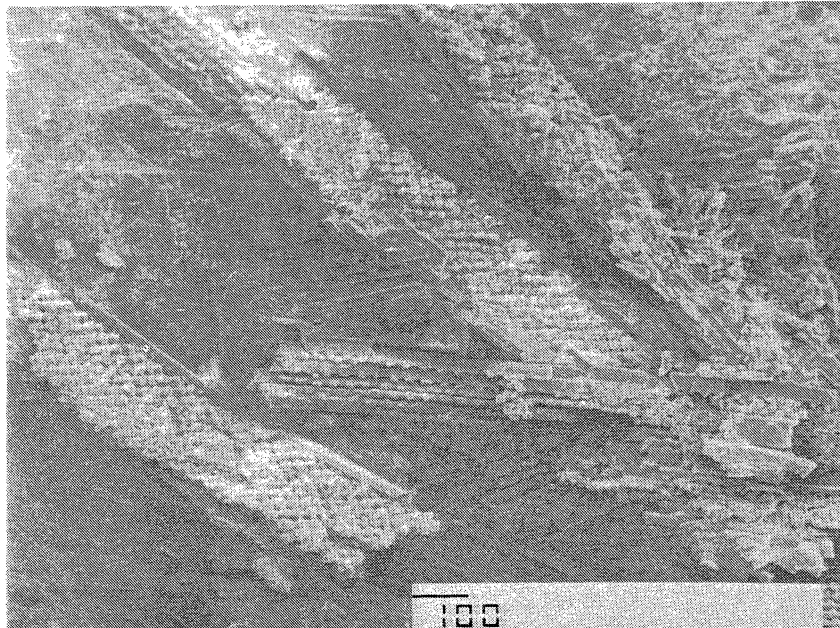


Figure 45. (a) Echinoid spines with ribbed margin and ornate center in basal lag deposit of the Anahuac Formation at 9,100.6 ft (2,773.9 m). (b) End view of spine showing ribbed margin and ornate center. Scale bar length in microns.

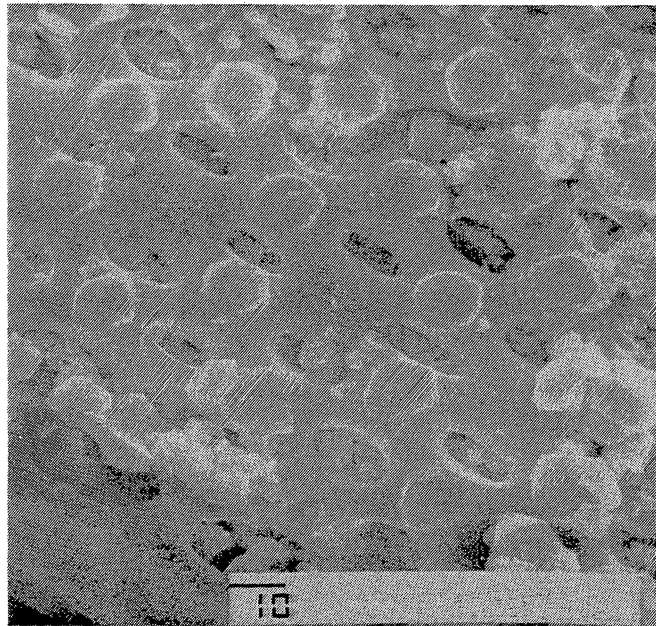


Figure 46. Close-up view of ornate center of echinoid spines in a basal lag deposit of the Anahuac Formation at 9,100.6 ft (2,773.9 m). Scale bar length in microns.

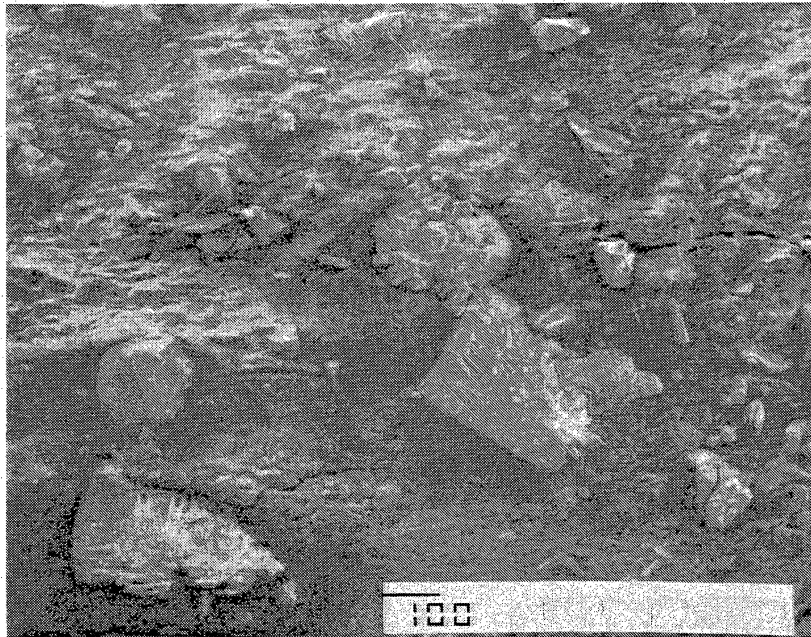


Figure 47. Rounded quartz grains, blocky feldspars, and organic spines in basal Anahuac lag deposit directly above the T2 marker horizon at 9,100.6 ft (2,773.9 m). Scale bar length in microns.

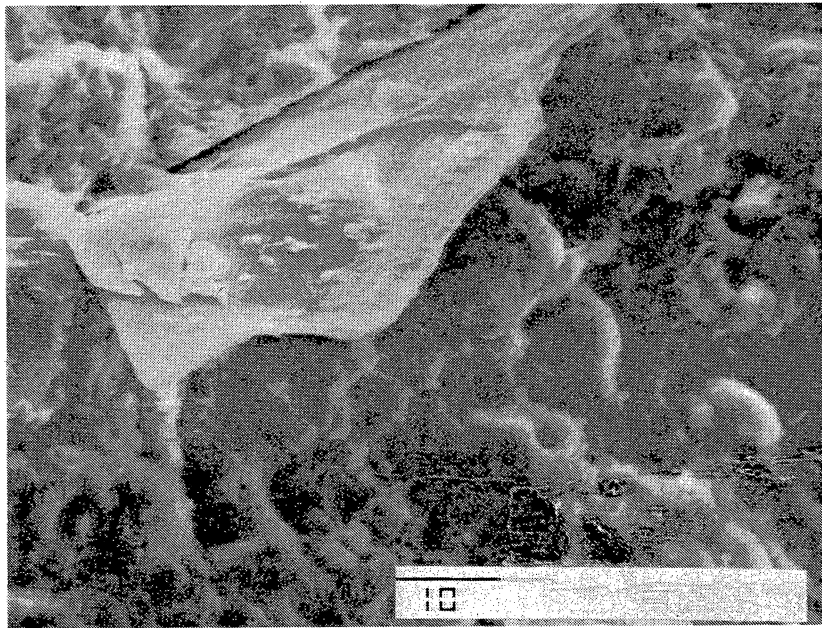


Figure 48. Shell fragment in basal Anahuac lag deposit directly above the T2 marker horizon at 9,100.6 ft (2,773.9 m). Scale bar length in microns.

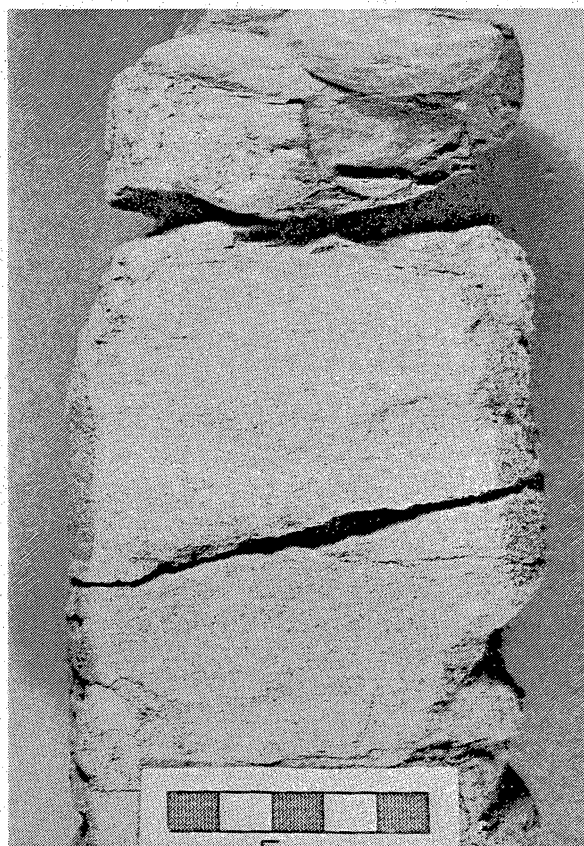


Figure 49. Anahuac basal shale lag erosively overlying the Upper Frio at 9,100.6 ft (2,773.9 m). This break locally represents the T2 marker horizon. Scale bar length 5 cm.

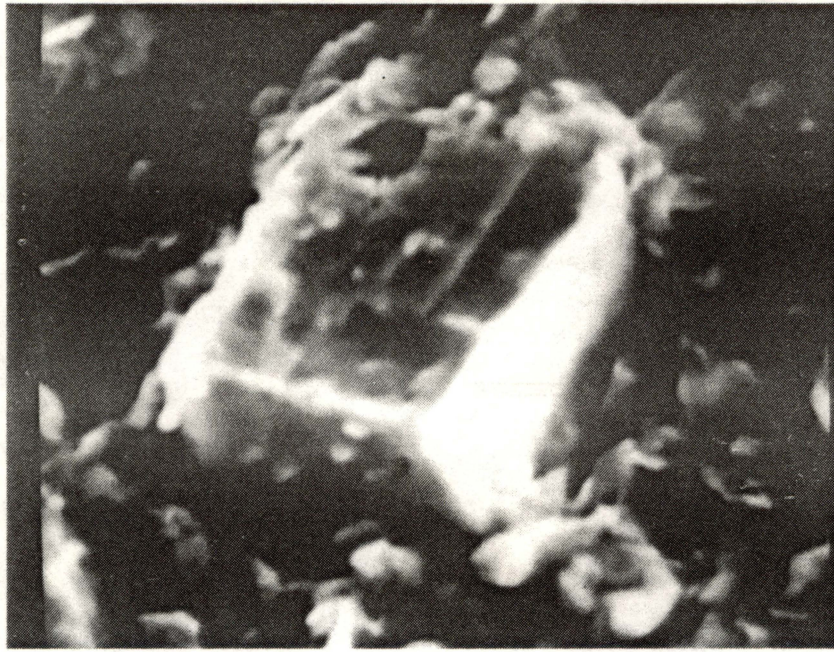


Figure 50. Corroded dolomite rhombohedron in the Anahuac shales at 9.092 ft (2.771 m) with fibrous illite overgrowths. Rhombohedron approximately 5μ wide.

Pelecypod (pecten) shells and molds (fig. 51) are abundant in the Anahuac Formation, as are planolites burrows. Pecten shells are indicative of a shallow-water near-shore marine environment with water depths between 5 and 20 ft (1.5 and 6.1 m) (Moore and others, 1952). Abundant planolites are characteristic of the nearshore (infralittoral - shoreface toe) and transitional zone in the offshore (shelf) with a water depth range of 66 to 591 ft (20 to 180 m) (Chamberlain, 1978).

DIAGENETIC HISTORY

Anahuac Formation

Abundant framboidal pyrite, siderite, and dolomite rhombohedrons identified by microprobe occur in the Anahuac shale below 9,092 ft (2,771 m) in the Delee No. 1 well. Some dolomite rhombohedrons are coated by clay, and the corners or cores commonly appear corroded or abraded. Siderite mud and argillaceous material are commonly deposited together in shallow marine waters or in stagnant lagoons and lakes, and pyrite and siderite also form early diagenetic minerals in marshy environments (Williams and others, 1954; Coleman and Prior, 1980).

Dolomite may be of clastic or early authigenic origin (Williams and others, 1954). Detrital abraded dolomite grains occur in Plio-Pleistocene Mississippi river sands while early diagenetic (isotopically light) diagenetic dolomites have formed on the shelf (K. L. Milliken, personal communication, 1984). The abraded nature of the dolomite rhombohedrons in the Anahuac shale and their fine silty grain size (.01 mm) suggest that they may represent either clastic or early diagenetic dolomites. Dolomite was either deposited or formed on the shelf during the Anahuac transgression and abraded by sea currents on the sea floor; it has been corroded during burial diagenesis. The dolomite rhombohedrons were later buried and developed wispy illite overgrowths.



Figure 51. Mold after pelecypod in Anahuac shales at 9,099.8 ft (2,773.7 m).

Ankerite also has been identified it forms in reducing environments where iron replaces calcium or magnesium in the carbonate structure (Long Liang, personal communication, 1985).

Frio 'A' Sandstones

The diagenetic sequence and its effect on porosity and permeability preservation in the Frio 'A' sandstone core from the Delee No. 1 well have been studied using 17 thin sections from four depths (9,156 ft, 9,166 ft, 9,177.5 to 9,178.5 ft, and 9,189.5 ft). At each level, 800 to 1,000 grains were point counted and the average mineral composition and porosity estimated (table 7). The sandstones are feldspathic litharenites (Folk, 1974). There is a direct relationship between the degree of winnowing (quartz content) and porosity (fig. 52).

Abundant authigenic kaolinite and white and pink detrital orthoclase feldspar are present in the coarse-grained basal tidal channel sandstones at 9,195.5 and 9,123.7 ft (2,782.5 and 2,781 m). Light-green, subrounded to well-rounded grains of microcline and some pink orthoclase feldspars are present in distributary-mouth-bar sandstones at 9,114 ft (2,778 m).

Detrital rutile and diagenetic framboidal pyrite are present in the 1-ft- (0.3-m-) thick crevasse splay sandstone above 9,101 ft (2,774 m). Stacked kaolinite flakes have developed on quartz overgrowths, so they probably postdate this diagenetic event. Iron chlorite formation appears to postdate the quartz overgrowths and framboidal pyrite on which it has formed.

A number of types of detrital grains appear in the basal 20 ft (6 m) of the Anahuac Formation and include rounded quartz, feldspar, volcanic rocks fragments, clay clasts, and shell fragments. Detrital grains have a coating of authigenic smectite-illite. Rare flakes of mica and corroded potassium feldspars replaced by kaolinite occur in the Anahuac shales.

Table 7. Frio 'A' sandstone components as percentages,
Delee No. 1 well.

Total no. of points counted	9156 ft 993	9166 ft 1009	9177.5- 9178.3 ft 847	9189.5 ft 812
Quartz	27.68	43.44	36.13	38.46
Plagioclase	14.78	7.4	6.19	6.85
K Feldspar	6.54	5.82	10.59	6.62
Muscovite	0.1			0.11
Biotite	0.28			
Glauconite	0.36	0.24	0.67	0.46
Chlorite clasts	3.55	2.51	4.91	5.1
Volcanic rock fragments	6.72	4.73	9.31	8.39
Cherts and accessories	12.98	8.61	9.48	8.22
Feldspar overgrowths		0.09	0.17	
Quartz overgrowths	0.74	0.85	0.95	0.34
Sparry calcites	0.92	0.38		0.57
Red carbonates	--	0.33	0.61	0.86
Clay	5.21	--	--	--
Chlorite cement	1.88	1.1	0.56	1.2
Kaolinite cement	2.39	3.5	1.95	3
Intergranular porosity	14.93	20.5	17.5	19.75
Dissolution porosity	1.04	0.5	1	0.12
	100.1	100	100.02	100.05
Quartz	38.3	59.9	47.16	52.2
Feldspar	29.51	18.23	21.9	18.28
Rock fragments	32.17	21.86	30.94	29.5
	99.98	99.99	100	99.98
Feldspars	21.32	13.31	16.95	13.47
Carbonate cements	0.92	0.71	0.61	1.43
Volcanic rock fragments and chlorite clasts	10.27	7.24	14.22	13.51

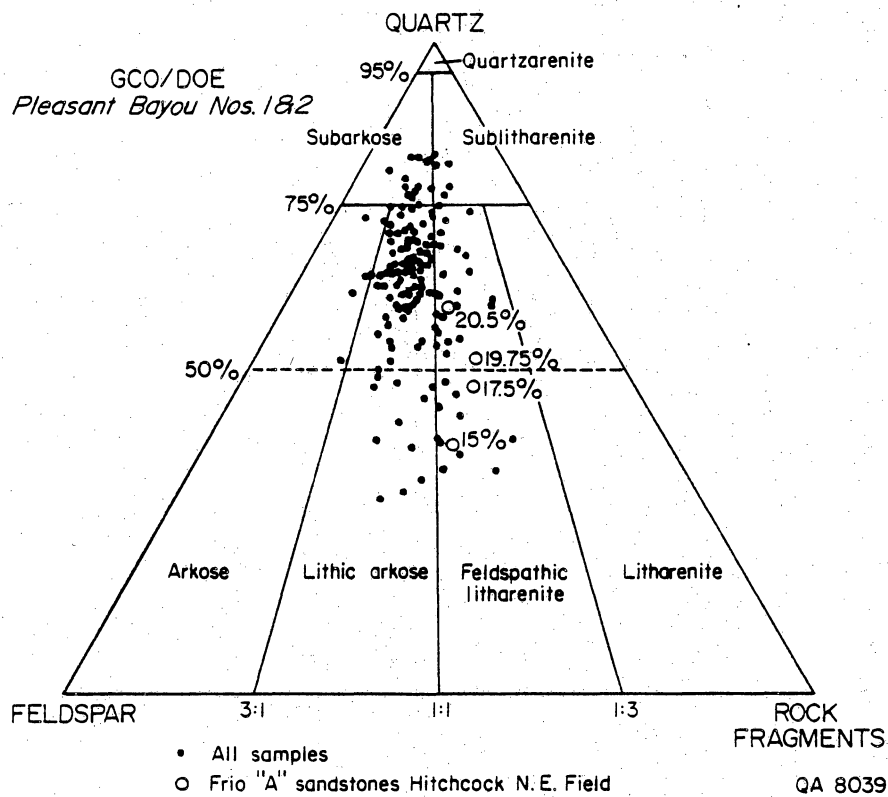


Figure 52. Sandstone compositions of Northeast Hitchcock samples compared with distribution of sandstone compositions from Pleasant Bayou samples. Sandstone classification after Folk (1974). Porosity given as a percentage.

Porosity Types in the Frio 'A' Reservoir

Loucks and others (1981) have subdivided porosity into "macroporosity" and "microporosity" depending on whether the average pore-throat diameter is greater or less than 1 micron, respectively.

Macroporosity

Primary Intergranular Porosity

This is the depositional porosity that remains after compaction and diagenesis (Loucks and others, 1981); it represents the largest apparent porosity component in the Frio 'A' sandstones (15 to 20 percent) (table 7). There is a direct relationship between the degree of winnowing (quartz to feldspar and volcanic rock fragment ratio) and amount of porosity, which indicates that most of the porosity is primary (fig. 52). Alternatively, secondary porosity could be better developed in the clean permeable sandstones.

Secondary Porosity

This is dissolution or replacement porosity that results from the intergranular dissolution or replacement of cements and intragranular dissolution of framework grains (Loucks and others, 1981). There is little petrographic evidence of dissolution porosity in the Frio 'A' sandstone; it reaches a maximum of 1 percent in these rocks. Total conversion of some minerals into cements (for example, plagioclase or potassium feldspar into kaolinite) may have increased the secondary porosity by up to 3.5 percent. This is because during hydration, potassium feldspar will produce only half

the volume of kaolinite, and 1 volume of plagioclase will produce 0.65 volumes of kaolinite.

Microporosity

This porosity occurs within authigenic clay, clay matrix, and fine-grained argillaceous rock fragments in reservoir sandstones. Microporosity is impossible to quantify petrographically, and it does not contribute measurably to permeability (Loucks and others, 1981). Microporosity is responsible for much of the irreducible water saturation in sandstones (Pittman, 1979).

Mineralogy of Frio 'A' Sandstones

The channel sandstone at 9,156 ft (2,791 m) is very poorly sorted and contains rounded and angular to elongate grains of quartz; feldspar (plagioclase, orthoclase, microcline, and microcline perthite) chert; volcanic, igneous and metamorphic rock fragments; chlorite and shale clasts; and accessory hyperthene, garnet, and opaque minerals. Feldspars are corroded, and skeletal and vacuolized feldspars that formed during secondary porosity development are abundant.

Authigenic kaolinite is a product of feldspar dissolution. Quartz overgrowths are present, and feldspars are sericitized. Plagioclase shows alteration to sericite along cleavages and is rimmed by later kaolinite. Late-stage chlorite cement crosscuts kaolinite cement. Dark-reddish-brown clay, and some sparry calcite cements occur in beds that show increased concentrations of chlorite clasts and volcanic rock fragments. This iron carbonate cement and sparry calcites rim corroded feldspars. Detrital biotite, muscovite, and chlorite occur rarely.

The channel sandstone at 9 189.5 ft (2.801 m) contains the same mineral assemblage as that described for the channel sandstone at 9156 ft (2.791 m). However, only a trace of reddish-brown iron calcite and sparry calcite cement occurs in the channel sand at 9,189.5 ft (2.801 m), whereas kaolinite cement is more abundant. Iron carbonate and sparry calcite cement rim quartz grains and is in turn rimmed by kaolinite cement. Chlorite was found to rim both unaltered and kaolinized feldspars.

Iron-poor calcite occurs earliest and is followed by ferroan calcite in Frio sandstones in Brazoria County; calcite leaching must have preceded or occurred contemporaneous with kaolinite precipitation (Kaiser and Richmann, 1981). Previous work on the Frio 'A' sandstones at the Northeast Hitchcock field have shown that iron-chlorite formation postdated quartz overgrowths and framboidal pyrite on which it has formed (Light, 1985).

The medium-grained distributary-mouth-bar sandstone at 9.166 ft (2.794 m) is very clean, well sorted, relatively uncemented and friable. The mouth-bar sandstone contains, in addition to the mineral assemblage already described, glauconite, rounded quartz grains, and elongated feldspar shards, probably of eolian and volcanic origin, respectively. Feldspars have been vacuolized during secondary porosity formation. Dolomite rhombohedrons are locally replaced by iron carbonate. However, carbonate forms a trace cement in this rock, but kaolinite is more abundant. Deformed shale clasts occur intergranularly to quartz and feldspar grains.

The indurated distributary-mouth-bar sandstone at 9.177.5 ft (2.797.3 m) has a similar mineral assemblage as that already described but contains in addition clear to milky quartz with quartz overgrowths, reddish microcline, kaolinized feldspars, carbonaceous fragments, glauconite, and a trace of amphibole. Kaolinite cement is fairly abundant and sporadically fills cavities between grains, producing a spotty

appearance to the rock. Reddish-brown iron carbonate forms a trace cement; it rims quartz overgrowths, indicating that it precipitated in a subsequent event.

Secondary porosity has formed from the partial or complete dissolution of feldspar (particularly plagioclase), which has resulted in only the authigenic cement rims of some crystals remaining. Some feldspar overgrowths appear to be formed of microcline, which surrounds a corroded feldspar core partly filled by successive inner rims of ferrous calcite and kaolinite. Kaolinite has also cemented completely vacuolized feldspars in which only the feldspar overgrowth has remained intact. Evidently during the diagenetic history of these rocks some feldspars were overgrown with feldspar overgrowths, after which the core was partly replaced by iron carbonate and kaolinite. Subsequent to kaolinite cementation some feldspars underwent dissolution and corrosion.

Depositional and Diagenetic Sequence

Loucks and others (1981) described the depositional and diagenetic history of Frio sandstones in the Chocolate Bayou/Danbury dome area using combined isotopic and petrographic techniques. Because of the proximity of the Northeast Hitchcock field to the Chocolate Bayou field, the sequence of diagenetic textures formed in the Frio 'A' sandstone was compared with the diagenetic history of the Chocolate Bayou/Danbury dome area.

The Anahuac Formation was deposited in a transgressive environment in a shallow-marine shelf environment above the regressive (deltaic) Frio Formation (Galloway and others, 1982). Dolomite rhombohedrons present in the Anahuac shales may be of clastic or early authigenic origin (Williams and others, 1954).

Initial Diagenesis and Leaching of Feldspars

Leaching of feldspars in Frio Formation sandstones in the Pleasant Bayou well (Brazoria County) has resulted in the formation of an intergranular, secondary porosity that has enhanced the primary porosity (Loucks and others, 1981). Compaction of clay clasts in the initial stages of burial can lead, however, to the formation of a pseudomatrix and the destruction of primary porosity (Loucks and others, 1981). No clear evidence of early leached feldspars was seen in the core cut in the Frio 'A' sandstone at the Delee No. 1 well.

Feldspar Overgrowth Formation

Feldspar overgrowths have formed on both potassium feldspars and plagioclases in the Frio 'A' sandstones and resulted in additional porosity destruction.

Poikilotopic Calcite Formation

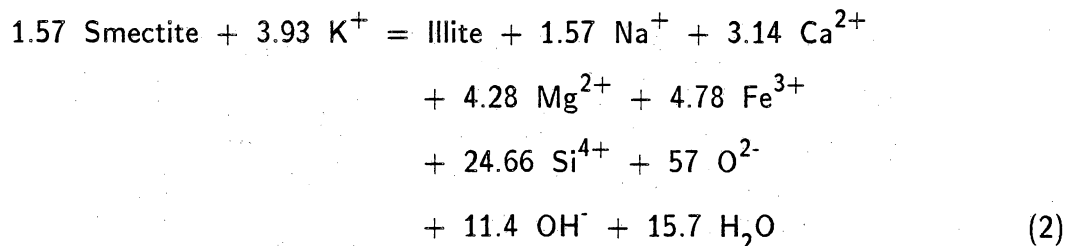
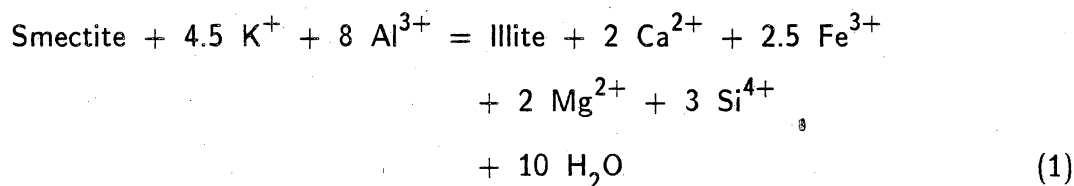
Poikilotopic calcite crystallization (mostly ferroan but some nonferroan grain replacement), which formed prior to quartz overgrowths, leads to porosity destruction in the Frio sandstones in the Pleasant Bayou well (Loucks and others, 1981). There is evidence for this type of cement in the Frio 'A' sandstones in the Delee No. 1 well.

Clay Coat Formation

Clay coat formation postdates early dolomites and feldspar overgrowths, and leads to porosity destruction in the Frio 'A' sandstones at the Northeast Hitchcock field.

Smectite-Illite Transformation and Formation of Quartz Overgrowths

Morton (1983) suggested that the Frio sandstones at the Pleasant Bayou well below 10,000 ft (3,050 m) were invaded by a K⁺- and Al³⁺-rich basinal brine less than 25 Ma ago that resulted in the alteration of smectite to illite. This transformation may have occurred by the following reactions (Boles and Franks, 1979):

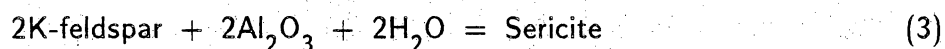


The increasing concentration of Si⁴⁺ released to the reservoir fluids has crystallized as euhedral quartz overgrowths (Boles and Franks, 1979) and resulted in porosity destruction.

Quartz overgrowths formed between 149 and 190.4°F (65 and 88°C), mostly below 12,000 ft in Brazoria County (Loucks and others, 1981; Morton, 1983). Quartz overgrowths are indented against volcanic rock fragments in the Frio 'A' sandstones in

the Delee No. 1 core, which may be due to the chlorite content of latter. However, no clear relationship exists between concentration of volcanic rock fragments and chlorite clasts and quartz overgrowths in the Northeast Hitchcock field (fig. 53).

Reaction of Al^{3+} -rich brines with potassium feldspars may have formed sericite at this time by the following reaction:



Invasion of early K^+ - and Al^{3+} -rich brine may have been undersaturated in H_2S and resulted in the formation of inclusion-free quartz overgrowths, then an increase in the H_2S content of the brine as a result of increasing maturity of organic materials (Hunt, 1979) in the sedimentary column could result in the subsequent formation of some pyrite. Isotopically heavy pyrite, which predates 5-Ma-old uranium deposits present in surface formations containing sulfur derived from deep in the Gulf Basin (Goldhaber and others, 1978, 1979), could have formed during this early H_2S -rich basinal-brine migration event.

From Rb/Sr dating of shales, Morton (1983) suggested that the smectite-illite transition and quartz overgrowth development occurred below 10,700 ft (3,261 m) in the Pleasant Bayou test well (Brazoria County) about 23.6 Ma ago at a temperature of approximately 154°F (68°C); the diagenetic reactions were caused by an upward flush of basinal fluids. However, the heavy $\delta^{18}\text{O}$ composition of quartz overgrowths at the Pleasant Bayou test well implies that they formed at much shallower levels (Loucks and others, 1981; Milliken and others, 1981). Present evidence from the Gulf Coast suggests that the smectite-illite transition begins at 176°F (80°C) (Freed, 1980; Loucks and others, 1981), but the major conversion of smectite to illite is only achieved at 212°F (100°C) (Freed, 1980). Hence the smectite-illite conversion postdates quartz overgrowth development at any stratigraphic level (Land and others, 1987), and

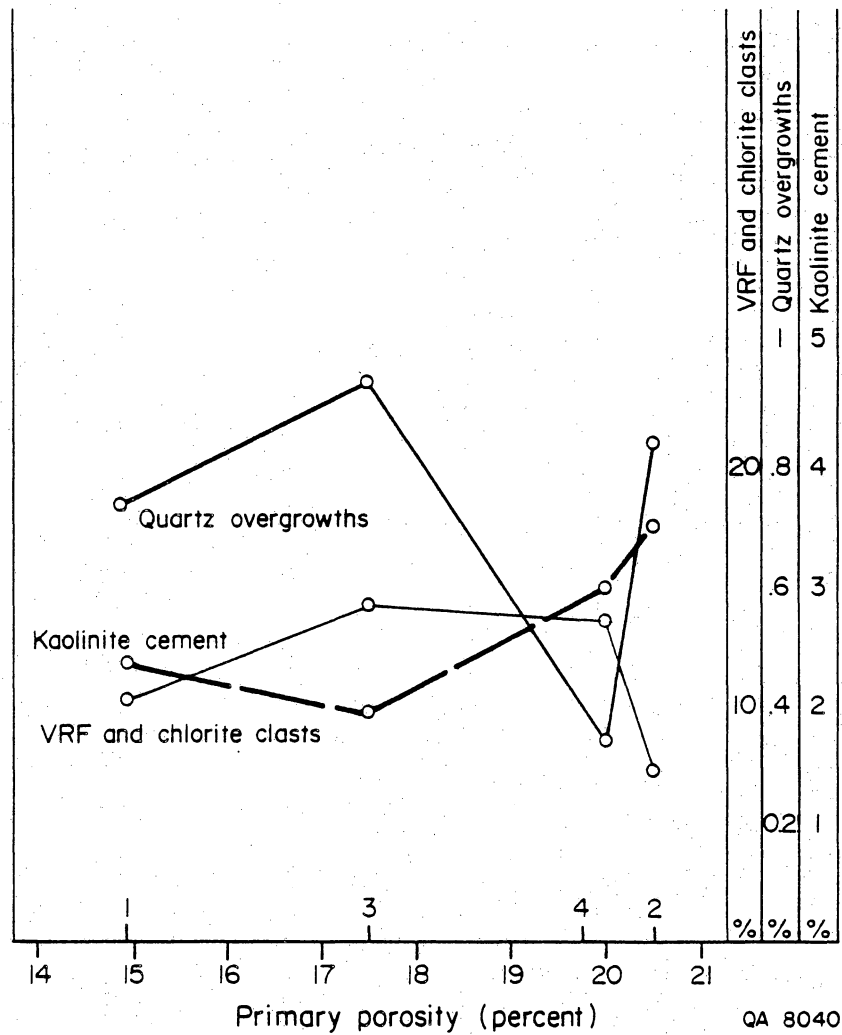


Figure 53. Concentration of quartz overgrowths, kaolinite cement and volcanic rock fragments/chlorite clasts versus primary porosity in the Frio 'A' sandstones, Northeast Hitchcock field.

upward transport of silica in solution is thus required for both these reactions to occur simultaneously. This idea is consistent with the model of the smectite-illite transition being a result of an upward flush of basinal water.

Leaching and Secondary Porosity Formation

Feldspar overgrowths have been corroded during leaching of feldspars, volcanic rock fragments and carbonates that resulted in the enhancement of porosity. Secondary porosity formation largely postdates the formation of quartz overgrowths in Brazoria County but occurred both before and after calcite cementation (Loucks and others, 1981). Leaching of feldspar overgrowths predates carbonate cementation in the Frio 'A' sandstones in the Northeast Hitchcock well.

The carbon dioxide and organic acid content of invading K^+ - and Al^{3+} -rich basinal brine was probably increased by decarboxylation and maturation of organics (Hunt, 1979; Kharaka and others, 1985). Acid waters with a pH of 4 to 6 can leach carbonates, feldspars, and volcanic rock fragments, resulting in pervasive secondary porosity formation (Loucks and others, 1981). Secondary porosity and feldspar overgrowths show similar concentration variations, implying that they were formed at similar times and probably in similar formation fluids (fig. 54).

Continued Transformation of Smectite to Illite and Formation of Late Fibrous Illite

Smectite continued to transform to illite as late fibrous illite formed on mixed-layer clay flakes in the lower Frio Formation in Brazoria County. Oxidized smectite-illite is generally confined to layers with high contents of muscovite and biotite mica, volcanic rock fragments, and chloritized clasts (9,156, 9,166, and 9,189.5 ft). At

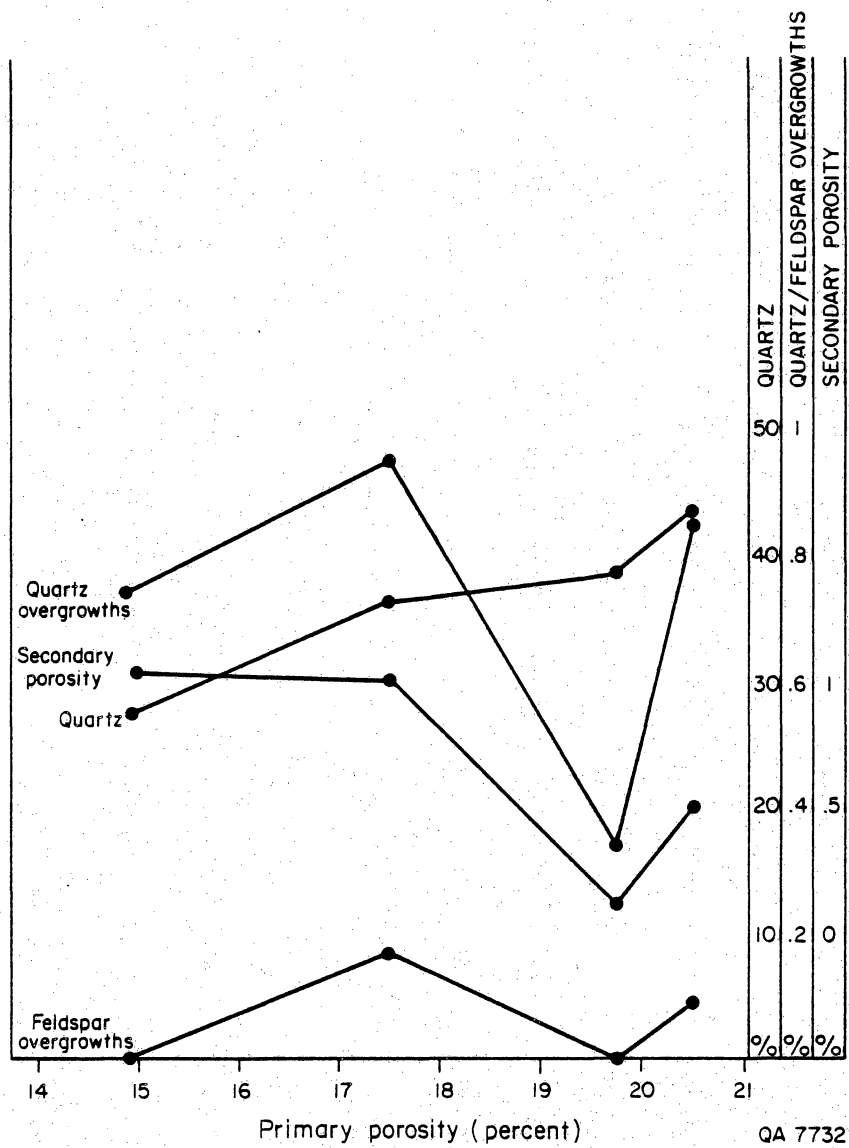


Figure 54. Concentration of quartz, quartz and feldspar overgrowths, and secondary porosity versus primary porosity, Frio 'A' sandstone, Northeast Hitchcock field.

9.156 ft. oxidized smectite-illite has a fibrous texture and is pseudomorphous after biotite. The invading brine must have continued to have high K^+ and Al^{3+} contents, and its temperature exceeded 194 to 212°F (90 to 100°C) (Foscolos and others, 1976; Powell and others, 1978). The conversion of smectite to illite releases 10 to 15 volume percent water of the compacted bulk volume of the argillaceous sediment (Burst, 1969).

Sparry Calcite Cements

Sparry calcite formation postdates quartz overgrowth development and leads to porosity destruction (Loucks and others, 1981). Sparry calcite crystals have filled corroded edges of quartz overgrowths (9.166 ft. 2.794 m) but have euhedral boundaries in pore spaces, suggesting that they postdate secondary porosity formation. Two periods of sparry calcite formation in the Frio 'A' sandstones are indicated by calcite veinlets that cut fractured sparry calcite crystals but are terminated by later red ferroan calcite cements.

An increase in concentration of Ca^{2+} in pore fluids as a result of the transition of smectite to illite probably resulted in the crystallization of poikilotopic and sparry calcites. Calcite also becomes more insoluble at higher temperatures (Kaiser and Richmann, 1981) as the sedimentary pile becomes buried to increasing depths. Pure calcite formation requires the virtual absence of ferrous iron in sulfide rich waters (Kaiser and Richmann, 1981).

Ferroan Calcite and Chlorite Cements

Ferroan calcite replaces plagioclase parallel to albite twins and microcline parallel to cross-hatching. The preferential replacement of albite twins in plagioclase indicates that albitization postdates red ferroan calcite crystallization. Ferroan calcite rims

corroded quartz and feldspar overgrowths and sparry calcites (9.156 and 9.189.5 ft) and it forms veins. Precipitation of ferroan calcite caused porosity destruction (Loucks and others, 1981). Ferroan calcite can replace calcite by the reaction given below (Kaiser and Richmann, 1981):



The ferroan calcite may have formed from increasing concentrations of Fe^{3+} in pore fluids due to the continued conversion of smectite to illite at high burial temperatures. Ferroan calcite is more insoluble than pure calcite at increasing temperature (Kaiser and Richmann, 1981).

Crystallization of chlorite from iron-rich solutions, which may have been generated by the transition of smectite to illite, continued to destroy porosity. In some places the chlorite appears to be directly derived from chloritized volcanic rock fragments. Chlorite has filled cores of ferroan-calcite-cemented zoned feldspars in the Frio 'A' sandstone, Northeast Hitchcock field, indicating that it postdates the carbonate cementation.

Sparry calcite, ferroan calcite, and chlorite have successively cemented leached quartz and feldspar overgrowths and corroded feldspars. These cements have similar concentration variations in the Frio 'A' sandstones, implying that they were formed at similar times and probably in similar pore waters (fig. 55). They show different concentration trends compared with the earlier overgrowths and the later kaolinite (figs. 54 and 56). Furthermore, the late carbonate and chlorite cements in the well-winnowed sandstones show an inverse concentration trend to the leached porosity, indicating that they caused porosity destruction (fig. 55).

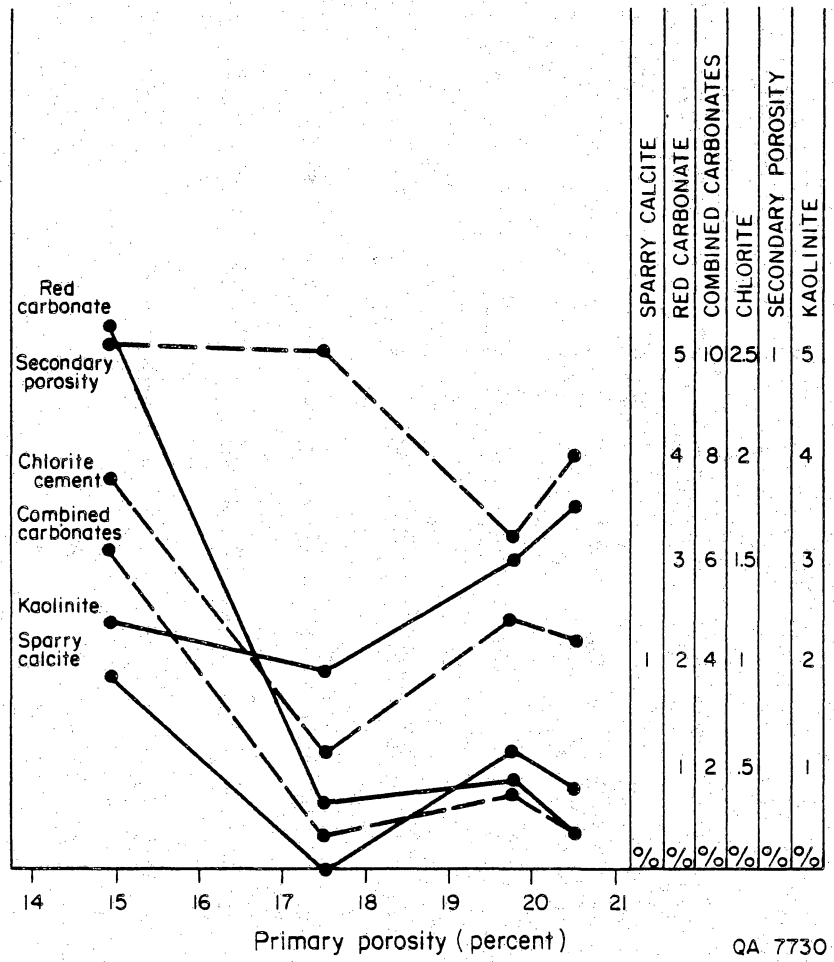


Figure 55. Concentration of carbonate, kaolinite and chlorite cements and secondary porosity versus primary porosity, Frio 'A' sandstones, Northeast Hitchcock field.

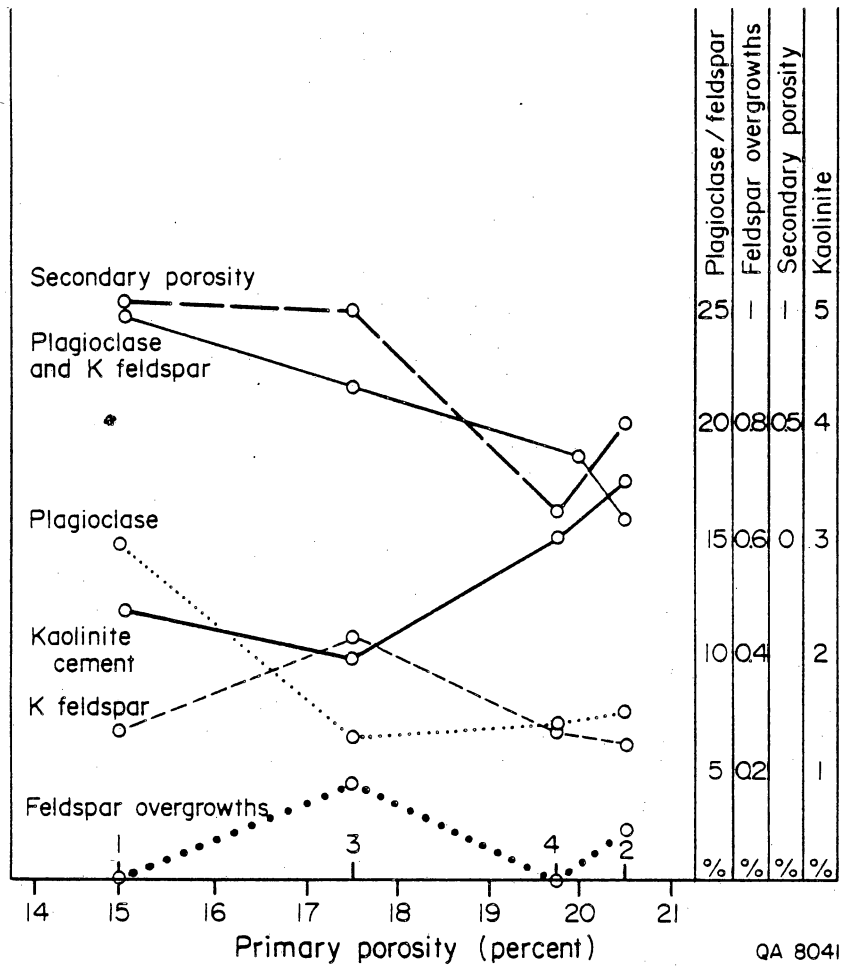
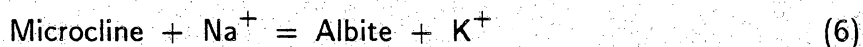
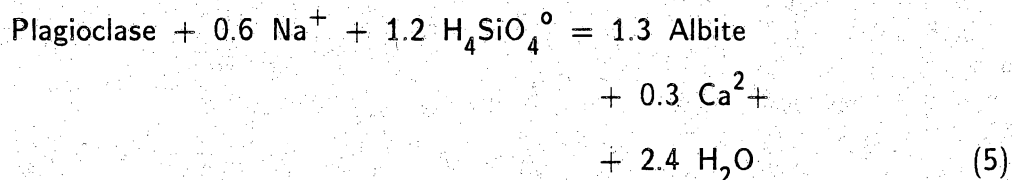


Figure 56. Concentration of plagioclase, potassium feldspar, feldspar overgrowths, kaolinite cement, and secondary porosity versus primary porosity, Frio 'A' sandstones, Northeast Hitchcock field.

Albitization of Feldspars

Feldspars have been albitized at temperatures above 122 to 248°F (50 to 120°C) (Loucks and others, 1981; Kaiser, personal communication, 1983). Two reactions have been suggested through which plagioclase and potassium feldspar are converted to albite (Kaiser and Richman, 1981):



Plagioclase was albitized earlier than potassium feldspar in the Frio in Brazoria County, but albite was stable before kaolinite precipitated, therefore albitization began earlier (Kaiser and Richmann, 1981). Isotopic data and trends in feldspar composition indicate that albitization in Brazoria County occurs slightly deeper than the smectite-illite transition (Loucks and others, 1981). Textures in calcitized feldspars suggest that feldspar grain replacement by calcite preceded complete albitization (Loucks and others, 1981).

Rare laumontite (a zeolite) has formed in the Frio sandstones in Pleasant Bayou (Brazoria County) and in the McAllen Ranch field (Loucks and others, 1981). The laumontite at McAllen Ranch field formed between 248 and 392°F (120 and 200°C) (Loucks and others, 1981) in formation water with a CO₂ content of less than 1 percent (Winkler, 1976).

The $\delta^{18}\text{O}$ of the albite in the Pleasant Bayou well is estimated at -13.2 o/oo (PDB) by Loucks and others (1981), and water in equilibrium with this albite should have a $\delta^{18}\text{O}$ ratio of -32.5 o/oo (PDB) using Friedman and O'Neil's (1977)

fractionation curve. Present formation waters in the Frio Formation are not in equilibrium with the albite at the present temperatures but would be in equilibrium at temperatures between 284 and 392°F (140 and 200°C) (Loucks and others, 1981). This suggests that the formation fluids in Pleasant Bayou have recently been replaced by basinal fluids that are now out of equilibrium with the albite.

The extremely depleted nature of the oxygen-isotopic composition of fluids that were in stable equilibrium with the albite in the Pleasant Bayou well at the time it formed suggests that they are saline waters of meteoric origin. The water may have entered the Lower Frio by brine density flow after having increased salinity by dissolution of salt domes near the surface (T. Jackson, personal communication, 1986). The period of brine density flow probably preceded the growth faulting because brine-bearing sandstones have been displaced by the major growth faults bounding the Chocolate Bayou field in Brazoria County. Hence, the brine density migration must have been an early event.

Kaolinite Cements

Kaolinite begins to crystallize when the temperature exceeds 190.4 to 248°F (88 to 120°C) (Loucks and others, 1981) but most of the kaolinite formed at 212°F (100°C) in acidic basinal brines (pH 4 to 6) that were undersaturated with respect to calcite (Kaiser and Richmann, 1981). Burial history data indicate that the temperature exceeded 212°F (100°C) in the Frio 'A' sandstones in the Northeast Hitchcock field less than 1 Ma ago, which suggests that kaolinite formation was a recent event.

The $\delta^{18}\text{O}$ of the kaolinite is estimated to be -10.5 o/oo (PDB) in the Pleasant Bayou well. This kaolinite is stable in formation waters with oxygen isotope ratios of -25.5 o/oo (PDB), similar to the isotopic ratio of present formation waters (Kharaka

and others 1977b, 1979). The invasion of a deeply sourced (temperature greater than 392°F [200°C]) CO₂-rich, acidic basinal brine less than 1 Ma could have caused precipitation of kaolinite and resulted in δ¹⁸O of the pore waters becoming heavier, and therefore no longer in equilibrium with albite.

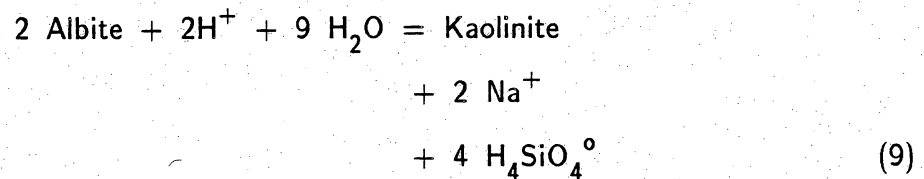
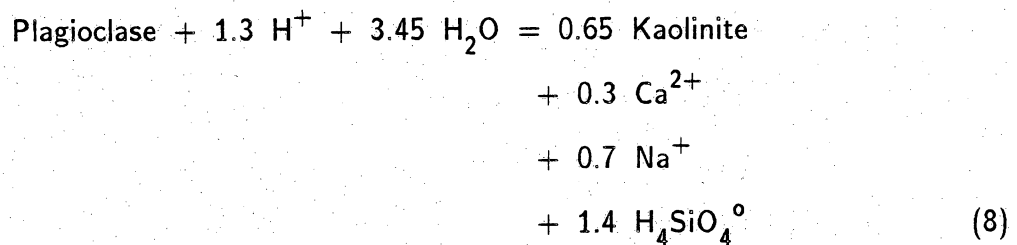
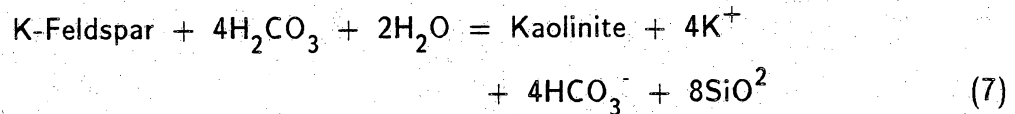
Kaolinite has cemented corroded feldspar and quartz overgrowths and ferroan calcite in the Frio 'A' sandstones, indicating that it postdates their formation. Kaolinite fills secondary pores and occludes porosity. Kaolinite crystallization postdates a period of secondary leaching (Kaiser and Richmann, 1981) and carbonate cementation, but some leaching must have occurred contemporaneously with kaolinite cementation (Loucks and others, 1981).

Kaolinite formed as a grain replacement of plagioclase that eventually consumed the whole grain as diagenesis proceeded (Kaiser and Richmann, 1981). The content of kaolinite is 3.5 volume percent in the well-sorted Frio 'A' sandstones in the Northeast Hitchcock field. Kaolinite content has an inverse concentration trend compared with that of potassium feldspar, which suggests that it has formed from potassium feldspar (fig. 56). The kaolinite concentration trend is quite different from the plagioclase concentration trend, so plagioclase appears to have formed a minor source for kaolinite in the Frio 'A' reservoir (fig. 56).

At surface conditions, potassium feldspar can be leached and altered to kaolinite by solutions with a low pH and high CO₂ content; the CO₂ may be a product of organic reactions (Mason, 1966). Hydration of potassium feldspar within the Frio 'A' sandstones by acidic (CO₂-bearing) waters will produce kaolinite and result in a porosity increase because of a volume reduction similar to the volume of kaolinite produced. In the well-sorted distributary-mouth-bar sandstones this could have caused a porosity increase of 3.5 percent. The high permeability of the well-sorted sandstones has apparently resulted in them preferentially acting as conduits for the

migration of acidic waters and the subsequent hydration of potassium feldspars.

The probable reactions through which feldspars are altered to kaolinite are given below (8 and 9 from Kaiser and Richmann, 1981):



Dissolution of Feldspars

Carbonate cements in the Pleasant Bayou well are dissolved (Kaiser and Richmann, 1981) where carbonate cementation preceded or occurred contemporaneously with kaolinite cementation (Loucks and others, 1981). Poikilitic laumontite crystals at McAllen ranch field have been also been leached (Loucks and others, 1981) by fluids with carbon dioxide contents greater than 1 percent (Winkler, 1976).

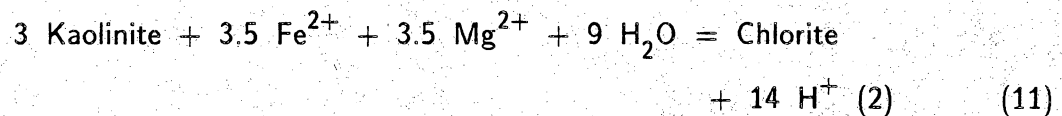
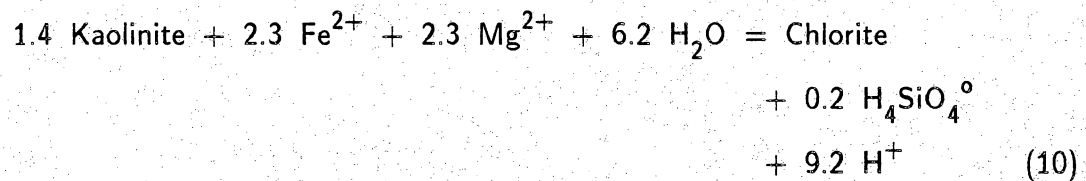
Many skeletal and vacuolized feldspars in the Frio 'A' sandstones at the Northeast Hitchcock field are rimmed and cemented by kaolinite, but the interior of

crystals are devoid of clay. This structure suggests that many feldspars have undergone dissolution and corrosion after the kaolinite precipitated. This leaching resulted in a further enhancement of the porosity.

Evidently the invading basinal brine was fairly acidic and initially formed kaolinite, but as more deeply sourced waters reached the Frio Formation, the CO₂ content and acidity increased and leaching began. Morton and others (1983) showed that the CO₂ content of brines in Brazoria County increases with increasing depth, consistent with the interpretation that increasingly deeply sourced brines will contain higher CO₂ contents.

Iron Chlorite

At the Northeast Hitchcock field, iron-chlorite formation appears to postdate quartz overgrowths and framboidal pyrite on which it has formed (Light, 1985). However, in the Pleasant Bayou well, chlorite rosettes have formed on euhedral kaolinite flakes and thus postdate the period of kaolinite cementation. Kaiser and Richmann (1981) indicate that iron chlorite crystallized from kaolinite between 302 and 347°F (150 and 175°C) by the reaction shown below:



Chlorite is stable in Brazoria County formation waters at temperatures between 302 and 347°F (150 and 175°C) and at pH from 4 to 6 (Kaiser and Richmann, 1981).

A late upward migration of basinal brines less than 1 Ma old is required to produce high temperatures necessary for chlorite crystallization. Formation water in the Lower Frio is not in isotopic equilibrium with albite, which implies that isotopically different fluids have invaded the formation (Loucks and others, 1981). Light hydrocarbons were introduced into the Frio reservoirs after chlorite precipitated because the presence of hydrocarbons in pores retards diagenetic reactions (Selley, 1970).

Similar hydrocarbon- and Fe-rich saline fluids may have produced pyrite-bearing calcite cap rocks on nearby salt domes (Light and others, in press). The high Cl/Br ratios of the present Frio formation fluids indicate they contain components of salt dissolution (Kharaka and others, 1979) and have therefore migrated past salt domes, probably on the downdip side of the fault blocks. The invading basinal brine appears to have become progressively more acidic and Fe- and methane-rich, with CO₂ forming more than 10 percent of the produced gas in the Lower Frio reservoirs in Brazoria County (Morton, 1981).

CONCLUSIONS

Depositional environment is the major control of the high porosity found in the Frio 'A' sandstones at the Northeast Hitchcock field, Galveston County. The high porosity (\pm 30 percent) and permeability (\pm 1,000 md, $0.99 \mu\text{m}^2$) of the Frio 'A' reservoir is largely the result of its deposition in a distributary-mouth-bar complex that was subsequently reworked by shallow-marine processes. The wide lateral extent of

the Frio 'A' sandstone, which is a consequence of extensive marine reworking, will allow free access to water influx from the southwest extension of this aquifer (Light, 1985).

The well-sorted sandstones have the highest porosities and permeabilities and contain the most abundant authigenic kaolinite, which suggests that they have acted as preferential conduits for the introduction of acidic waters that hydrated the potassium feldspar to kaolinite. Hydration of potassium feldspar to kaolinite by migrating acidic waters prior to the introduction of hydrocarbons resulted in a porosity increase of up to 3.5 percent in the well-sorted distributary-mouth-bar Frio 'A' sandstones. The removal of potassium feldspar grains and their redistribution as kaolinite cement could explain the open texture of some of the sandstones, in which many of the quartz grains appear unsupported. Because the conversion of potassium feldspar to kaolinite results in a decrease in volume of about 50 percent, the percentage concentration of kaolinite is a rough estimate of the volume of secondary porosity produced by this process.

Well-sorted sandstones with high porosities and permeabilities contain the most abundant authigenic kaolinite; these sandstones have acted as preferential conduits for migrating acid waters and for major fluid flow during co-production. Authigenic kaolinite can create fluid production problems because its delicate structure is fragile. In addition, chlorite cements and chlorite rims on quartz overgrowths are present in some sandstones, and these may also be dislodged during high production rates. The dislodged clay and chlorite flakes will accumulate at and obstruct pore throats at high production rates.

A maximum safe rate of fluid production will need to be determined for co-produced wells that will not result in dislodgement and migration of kaolinite and

chlorite into pore throats. Experimental flow tests conducted at different flow rates on kaolinite-rich sandstones and measurement of resulting changes in permeability could assist in determining the safe upper flow rate.

FLUID-INJECTION POTENTIAL OF PROPOSED MIOCENE BRINE-DISPOSAL SANDS IN THE NORTHEAST HITCHCOCK AND ALTA LOMA FIELDS, GALVESTON COUNTY, TEXAS

by William A. Ambrose

INTRODUCTION

Economically favorable production of gas and water from hydro pressured reservoirs in the Texas Gulf Coast has been effectively demonstrated by Gregory and others (1983) and Anderson and others (1984), who have presented preliminary results of co-production activity from the hydro pressured and geopressed Frio 1-A (9,100 ft) sand in Northeast Hitchcock field in Galveston County, Texas. Large amounts of brine are also produced with gas from the Frio 1-A sand; cumulative production of brine from the Frio 1-A sand in Northeast Hitchcock field to August 1984 has been 7,990,000 bbl (Anderson and others, 1984).

Miocene sands, buried at depths from 2,000 to 6,800 ft (610 to 2,073 m), have been targeted to receive brines co-produced from the Frio 1-A sand. Up to 7,500 bbl of brine per day in each of three wells are to be disposed of into the most optimum Miocene sands within a small disposal site in Northeast Hitchcock field. The selection of these brine-disposal sands was in part based on a study of their continuity, thickness, and documented fluid-injection potential in Northeast Hitchcock field and surrounding areas.

Objectives

The Bureau of Economic Geology developed five specific objectives to be met in order to successfully select appropriate Miocene brine-disposal sands in Northeast Hitchcock field. Those objectives were:

(1) To determine the extent of the fault block containing Northeast Hitchcock field and adjacent Alta Loma field in order to define the maximum area where Miocene sands are continuous by not having been offset by faults.

(2) To provide three primary and three alternate Miocene sands for disposal of brines by evaluating their potential aquifer volumes and heterogeneity on the basis of analysis and interpretation of several structural cross sections, net-sand maps, and depositional facies maps of the most laterally extensive and thickest Miocene sands in Northeast Hitchcock and Alta Loma fields.

(3) To document known brine-disposal potential of Miocene sands in Northeast Hitchcock, Alta Loma, and in nearby fields where significant brine disposal has occurred in analogous and correlative Miocene sands. These data were obtained from the Texas Railroad Commission of Texas.

(4) To select potential sites for brine disposal in Northeast Hitchcock and Alta Loma fields on the basis of the common occurrence of the thickest and most laterally continuous portions of potential brine-disposal Miocene sands.

(5) To evaluate factors that would limit the optimum brine-disposal potential of Miocene sands in Northeast Hitchcock and Alta Loma fields, such as sand-body heterogeneity due to facies architecture, and cementation due to diagenesis.

Study Area, Data Base, and Methods

Northeast Hitchcock and Alta Loma fields are located in Galveston County, Texas (fig. 57). Alta Loma field was included in the study because it is located within the same major fault block that contains Northeast Hitchcock field. Hence, brines injected into Northeast Hitchcock field have the potential to flow also into Alta Loma field.

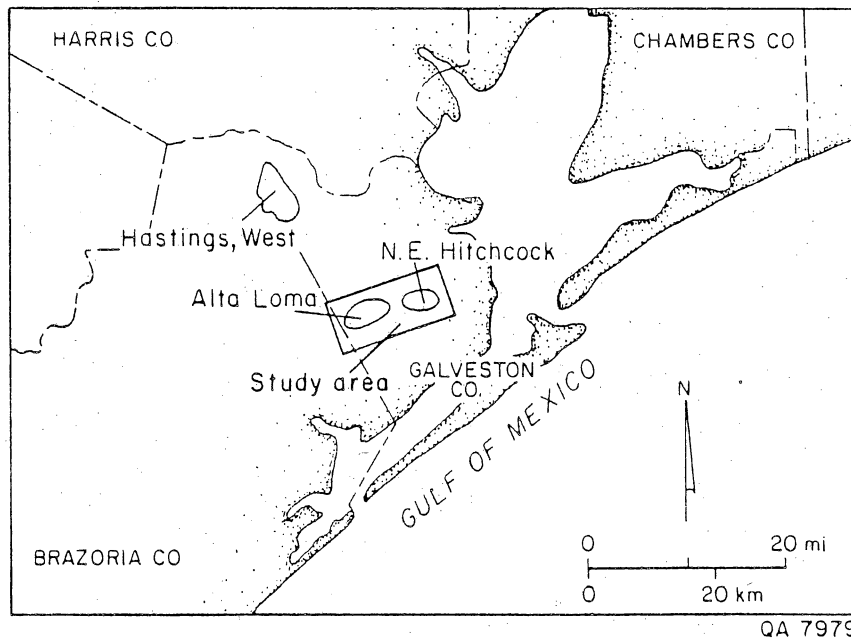


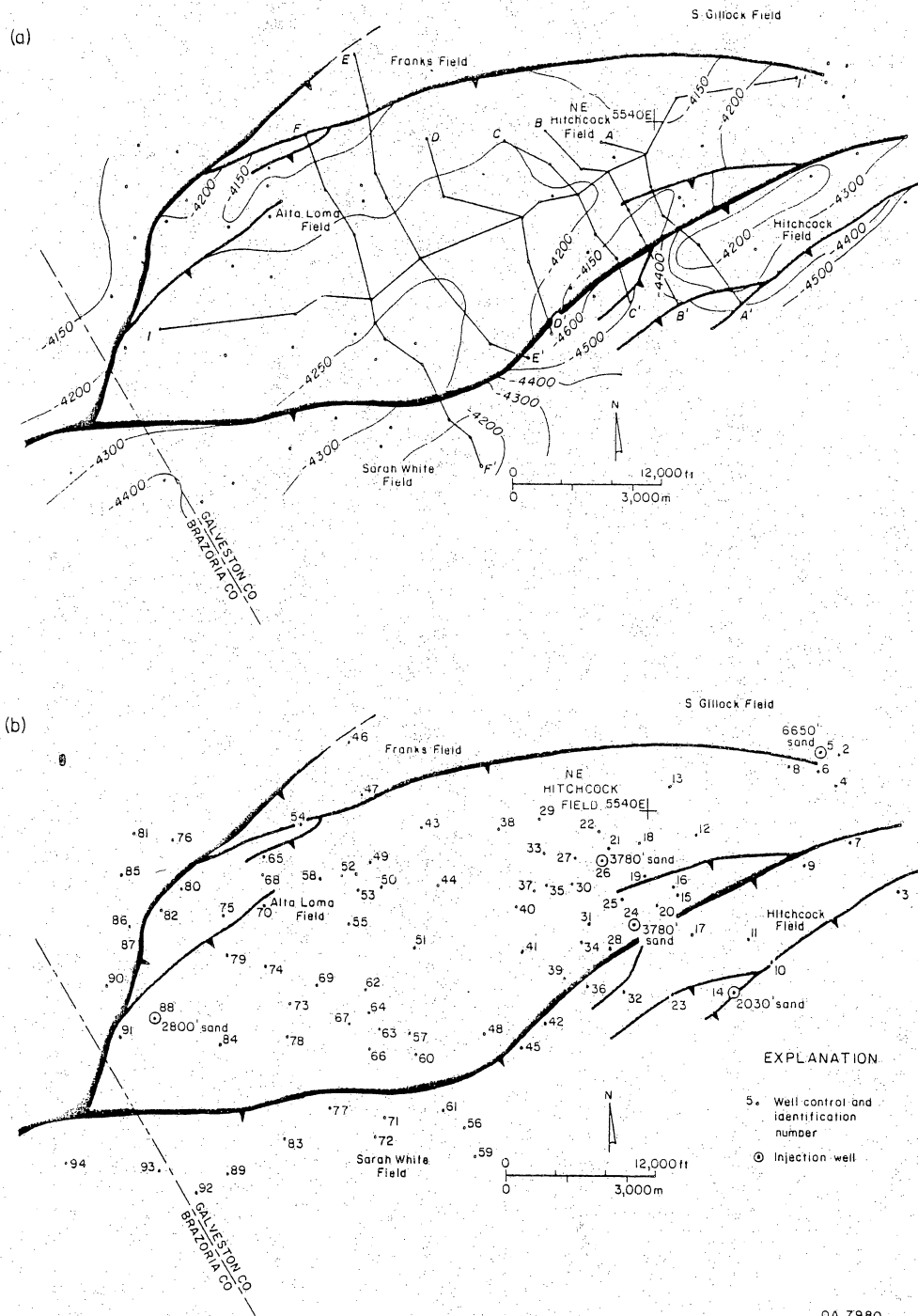
Figure 57. Location of Northeast Hitchcock field, in which six Miocene sands (2,000 to 6,150 ft deep) have been proposed for disposal of brines associated with methane co-produced from the underlying Frio Formation. Hastings West field contains 43 wells that have been used to inject brines into several Miocene sands analogous to those of the Northeast Hitchcock field.

Details of this fault block are illustrated on a structure map of Northeast Hitchcock and Alta Loma fields, which is contoured on the top of the 4,240-ft sand (fig. 58). Two major growth faults that offset Miocene sands from 50 to 200 ft (15 to 61 m) isolate the two fields into a block covering approximately 35 mi² (89.6 km²). Northeast Hitchcock field is located in a structurally high area within the fault block; many of the minor faults that offset the underlying Frio 1-A sand in this area die out in the Miocene section.

The data base consisted of 94 well logs distributed throughout Northeast Hitchcock and Alta Loma fields, as well as portions of nearby Franks, Gillock South, Hitchcock, and Sarah White fields (fig. 58). The names of the well logs are listed in table 8.

Other data incorporated into the study were brine-disposal histories of Miocene sands in five of the wells in the Bureau of Economic Geology data base. These wells are also indicated in figure 58. Similar but more extensive brine-disposal data from analogous and correlative Miocene sands in Hastings West field (fig. 57) were analyzed in order to determine the maximum brine-disposal potential of Miocene sands in the region.

Six structural dip sections and one structural strike section were constructed in Northeast Hitchcock and Alta Loma fields in order to document the location and offset of the major bounding faults and to determine the lateral extent and thickness of Miocene depositional units to be considered for brine disposal. Net-sand and depositional facies maps based on SP log patterns were constructed for thirteen Miocene sands (fig. 59). Net-sand thickness was determined from SP logs by using a cutoff line drawn 35 percent of the distance from the SP baseline to a normalized maximum SP deflection for the Miocene in the study area. This value has been successfully used for accurate determination of net sand in studies of other Tertiary formations in the Texas Gulf Coast by the Research Planning Institute, which based the value on electric log crossplots and whole core data, and by the Bureau of



QA 7980

Figure 58. Structure map of Northeast Hitchcock and Alta Loma fields, contoured on the top of the 4,240-ft sand. Two major growth faults, with throws from 50 to 200 ft (15 to 61 m), serve to isolate these two fields into a 35-mi² (89.6-km²) fault block. Miocene sands in five wells in the study area have recently received brines; these sands and wells are indicated on the map above. Amounts of disposed brine are illustrated on the net-sand map of each indicated sand (figs. 62 to 70).

Table 8. Well logs used in brine-disposal study of Northeast Hitchcock and Alta Loma fields.

<u>Well</u>	
<u>No.</u>	<u>Operator and Lease</u>
1	Pan Am. #1 State Moses Lake
2	Pan American #2 Scofield Comm.
3	Mecom #A-1 Univ. of Texas
4	Pan American #D-4 Kohfeldt
5	Pan Am. #D-3 S. Gillock Un.
6	Pan American #DD-1 S. Gillock
7	Pan American #B-1 S. Gillock
8	Pan American #1-N S. Gillock
9	Mid Sts. #1 Westbridge Un.
10	Cockburn #1 Dobbs. et al
11	Hanson #2 Title and Guar.
12	Total Pet. #1 Stuart
13	Pan American #1 Bogatto Comm.
14	Cockburn #1 Aarco
15	Sue-Ann #1 Dynamic Land Devel.
16	L.B. Wright #1 Schaub
17	Adobe & Cameron #1 Stubbs
18	Phillips #1-A Fox
19	Phillips #1-D Davis
20	Cockrell #1 Lemm
21	Phillips #1 Delaney
22	R.L. Burns #1 Delaney
23	Humble #1 Coon Fee
24	Phillips #1-A Huff

25 Phillips #1 Prets
26 Phillips #1 Thompson
27 Kennedy and Mitchell #1 Delaney
28 Phillips #1 Sundstrom
29 Placid #1 Weidman
30 Phillips #1-A Louise
31 Mecom #1 Kipfer
32 Tx. E. Trans. #1 Hitchcock G.U.
33 Mecom #1 Wittgen
34 Phillips #1 Lasalo
35 J.S. Michael #1 Newman
36 Slater et al #1 Flake G.U.
37 Kimball #1 Knox est.
38 Placid #1 Camp Wallace G.U.
39 Slater et al #1 Delasandre
40 H&M Gas and Oil #1 Reichmeyer
41 Aikman Pet. #1 Drew Unit
42 Tx. E. Trans. #1 White G.U. 4
43 Placid #1 Lobit
44 Hassie Hunt #1-A Ghino
45 Tx. E. Trans. #1 White G.U. 3
46 Placid #1 Thompson G.U. 1
47 Placid #1 Crane G.U.
48 Tx. E. Trans. #1 Henck
49 Hassie Hunt #1 S.H. Green
50 Hassie Hunt #3 S.H. Green
51 Hassie Hunt #1-A Brister
52 Hassie Hunt #1 H. Sealy

53 Hassie Hunt #1 M. David
54 Hassie Hunt #1 Nelson
55 Hassie Hunt #1 R.B. Wilkins
56 Gulf #2 Emil Firth est.
57 Phillips #1-A Tacquard
58 Hassie Hunt #1 M. Rogers
59 Alamo Pet. #1 Firth est.
60 Damson #1 G. Latimer
61 Gulf #1 Lowenstein
62 Phillips #1 O'Daniel Un.
63 Phillips #2 O'Daniel Un.
64 Phillips #3-A O'Daniel Un.
65 Hassie Hunt #1 Sayko
66 Phillips #1-A Evans
67 Phillips #1 McVea
68 Hassie Hunt #2 Sayko
69 Hassie Hunt #1 M. Jensen
70 Phillips #2-B Pabst
71 Tx. E. Trans. #4 Craig
72 Tx. E. Trans. #3 Craig
73 Phillips #1 Lauzon
74 Jolensky-Gideon #1 Tacquard
75 Phillips #1-B Pabst
76 Reb. Pet. #1 Chapman
77 Mecom #1 Roos Trustee
78 Phillips #A-1 Christensen
79 Crystal Oil #1 McIlvane
80 Del Mar #1 W.N. Zinn

81 M.P.S. Prod. #1 Chapman
82 Del Mar #1 Harris
83 Tx. E. Trans. #1 Halls Bayou R.
84 Buttes #1 Sun Amoco Fee
85 The Texas Co. #1 Joe Tucker
86 The Texas Co. #B-1 J.W. Harris
87 Tx. E. Trans. #1 Newton
88 Gen. Crude #1 Reitmeyer-Briscoe
89 Edwin Cox #1 Halls Bayou Ranch
90 Tx. E. Trans. #1 Nana
91 Pan American #1 R.E. Brading
92 Buttes #2 A.B. Marshall
93 Fina. et al #1 Marshall
94 Phillips #1 McIlvane

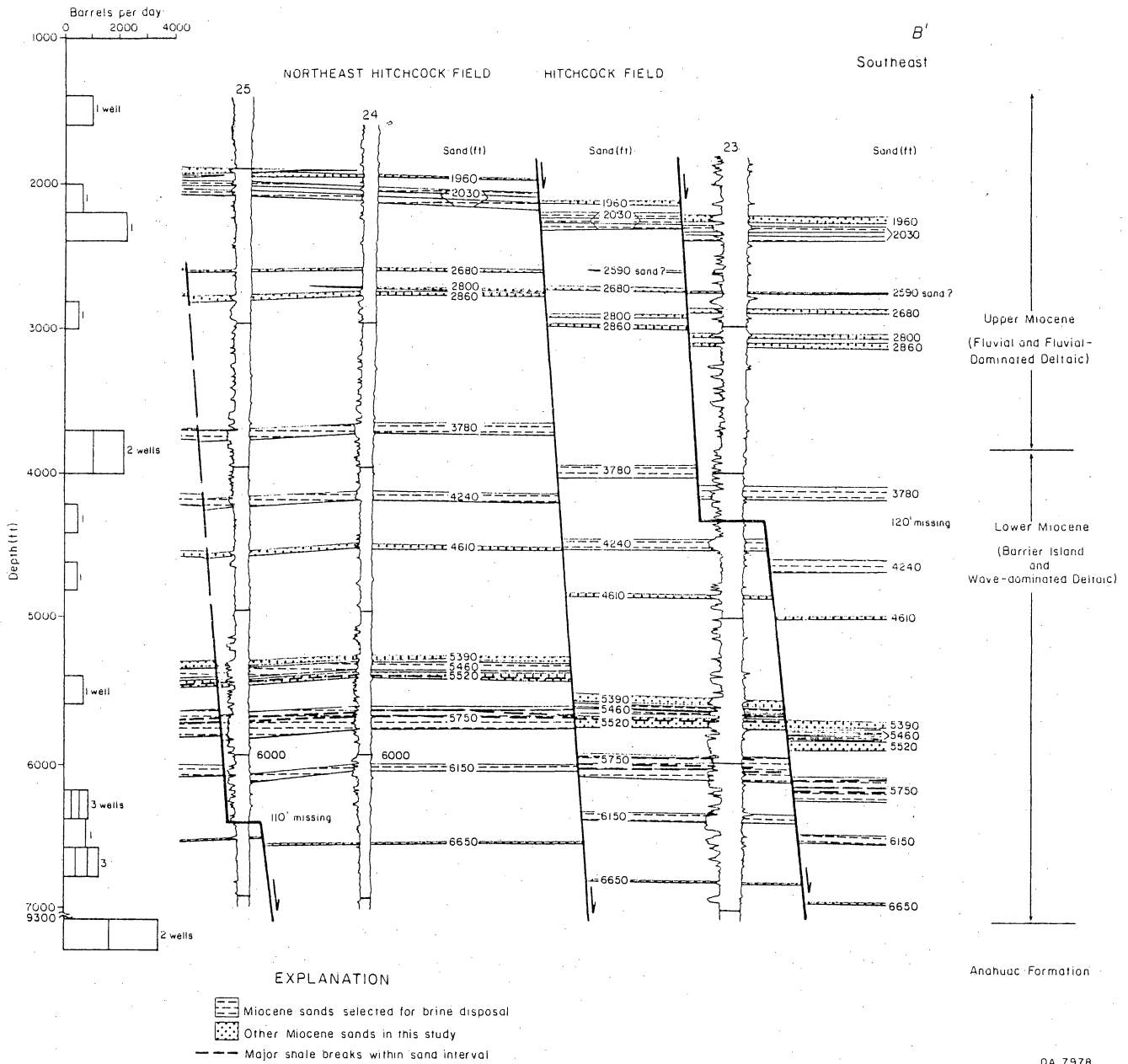


Figure 59. South end of structural dip-section B-B' through Northeast Hitchcock and Hitchcock fields (see fig. 58 for location of cross section). Five lower Miocene sands and one upper Miocene sand are proposed for brine disposal.

Economic Geology in its studies of the Frio barrier-strandplain trend in the Texas Gulf Coast (Tyler and Ambrose, 1985).

Depositional facies maps of each Miocene sand selected for study were based on characteristic SP patterns that were interpreted in conjunction with the net-sand maps. Application of SP patterns to depositional systems interpretation has been effectively demonstrated in previous studies of the Miocene in the Texas Gulf Coast (Morton and others, 1985) and of other Tertiary units (Galloway and Cheng, 1985; Tyler and Ambrose, 1985).

MIOCENE DEPOSITIONAL SYSTEMS IN THE TEXAS GULF COAST

Regional Miocene Depositional Systems

Miocene sediments of the Texas Gulf Coast were deposited by several stages of deltaic progradation over the Frio paleocontinental margin. In the Texas Gulf Coast, the Miocene clastic wedge thickens from less than 2,000 ft (610 m) updip to a maximum of 10,000 ft (3,050 m) offshore, 45 mi (72 km) from the present coastline (Rainwater, 1964). The lower Miocene in the region of Northeast Hitchcock and Alta Loma fields was deposited in a prograding barrier-strandplain system that formed a prominent strike-parallel belt of sand, bounded seaward by a transitional zone of thin distal-shoreface and inner-shelf sandstone and siltstone interbedded with shelf mudstone. The barrier-strandplain system is bounded landward by massive mudstone containing thin sandstone channel units deposited in a muddy coastal plain (Galloway and others, 1986).

Upper Miocene sediments were deposited in a succession of fluvial, fluvial-dominated deltaic, and strandplain environments superimposed over older lower Miocene progradational wedges (Doyle, 1979). These facies are commonly comprised of

abundant lenticular fluvial and distributary channel sands encased in silty and muddy coastal plain sediments.

Miocene Depositional Systems, Northeast Hitchcock and Alta Loma Fields

The Miocene in Brazoria and Galveston Counties was deposited as a succession of deltaic and barrier-strandplain facies overlain by fluvial and deltaic facies (Doyle, 1979). The Miocene in Northeast Hitchcock and Alta Loma fields has been informally subdivided in this study into a lower barrier island and wave-dominated deltaic interval, 3,000 to 3,500 ft (915 to 1,070 m) thick, and an upper fluvial and fluvial-dominated deltaic interval, 1,800 to 2,200 ft (550 to 670 m) thick (fig. 59). In Northeast Hitchcock and Alta Loma fields, the lower Miocene barrier island and deltaic sequences, which may consist of up to four separate sand bodies, each up to 50 ft (15 m) thick, are generally thicker and more continuous than the lenticular, laterally discontinuous fluvial and fluvial-dominated deltaic sequences of the upper Miocene. Because of the greater thickness and lateral extent of lower Miocene sands, more attention and effort was directed toward choosing these as potential units for brine disposal. The thickest upper Miocene units that were selected for study were chosen not only for the sake of comparison with lower Miocene units, but also because of their shallow depth, which makes them economically favorable in terms of drilling costs.

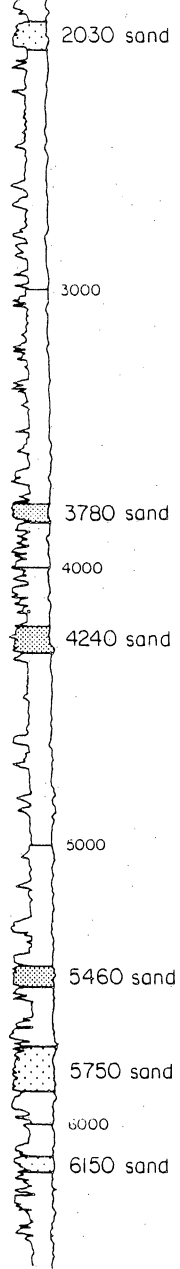
PROPOSED BRINE-DISPOSAL SANDS, NORTHEAST HITCHCOCK AND ALTA LOMA FIELDS

Factors Considered in Selection of the Brine-Disposal Sands

Five lower Miocene sands and one upper Miocene sand are proposed for brine disposal in Northeast Hitchcock and Alta Loma fields (fig. 60). Of these six sands,

Type Log
 PHILLIPS
Thompson No. 1
 Galveston County, Texas
 Northeast Hitchcock Field

Sp Res



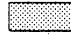

 Primary sand for fluid injection
 Alternate sand for fluid injection
 QA 7730

Figure 60. Type log from Northeast Hitchcock field, featuring proposed primary and alternate brine-disposal sands in the Miocene.

three are designated as primary choices (the 3,780 ft., 4,240 ft., and 5,460 ft., all lower Miocene) and three are selected as alternates (2,030 ft., upper Miocene, and 5,750 ft., 6,150 ft., lower Miocene).

Four major factors were taken into consideration in the selection of these sands:

- (1) sand-body complexity due to high number and diversity of component depositional facies.
- (2) thickness of brine-disposal sand.
- (3) previously documented brine-disposal capacity, both in Miocene sands in Northeast Hitchcock and Alta Loma fields and in analogous, correlative sands in nearby fields, and
- (4) depth of the brine-disposal sand.

Sand-Body Complexity

The majority of the proposed brine-disposal sands are simple genetic units consisting of only one major sand body interbedded with one or two minor shale stringers, rather than thick, composite intervals of sand and shale. By focusing on simple genetic units, it is possible to select more homogeneous aquifers for brine disposal. Thick sequences of sand interbedded with shale commonly contain numerous heterogeneities that reflect the high number of component sand bodies and depositional facies in the interval.

Additionally, original depositional environment plays a key role in determining aquifer complexity. Large and relatively continuous sand bodies tend to be more common in barrier-strandplain and delta-front sands rather than in fluvial-channel deposits, which are associated with such discontinuities as abandoned-channel-fill, levee, crevasse splay, and floodplain deposits (Morton and others, 1983). The presence of these fluvial facies, most of which feature large grain-size variations, results in complex aquifers subdivided into many compartments separated by permeability

barriers. Additionally, many fluvial facies contain internal permeability differences, which result in further complications.

Barrier-island and delta-front sands reworked by marine processes, in contrast, are commonly well sorted and laterally continuous. These properties result in excellent reservoirs (Tyler and others, 1984). Heterogeneities within these systems are minimal, although the presence of modifying facies such as tidal channels and washover fans may locally disrupt aquifer continuity.

Thickness of the Brine-Disposal Sand

Thickness of the depositional unit for use as a brine-disposal sand also is an important factor. Both the thickest Miocene depositional sequences and the thickest individual sand bodies in Northeast Hitchcock and Alta Loma fields are found in the lower Miocene. Accumulation of up to 300 ft (90 m) of sand in some lower Miocene depositional sequences such as the 5,750 ft sand was probably the result of intermittent subsidence along reactivated Frio growth faults that occurred as delta and barrier-island systems prograded over the Frio paleocontinental margin early in the Miocene. Relatively thin (less than 150 ft, 46 m) upper Miocene depositional sequences in Northeast Hitchcock and Alta Loma fields were probably associated with diminishing rates of subsidence as the lower Miocene shelf margin became more stable (Galloway and others, 1986).

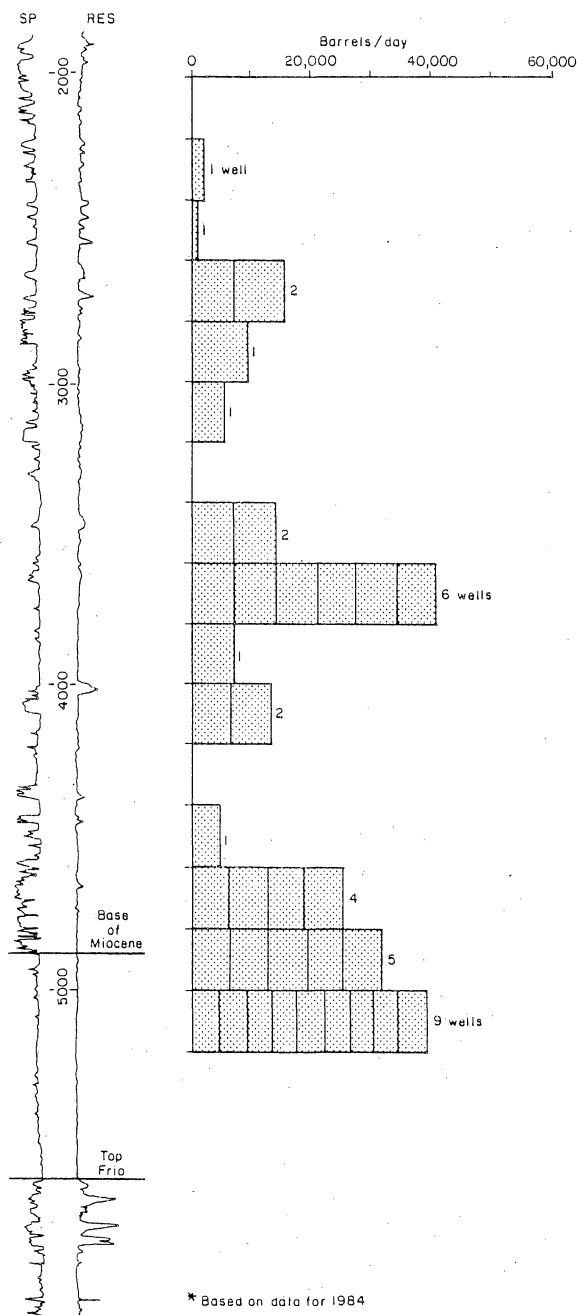
Previously Documented Brine-Disposal Capacity

Northeast Hitchcock and Alta Loma Fields

Because only a few scattered wells in Northeast Hitchcock and Alta Loma fields have available brine-injection information, it was impossible to make a statistically valid correlation between depositional systems and thicknesses of brine-disposal sands and amounts of brine injected. Documented rates of brine injection in Northeast Hitchcock and Alta Loma fields vary considerably, with a range of values from 622 to 72,000 bbl of brine per well per month. For instance, in the 3,780-ft sand there is a large difference (622 versus 20,200 bbl of brine per month) in amounts of brine disposed into two nearby wells in identical depositional environments, which suggests that factors other than aquifer quality and depositional environments are controlling amounts of brines disposed of in Northeast Hitchcock field. Therefore, it was necessary to document brine-disposal rates in other Miocene sands in an area represented by a larger, more consistent data base.

Hastings West Field (Brazoria County)

Hastings West field, which contains 43 active Miocene disposal wells, is located 15 mi (24 km) northwest of the Alta Loma field (fig. 57). Although Hastings West field is situated in an area slightly updip from Northeast Hitchcock and Alta Loma fields, the Miocene there is also composed of a succession of thick (300 ft [91 m] or more), laterally continuous sands overlain by a succession of relatively thin (commonly less than 70 ft [21 m] thick), discontinuous fluvial and moderately continuous fluvio-deltaic sands, locally up to 150 ft (45.7 m) thick (fig. 61).



QA 7967

Figure 61. Type log in Hastings West field, located 15 mi (24 km) northwest of Northeast Hitchcock and Alta Loma fields (fig. 57). Marine and fluvio-deltaic sands received 242,000 barrels of brine per day in 1985 from 43 wells in Hastings West field. Lower Miocene sheet sands and other shallow sands are capable of receiving up to 10,000 barrels of brine per day per well. Figures obtained from the Railroad Commission of Texas.

Thick lower Miocene sands in Hastings West field received 88,000 bbl of brine per day from 19 wells in 1985. These sands, which are correlative with other lower Miocene sands in Northeast Hitchcock and Alta Loma fields, are capable of receiving up to 9,500 bbl of brine per well per day. Therefore, by analogy with other lower Miocene sands in Hastings West field, lower Miocene barrier-island and wave-dominated deltaic sands in Northeast Hitchcock and Alta Loma fields should be capable of receiving the required 7,500 bbl of brine per day in each of three disposal wells.

Depth of the Brine-Disposal Sand

Because of cheaper drilling and other related costs associated with shallow sands, certain of the thickest and laterally continuous upper Miocene sands were considered for study. However, other factors such as aquifer heterogeneities due to distribution of discontinuous depositional facies strongly offset the economically favorable shallow depth factor of the upper Miocene sands in the study area.

Lower Miocene Brine-Disposal Sands, Northeast Hitchcock and Alta Loma Fields

Primary Brine-Disposal Sands

All of the proposed primary brine-disposal sands in Northeast Hitchcock and Alta Loma fields are in the lower Miocene and consist of the 3,780-ft sand (fig. 62), 4,240-ft sand (fig. 63), and 5,460-ft sand (fig. 64). All of these sands were deposited in either elongate, strike-parallel barrier-island, sandy shoreface, or wave-reworked deltaic systems. These units are relatively simple, individual genetic sand bodies featuring only a minor number of interbedded shales. Consequently, the depositional facies tracts within these sands are relatively simple, only slightly modified by minor

crosscutting features such as sand-filled tidal channels and sandy, lobate washover fans. By virtue of their average individual thickness of 70 to 90 ft (21 to 27 m) and lateral continuity, the 3,780-ft, 4,240-ft, and 5,460-ft sands should be excellent aquifers for brine disposal in Northeast Hitchcock and Alta Loma fields. Key aspects of these and all other potential brine-disposal sands presented in this report are summarized in tables that accompany the net-sand maps.

Alternate Brine-Disposal Sands

Although the 5,750-ft and the 6,150-ft sands exhibit sheetlike and lobate net-sand patterns that are similar to those of the primary sands previously described, these two sands are designated as alternate choices owing to certain offsetting factors. The 5,750 ft sand (fig. 65), although the thickest of those proposed in the study, is the most complex and features several major interbedded shale stringers, each up to 25 ft (7.6 m) thick. These shale stringers serve as barriers to fluid flow that may limit the overall capacity of the aquifer. The 6,150-ft sand (figs. 66 and 67), although sheetlike and continuous as a consequence of being deposited in a barrier island and high-energy shoreface system, is the deepest and thinnest (generally 40 to 60 ft, 12 to 18 m) of the six proposed brine-disposal sands.

Upper Miocene Brine-Disposal Sands, Northeast Hitchcock and Alta Loma Fields

Upper Miocene fluvial sands, typified by the 2,800-ft sand (figs. 68 and 69), are poor choices for brine disposal due to the abundance of lenticular, isolated fluvial-channel sands encased in muddy and silty overbank and floodplain deposits. However, the 2,030-ft sand (figs. 70 and 71), deposited in a fluvio-deltaic setting, is offered as

DEPOSITIONAL SYSTEMS AND BRINE-DISPOSAL
POTENTIAL OF THE 3,780-FT SAND (LOWER MIOCENE).
NORTHEAST HITCHCOCK AND ALTA LOMA FIELDS

I. Interval Description

A. Sand-Body Geometry:

Continuous sand sheet developed parallel to depositional strike: up to 110 ft (33.5 m) of sand along the main axis of deposition, which runs through Northeast Hitchcock and Sarah White fields. This unit is thinner and less sandy updip toward Alta Loma field, where it is only 40 ft (12 m) thick.

B. Depositional Facies:

Barrier-island system deposited in a 1- to 4-mi- (1.6- to 6.4 km) wide belt along depositional strike. The barrier core, distributed in a continuous band from Northeast Hitchcock field to an area between Sarah White and Alta Loma fields, is transected by sand-poor tidal channel deposits in Northeast Hitchcock field. Small-scale, lobate washover deposits grade updip into a back-barrier lagoon system located in Alta Loma and Franks fields.

II. Reservoir Characteristics

A. Brine-Disposal Potential in Northeast Hitchcock and Alta Loma Fields:

Excellent, due to development of a continuous sheet sand 70 to 110 ft (21.3 to 33.5 m) thick along the main depositional axis. Areas where brine disposal may be less optimum are in sand-poor areas such as the complex lagoonal facies (Alta Loma field) and in crosscutting tidal channel deposits (Northeast Hitchcock field).

B. Brine-Disposal History:

Northeast Hitchcock field: 20,240 bbl per month in well 26, situated in barrier core deposits marginal to a tidal channel system; 622 barrels per month in well 24, situated in a similar setting.

C. Area of Greatest Sand Thickness and Best Continuity For Brine Disposal:

Within barrier-island core facies, specifically between Alta Loma and Sarah White fields (wells 57, 63, and 66) and in similar facies in Northeast Hitchcock field (wells 25, 31, and 34).

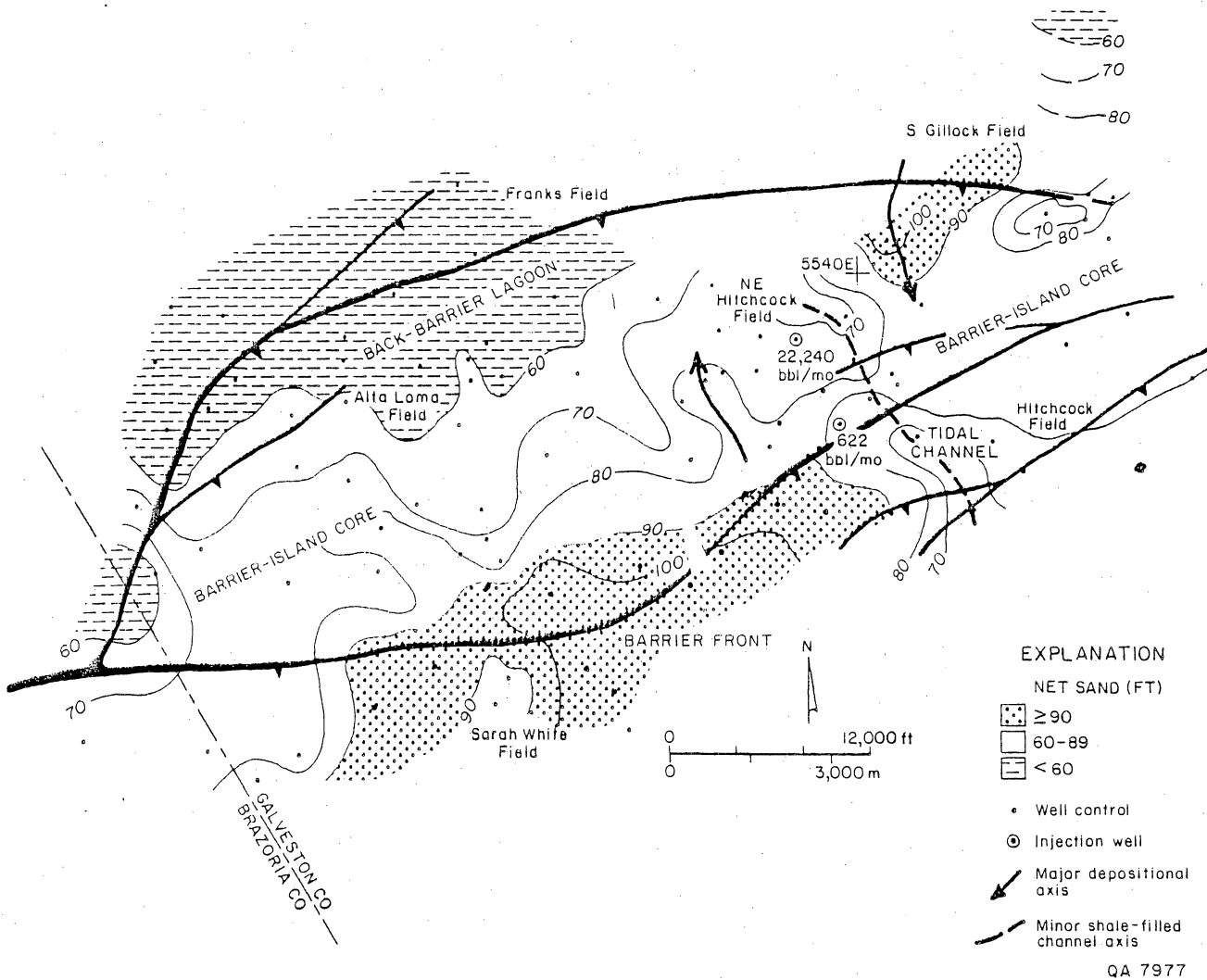


Figure 62. Net-sand and depositional facies map of the 3,780-ft sand (lower Miocene). This sheet sand, deposited in a barrier island environment, is a primary choice for brine disposal, based on excellent sand continuity and an average thickness of about 70 ft (21.3 m) in the study area.

DEPOSITIONAL SYSTEMS AND BRINE-DISPOSAL
POTENTIAL OF THE 4240-FT SAND (LOWER MIOCENE),
NORTHEAST HITCHCOCK AND ALTA LOMA FIELDS

I. Interval Description

A. Sand-Body Geometry:

Primarily an irregular belt, 60 to 110 ft (18.3 to 33.5 m) thick, developed parallel to depositional strike, but also consisting of a series of lobate and lenticular sand bodies that pinch out downdip.

B. Depositional Facies:

A system of lobate, wave-reworked deltas. Individual lobes (0.4 to 1.8 mi [0.64 to 2.9 km] wide) are composed of 80 to 100 ft (24.4 to 30.4 m) of sand. Reworked delta-front deposits are most extensive south of Alta Loma field and also in Hitchcock field. Distal delta-front and interdeltatic deposits are well developed in Sarah White field and in the southern part of Northeast Hitchcock field, respectively.

II. Reservoir Characteristics

A. Brine-Disposal Potential in Northeast Hitchcock and Alta Loma Fields:

Good to excellent. Continuous, wave-reworked delta-front sands are extensively developed throughout the area and constitute most of the potential reservoir sand in Northeast Hitchcock and Alta Loma fields.

B. Brine-Disposal History:

None available in the study area.

C. Area(s) of Greatest Sand Thickness and Best Continuity For Brine Disposal:

Within wave-reworked delta-front facies in Alta Loma field (wells 50, 51, 53, and 55 for example) and, to a lesser extent, within distributary-channel and delta-front facies in Northeast Hitchcock field (wells 18, 21, 26, and 27).

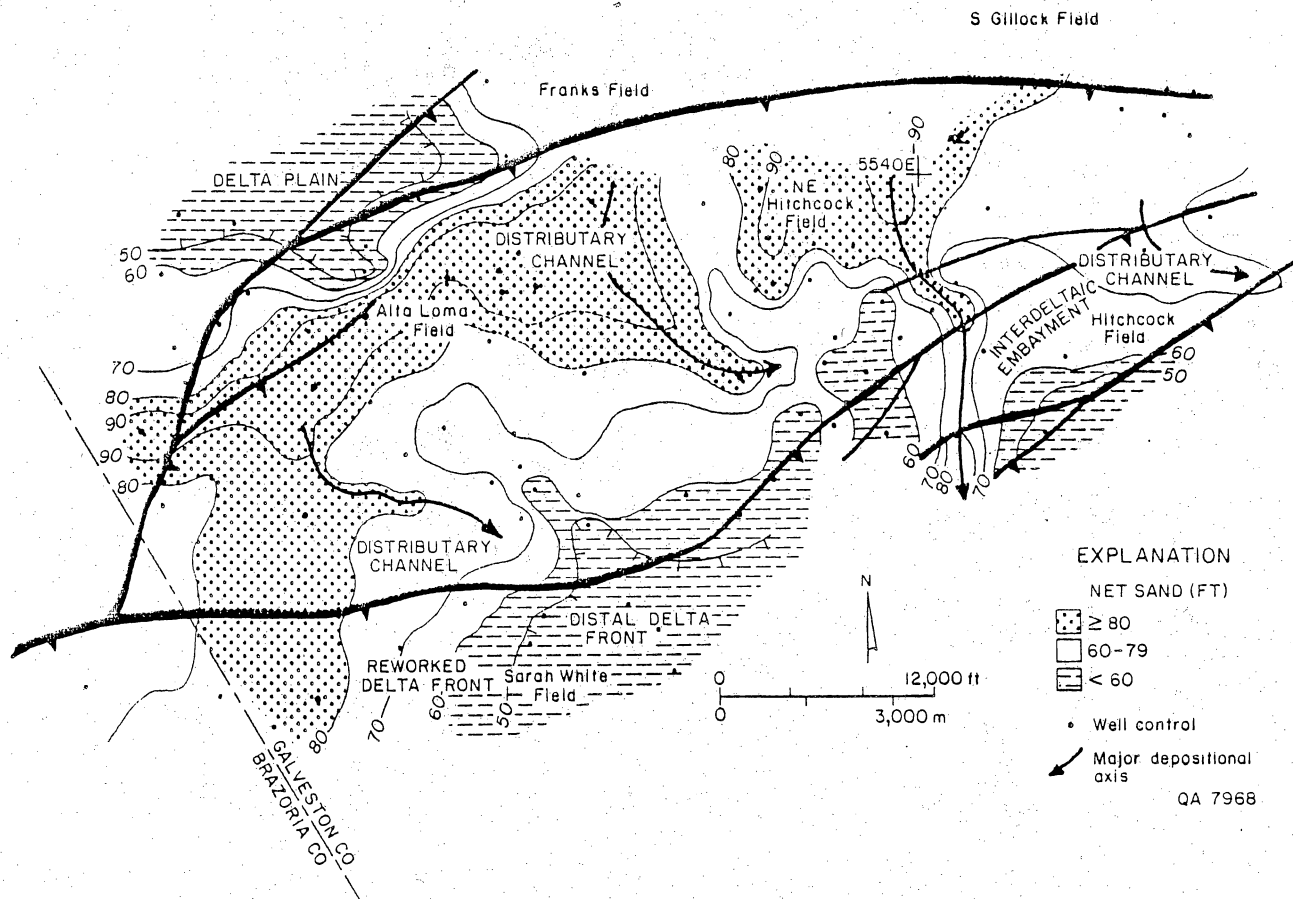


Figure 63. Net-sand and depositional facies map of the 4,240-ft sand (lower Miocene). The 4,240-ft sand, deposited as a series of lobate, wave-dominated deltas, is proposed as a primary brine-disposal sand because of its good sand continuity and thickness of 70 to 110 ft (21.3 to 33.5 m) in a strike-elongate band throughout the Northeast Hitchcock and Alta Loma field area.

DEPOSITIONAL SYSTEMS AND BRINE-DISPOSAL
POTENTIAL OF THE 5.460-FT SAND (LOWER MIOCENE).
NORTHEAST HITCHCOCK AND ALTA LOMA FIELDS

I. Interval Description

A. Sand-Body Geometry:

Sheet sand developed parallel to depositional strike, with minor dip-elongate elements on the basinward edge. Thickest sand (60 to 70 ft [18.3 to 21.3 m]) is concentrated in a strike-parallel band, roughly 1 mi (1.6 km) wide, within Northeast Hitchcock and Alta Loma fields.

B. Depositional Facies:

Barrier-island system, with barrier-island core facies ranging in width from 1.7 to 4.5 mi (2.7 to 7.2 km). The seaward edge is modified by small-scale tidal-channel and ebb-tidal delta deposits, approximately 0.5 mi (0.8 km) across at their widest. The barrier system pinches out over a short distance downdip into thin barrier-front and shelf sands and silts in the region of Sarah White field.

II. Reservoir Characteristics

A. Brine-Disposal Potential in Northeast Hitchcock and Alta Loma Fields:

Excellent, due to deposition of continuous sheet sands throughout the entire field area.

B. Brine-Disposal History:

None available in the study area.

C. Area(s) of Greatest Sand Thickness and Best Continuity For Brine Disposal:

Within barrier-island core facies in belt of 60 to 70 ft (18.3 to 21.3 m) of sand connecting Northeast Hitchcock and Alta Loma fields (refer to net-sand map).

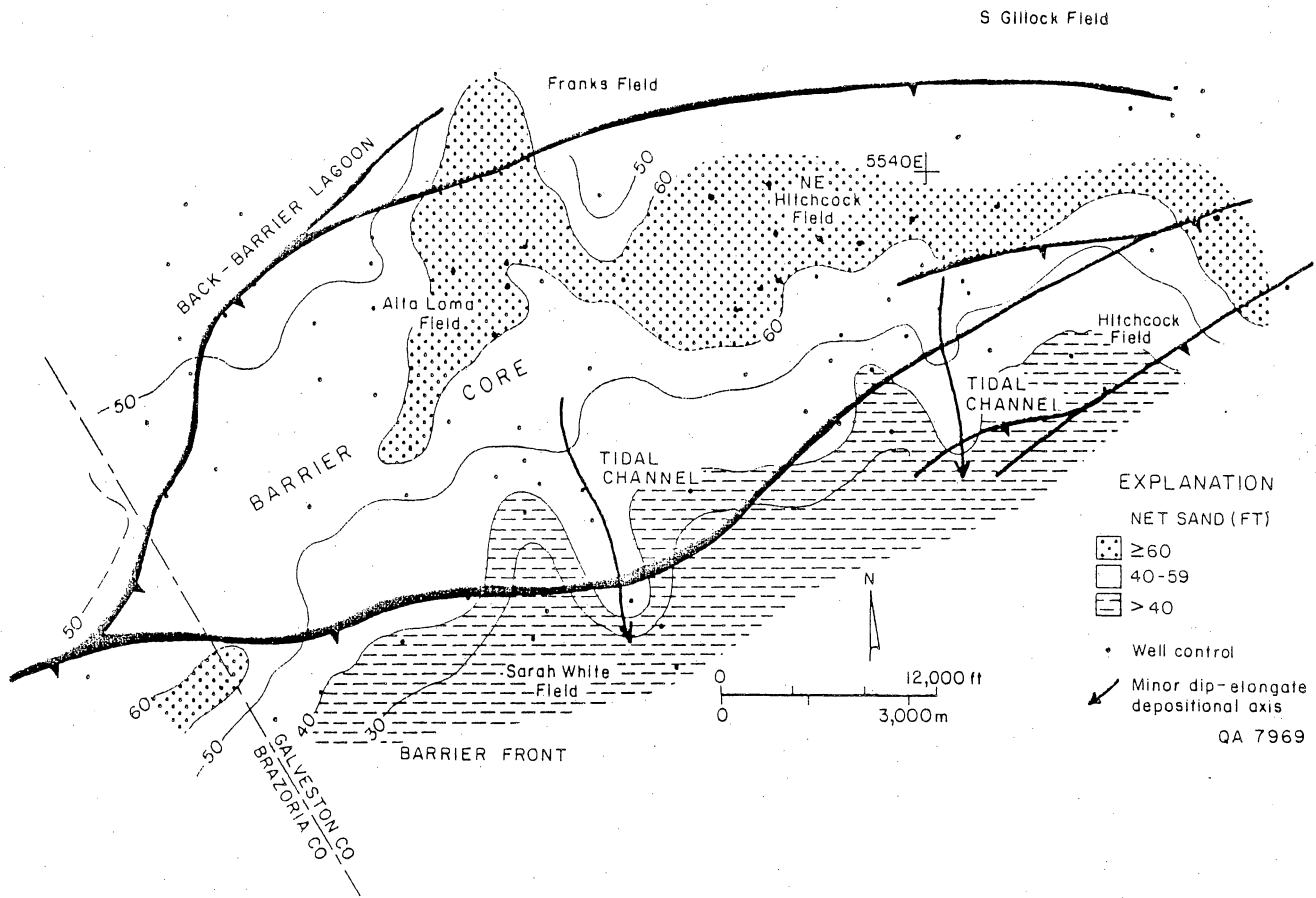


Figure 64. Net-sand and depositional facies map of the 5,460-ft sand (lower Miocene). Another primary sand for brine disposal, the 5,460-ft sand was deposited in a barrier-island environment. Maximum thickness of 70 ft (21.3 m) of sand in this simple unit is developed in a strike-parallel band linking Alta Loma and Northeast Hitchcock fields.

DEPOSITIONAL SYSTEMS AND BRINE-DISPOSAL
POTENTIAL OF THE 5,750-FT SAND (LOWER MIOCENE),
NORTHEAST HITCHCOCK AND ALTA LOMA FIELDS

I. Interval Description

A. Sand-Body Geometry:

Multiple lobate and digitate sand bodies (175 to 250 ft [53.3 to 76.2 m] thick) oriented parallel to depositional dip, cutting across the field area. Associated sheetlike, strike-parallel component of 150 to 175 ft (45.7 to 53.3 m) of sand is developed lateral to and downdip from these lobate sand bodies.

B. Depositional Facies:

Composite interval consisting of several progradational wedges, each consisting of small- to medium-sized wave-modified deltas ranging in width from 1.5 to 3.5 mi (2.4 to 5.6 km). Associated facies are laterally extensive delta-front and sandy shoreface deposits developed along depositional strike. Minor occurrence of sand-poor delta-plain deposits north of Alta Loma field.

II. Reservoir Characteristics

A. Brine-Disposal Potential in Northeast Hitchcock and Alta Loma Fields:

Fair to good, due to complex internal reservoir structure resulting from the composite nature of the interval, although it is the thickest of those chosen in this study.

B. Brine-Disposal History:

None available in the study area.

C. Area(s) of Greatest Sand Thickness and Best Continuity For Brine Disposal:

In wave-modified delta and delta-front deposits, east of Alta Loma field (wells 44, 51, and 55).

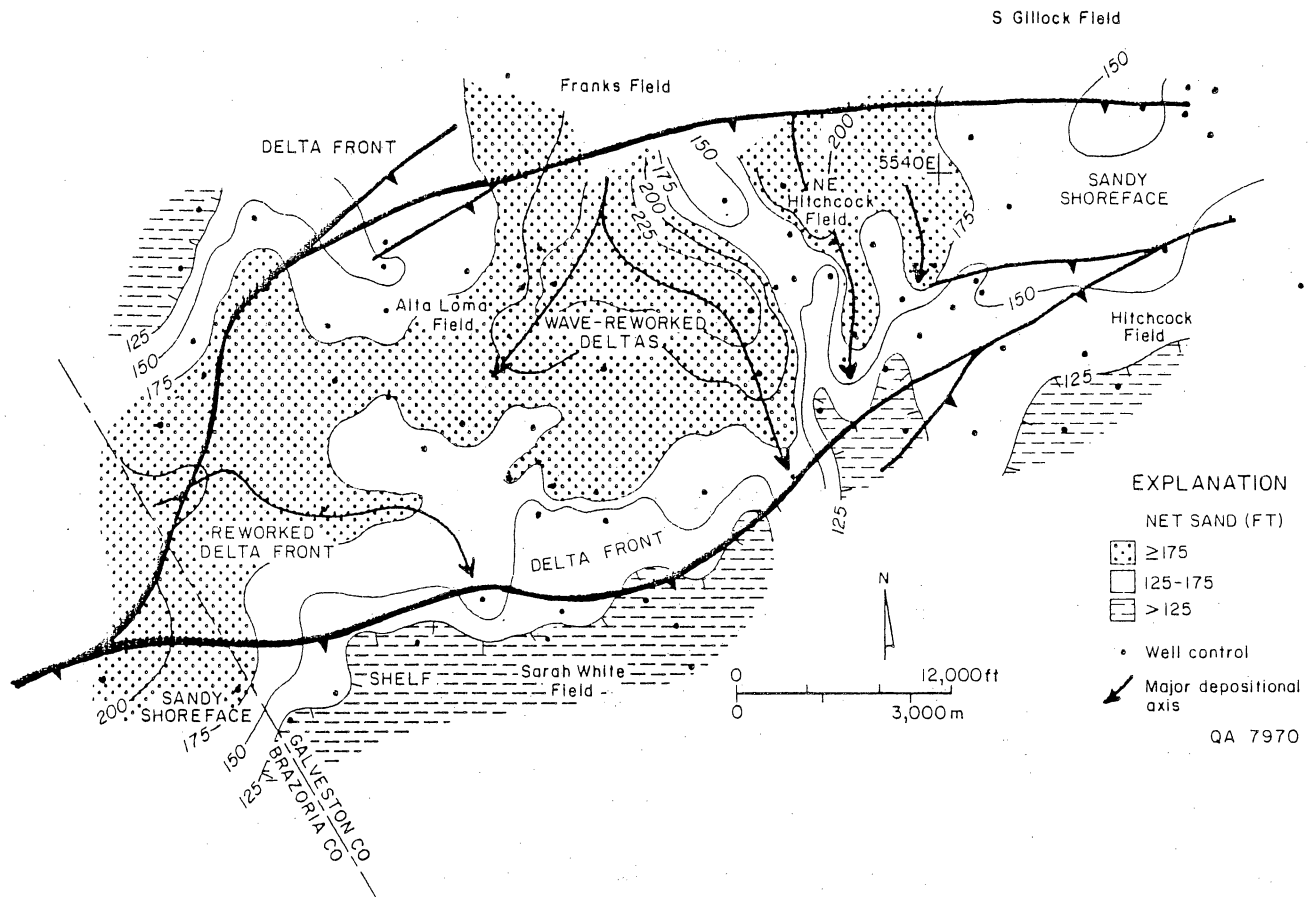


Figure 65. Net-sand and depositional facies map of the 5,750-ft sand (lower Miocene). Although this unit reaches a maximum thickness of up to 250 ft (76 m) in Northeast Hitchcock field, it may not be an optimum brine-disposal sand because of the high number of shale breaks and isolated sands as a consequence of having been deposited as a complex of several lobate wave-dominated deltaic sand bodies.

DEPOSITIONAL SYSTEMS AND BRINE-DISPOSAL
POTENTIAL OF THE 6.150-FT SAND (LOWER MIOCENE),
NORTHEAST HITCHCOCK AND ALTA LOMA FIELDS

I. Interval Description

A. Sand-Body Geometry:

Sheet sand developed parallel to depositional strike, reaching a maximum thickness of 64 ft (19.5 m) in the Sarah White field. Scattered occurrences of sand-poor pockets noted throughout the area.

B. Depositional Facies:

Single genetic unit consisting of a barrier-island system modified by tidal channels and back-barrier washover fans.

II. Reservoir Characteristics

A. Brine-Disposal Potential in Northeast Hitchcock and Alta Loma Fields:

Good to excellent, based on sheetlike sand geometry, although the unit is only about 50 ft (15.2 m) thick on average. Northeast Hitchcock field contains the greatest number of reservoir heterogeneities, but these are limited to small areas.

B. Brine-Disposal History:

None available in the study area.

C. Area(s) of Greatest Sand Thickness and Best Continuity For Brine Disposal:

Within barrier-island core facies in an irregular band (0.4 to 3.0 mi [0.6 to 4.8 km] wide) connecting Northeast Hitchcock field to an area south of Alta Loma field.

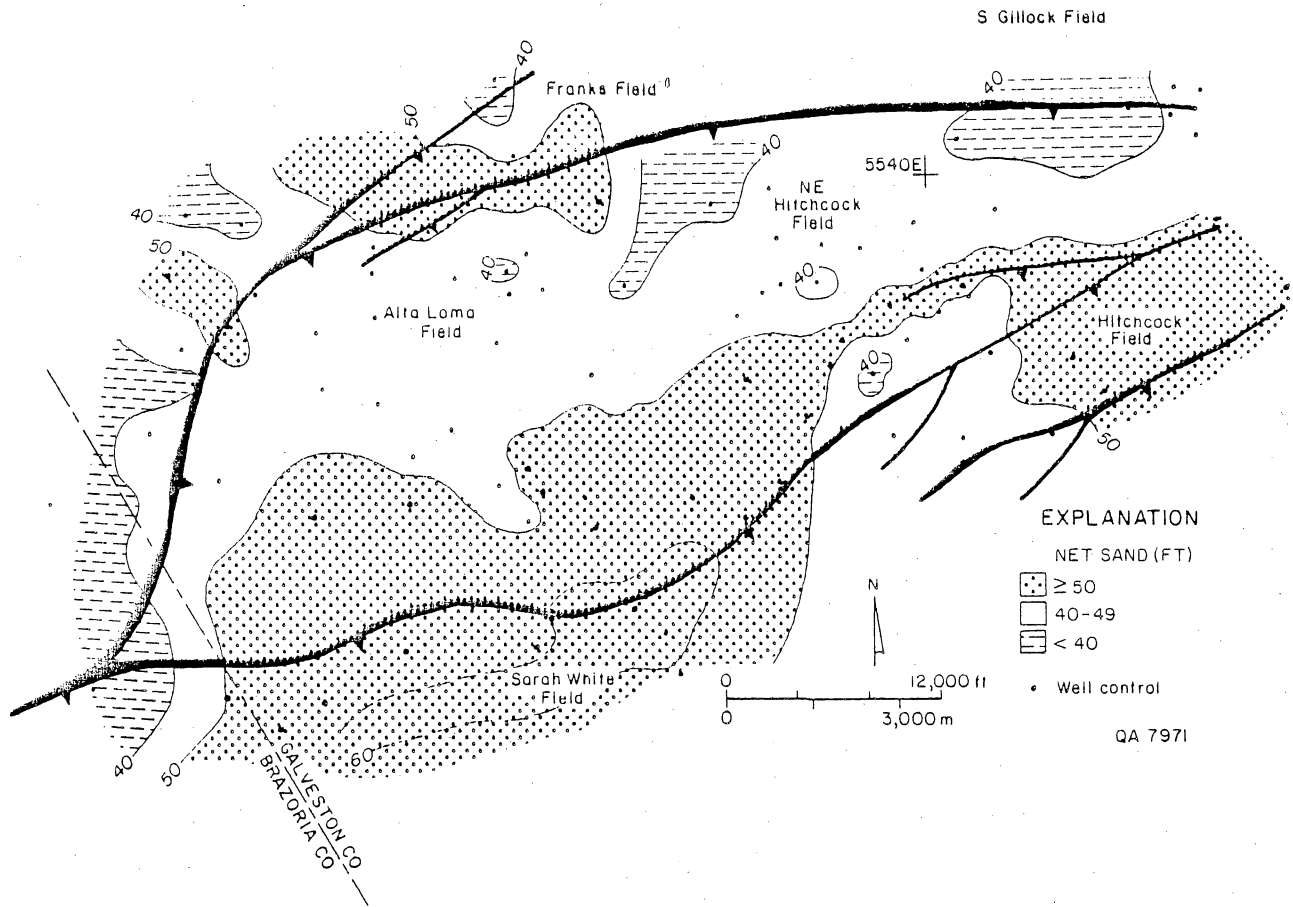


Figure 66. Net-sand map of the 6,150-ft sand (lower Miocene), an alternate brine-disposal sand. Good sand continuity is developed throughout Alta Loma and Northeast Hitchcock fields, although maximum sand thickness is only 60 ft. The strike-parallel net sand trend is consistent with a barrier-island or wave-dominated coastline environment (see SP log facies map, fig. 67), where high wave energy winnowed muds, resulting in the deposition of a clean, homogenous sand body.

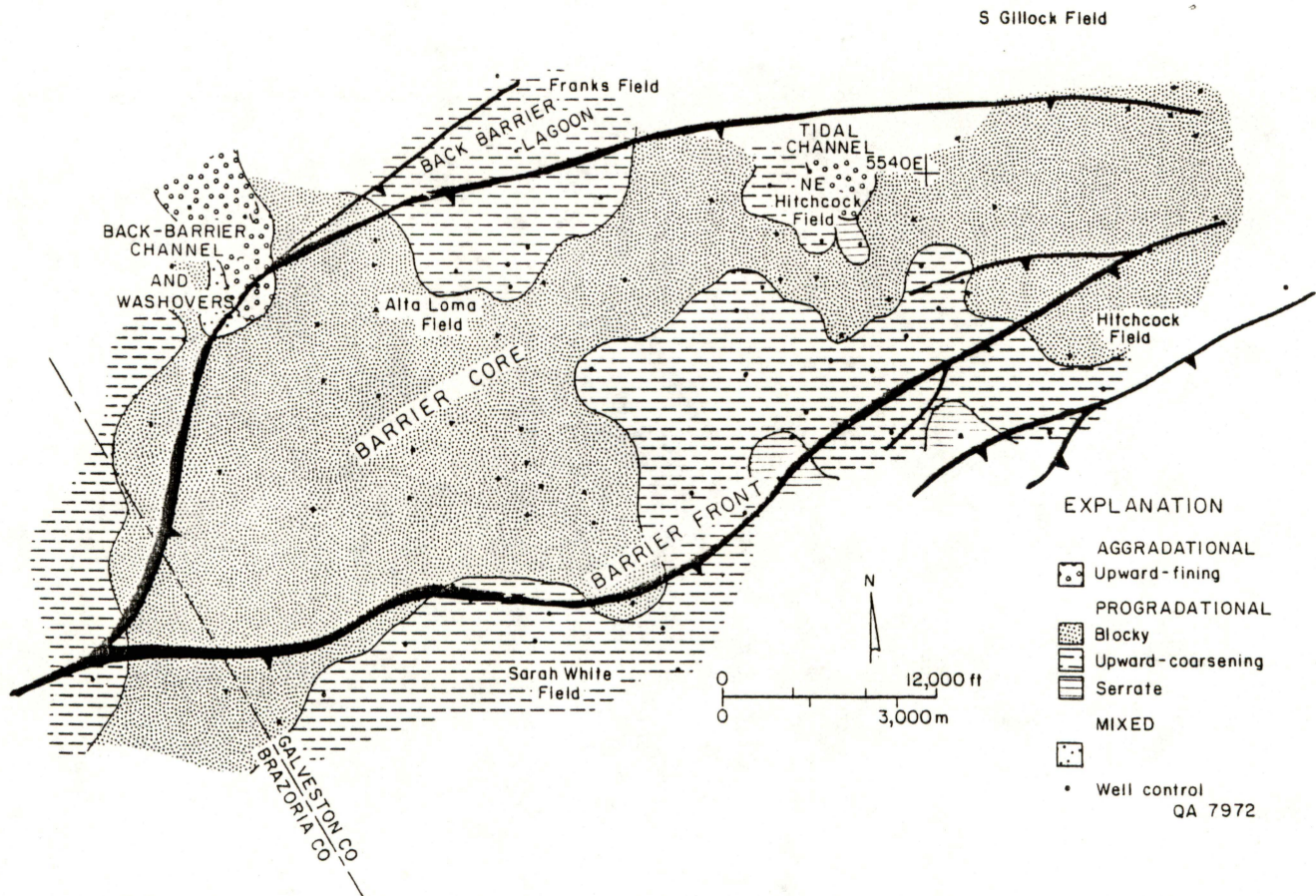


Figure 67. SP log facies map of the 6,150-ft-sand (see net-sand map, fig. 66). The 6,150-ft sand was deposited in a barrier-island environment and is a simple, homogenous sand throughout most of the fault block containing Alta Loma and Northeast Hitchcock fields. Minor shale breaks occur in tidal-channel deposits (Northeast Hitchcock field) and back-barrier channel and washover deposits (west of Alta Loma field).

an alternate choice for brine-disposal. Favorable properties of the 2,030-ft sand that make it attractive as a brine-disposal sand are shallow depth and thickness of up to 95 ft (29 m) in a sheetlike area in the northern half of the Northeast Hitchcock - Alta Loma fault block. A major factor that detracts from the brine-disposal potential of the 2,030-ft sand is the occurrence of several lenticular distributary-channel sand bodies surrounded by muddy delta-plain and interdistributary-marsh deposits (fig. 71).

POTENTIAL SITES FOR BRINE DISPOSAL, NORTHEAST HITCHCOCK FIELD

Although the proposed brine-disposal sands were mapped throughout the entire fault block containing Northeast Hitchcock and Alta Loma fields, a brine-disposal site only within Northeast Hitchcock field is more practical because it is in the area of current methane and brine co-production. The optimum brine-disposal site in Northeast Hitchcock field should be located where the combined thicknesses of the three primary disposal sands are greatest, and also where these sands are most laterally continuous. Therefore, the three primary sands at the brine-disposal site should be relatively free from aquifer discontinuities introduced by the presence of lenticular or isolated facies such as fluvial, distributary, or tidal channels, washover fans, and overbank deposits such as levees and crevasse splays.

On the basis of these criteria and other economic considerations, the Phillips Thompson No. 1 well (number 26 in this study) has been selected as the initial site for brine disposal. Within the Phillips Thompson No. 1 well, a total of 218 ft (66.4 m) of sand from the three primary brine-disposal sands is intersected. These sands at the disposal site were deposited in barrier-island core (3,780 ft and 5,460 ft) and wave-reworked delta-front (4,240 ft) environments. These depositional

DEPOSITIONAL SYSTEMS AND BRINE-DISPOSAL
POTENTIAL OF THE 2,800-FT SAND (UPPER MIOCENE),
NORTHEAST HITCHCOCK AND ALTA LOMA FIELDS

I. Interval Description

A. Sand-Body Geometry:

System of lenticular, dip-elongate pods crosscutting Northeast Hitchcock and Alta Loma fields. These sands reach combined thicknesses of up to 70 ft (21.3 m) in Alta Loma field, and individual, thinner (20 to 40 ft [6 to 12 m]) pods associated with sand pinch-outs are located in Northeast Hitchcock field.

B. Depositional Facies:

Single genetic unit consisting of a fluvial system dividing Northeast Hitchcock and Alta Loma fields into elongate bands of individual (upward-fining SP pattern) and aggraded (blocky SP pattern) point-bar sands, and levee and floodplain silts and muds (serrate SP pattern). Progradational sands in Sarah White field may represent lacustrine delta deposits.

II. Reservoir Characteristics

A. Brine-disposal Potential in Northeast Hitchcock and Alta Loma Fields:

Alta Loma field area--fair

Other areas--poor, due to abundance of lenticular, isolated point-bar sands encased in floodplain muds.

B. Brine-Disposal History:

West Alta Loma field: 17,000 bbl per month in well 88, situated in stacked point-bar sands.

C. Area(s) of Greatest Sand Thickness and Best Continuity For Brine Disposal:

Alta Loma field, in area of wells 55, 62, and 69.

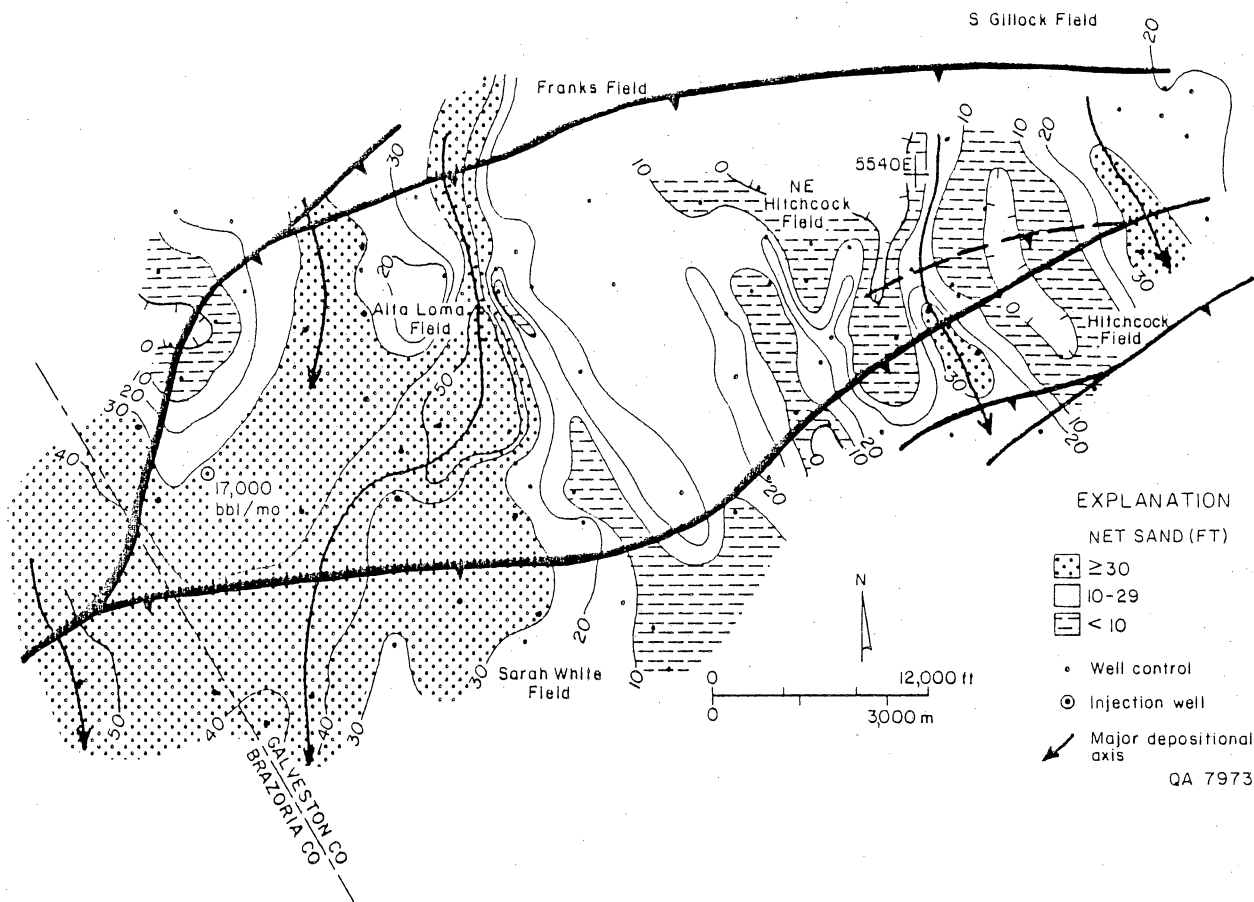


Figure 68. Net-sand map of the 2,800-ft sand, a typical upper Miocene fluvial sand, which is a poor choice for brine disposal because of the isolated, lenticular nature of point-bar deposits (see fig. 69). Although this sand has a fair injection potential in Alta Loma field, where it has a thickness of up to 55 ft (16.8 m) due to the presence of several stacked point bars, the occurrence of many sand pinch-outs in Northeast Hitchcock field precludes this unit as a good sand for brine disposal.

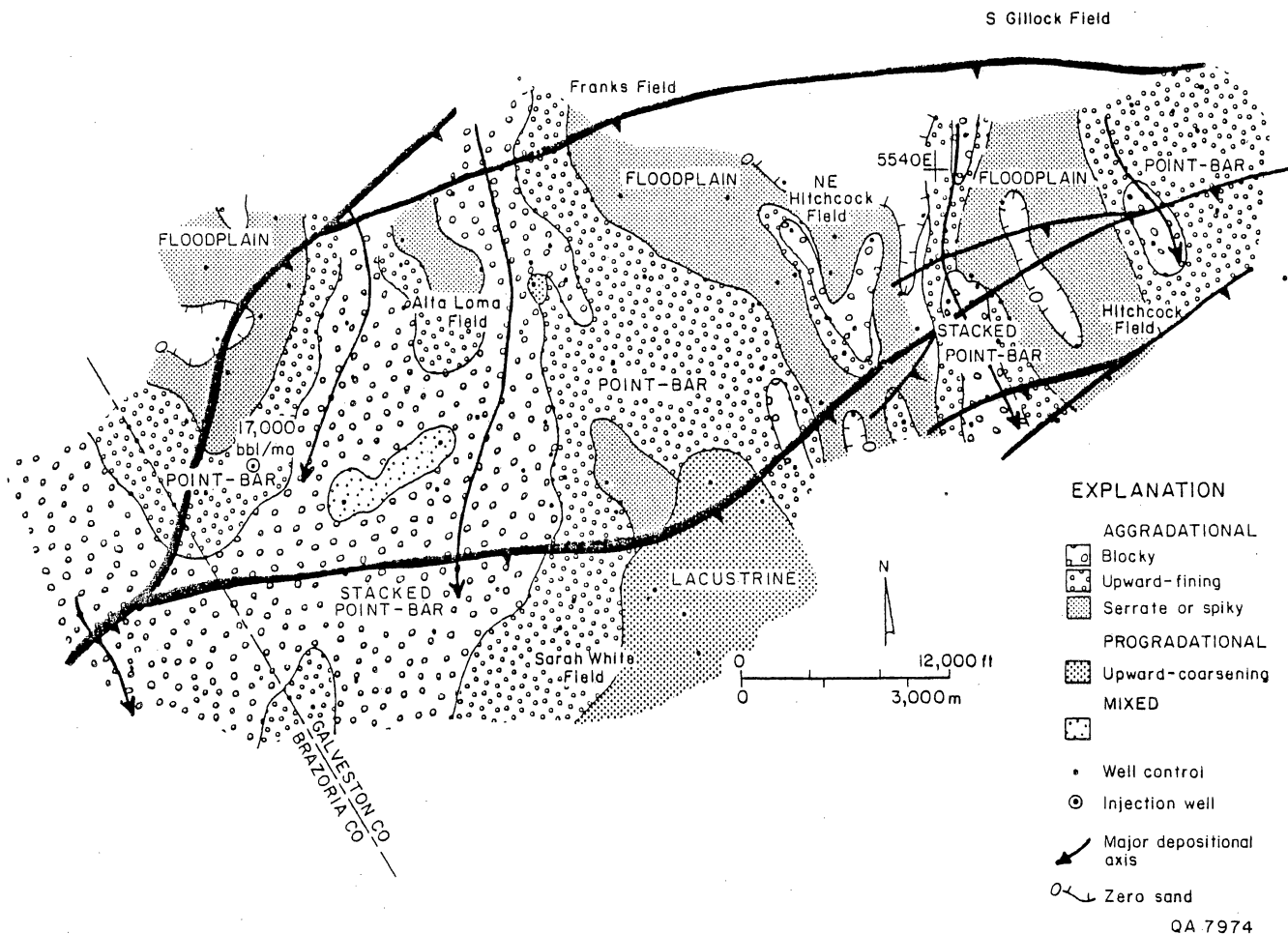


Figure 69. SP log facies of the 2,800-ft sand (upper Miocene). This sand is a poor choice for brine disposal because it is composed of isolated, lenticular ribbons of fluvial-channel sand encased in floodplain muds. Refer to figure 68 for the net-sand map of the 2,800-ft sand.

environments are prime brine-disposal facies. Good alternate disposal sites for the 3,780-ft, 4,240-ft, and 5,460-ft sands are in wells 21, 25, 27, 31, and 34.

Assuming that all of the pore volumes in the three primary sands can be contacted within the Northeast Hitchcock - Alta Loma fault block, a total volume of 8,105,700,000 bbl is available for brine disposal (table 9). Even within Northeast Hitchcock field, which constitutes approximately 30 percent of the fault block, a volume of approximately 2,000,000,000 bbl of pore space is available, a number that far exceeds the estimated total of 36,000,000 bbl of brine that are planned for disposal from the Northeast Hitchcock co-production project.

POTENTIAL PORE VOLUMES AVAILABLE IN PROPOSED BRINE-DISPOSAL SANDS, NORTHEAST HITCHCOCK AND ALTA LOMA FIELDS

Most of the Miocene sands proposed for brine disposal by this study are highly continuous throughout the Northeast Hitchcock - Alta Loma fault block. Other, minor faults within this block offset Miocene units only 40 ft (12.2 m) or less and generally do not serve to isolate the reservoirs into separate, structurally bounded pieces.

Potential pore volumes in the proposed sands in Northeast Hitchcock and Alta Loma fields were calculated by determining the total volume of sand 40 ft (12.2 m) or more in thickness within the Northeast Hitchcock - Alta Loma fault block. The volumes of sand thus derived were multiplied by a factor of 25 percent, which represents the weighted average porosity ranging from 16 to 30 percent for Miocene sands in the Texas Gulf Coast. Miocene porosity values were taken from Doyle (1979), Morton and others (1985), and Galloway and others (1986).

DEPOSITIONAL SYSTEMS AND BRINE-DISPOSAL
POTENTIAL OF THE 2,030-FT SAND (UPPER MIOCENE),
NORTHEAST HITCHCOCK AND ALTA LOMA FIELDS

I. Interval Description

A. Sand-Body Geometry:

Dip-elongate system of lenticular sands, 50 to 70 ft (15.2 to 21.3 m) thick, merging updip into a sheetlike system of sands, 70 to 95 ft (21.3 to 28.9 m) thick. Numerous occurrences of sand-poor areas throughout the downdip half of the study area. Bifurcating trends noted in lenticular sand bodies in Alta Loma field.

B. Depositional Facies:

Fluvial-dominated deltaic system, represented by a transition from upper delta-plain facies in Franks field to a lower delta-plain system in Northeast Hitchcock and Alta Loma fields. Distributary channels transect the lower delta-plain facies and merge downdip into upward-coarsening delta-front deposits.

II. Reservoir Characteristics

A. Brine-disposal Potential in Northeast Hitchcock and Alta Loma Fields:

Fair to medium, due to occurrence of numerous lenticular sands separated by floodplain and interdeltic muds. Redeeming features are shallow depth (economically favorable) and possibly higher permeabilities along main depositional axes.

B. Brine-disposal history:

Hitchcock field: 72,000 bbl per month in well 14, situated in crevasse splay sands lateral to channel axes.

C. Area(s) of greatest sand thickness and best continuity for brine disposal:

In stacked distributary-channel sands within Northeast Hitchcock field (wells 18, 20, and 26) and in a similar area east of Alta Loma field (wells 38, 43, and 44).

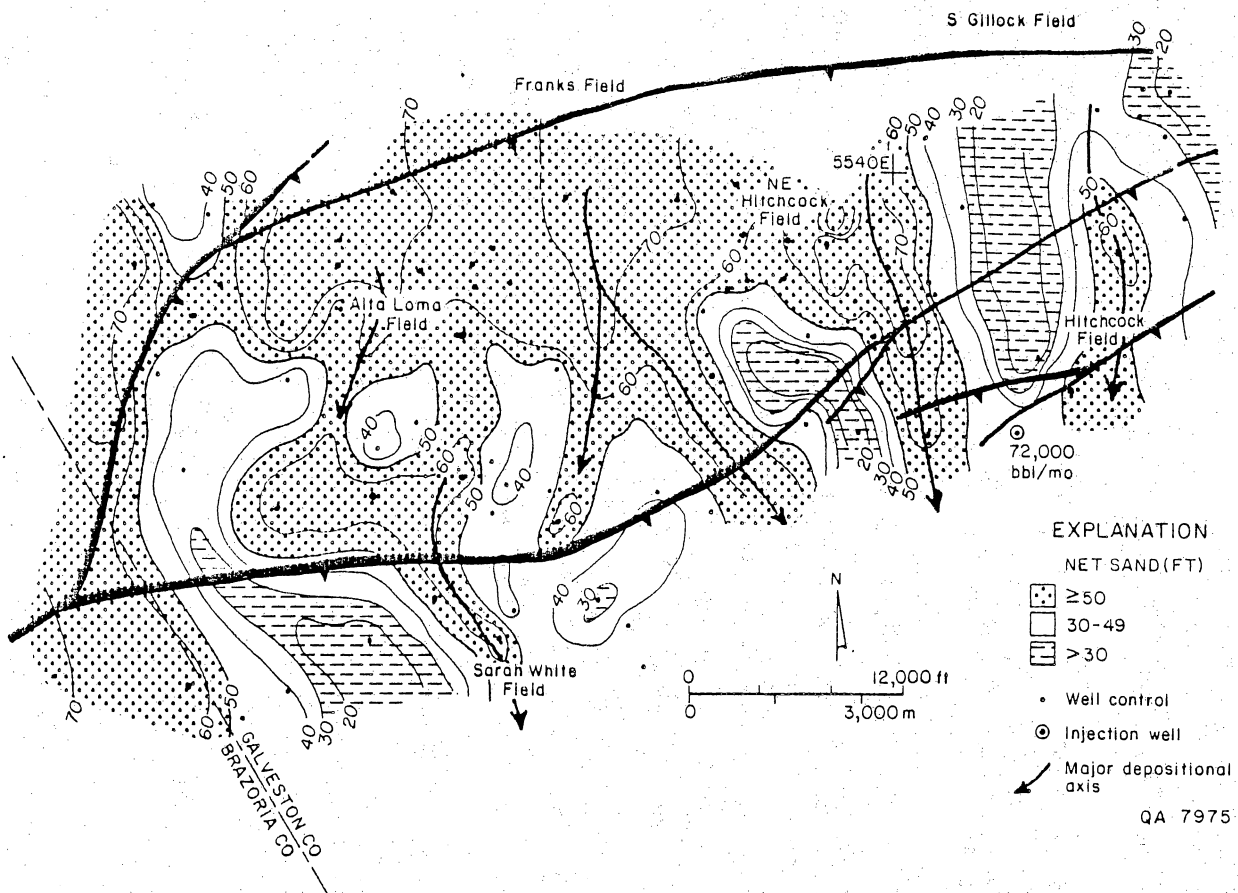


Figure 70. Net-sand map of the 2,030-ft sand (upper Miocene), which is included as an alternate choice for brine disposal because of (1) its shallow depth of burial, and (2) extensive development of 50 to 75 ft of sand in Alta Loma and Northeast Hitchcock fields. However, several sand-poor areas exist within this unit, owing to the lenticular nature of distributary sand bodies in the southern part of the study area (see fig. 71).

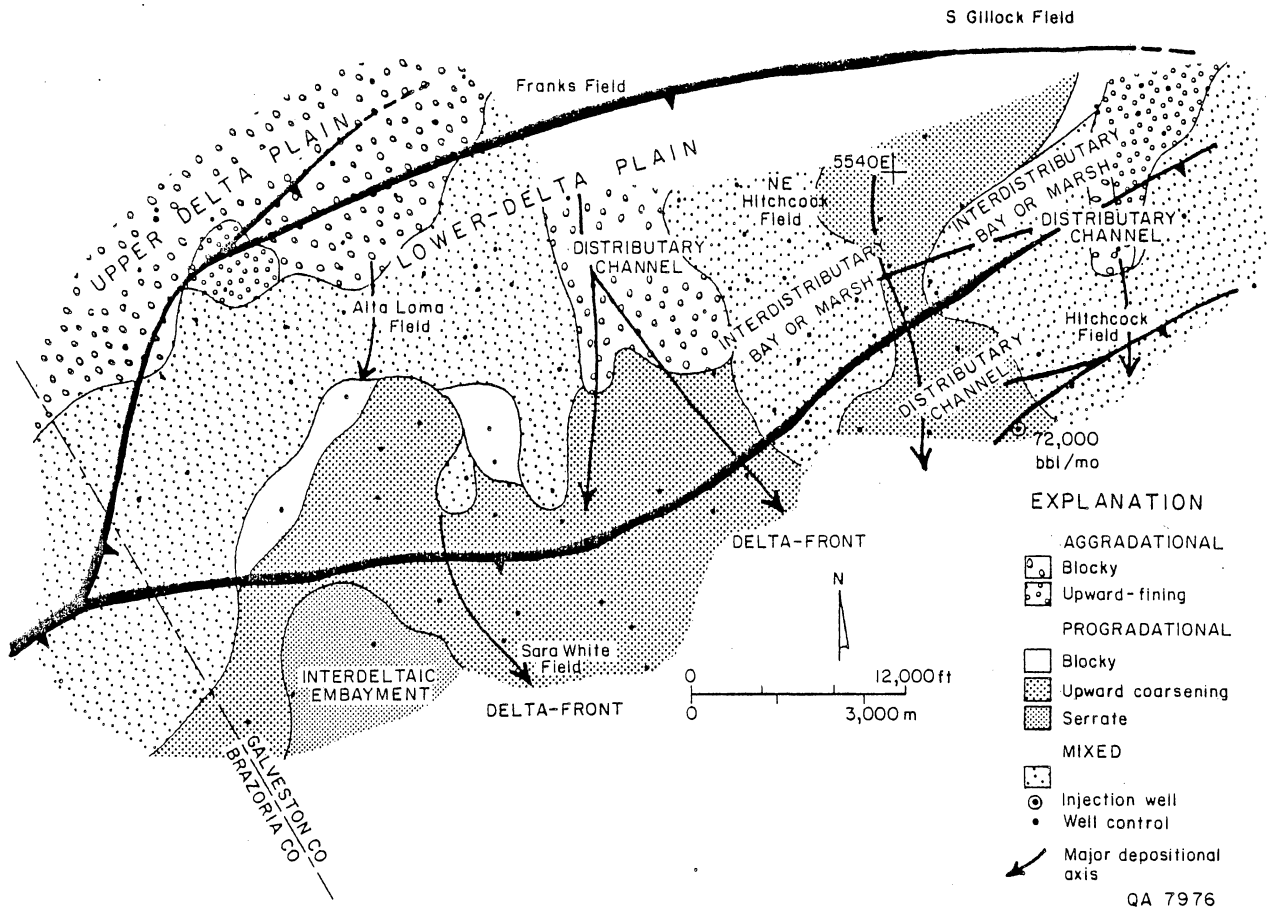


Figure 71. SP log facies map of the 2,030-ft sand (compare with net-sand map, fig. 70). Although this shallow unit is a good alternate choice for brine disposal, several heterogeneities exist because of the occurrence of lenticular distributary sand bodies and the presence of muddy interdistributary bay and marsh deposits.

Table 9. Volumes available for brine disposal into sand greater than 40 ft thick calculated for the three primary and three alternate brine-disposal Miocene sands within the fault block containing Northeast Hitchcock and Alta Loma fields.

A. <u>Primary brine-disposal sands</u>		
<u>Sand</u>	<u>Pore volume (bbl)</u>	<u>Limiting factors</u>
3780 ft	2,903,700,000	Virtually none: sheet sand with minor heterogeneities due to tidal channels and washovers.
4240 ft	3,071,000,000	Minor number of sand-poor areas separated by lobate distributary-channel sand bodies.
5460 ft	2,131,000,000	Virtually none: barrier-island sheet sand.
<u>Total pore volume, primary sands:</u>		
	8,105,700,000 bbl	
B. <u>Alternate brine-disposal sands</u>		
<u>Sand</u>	<u>Pore volume (bbl)</u>	<u>Limiting factors</u>
2030 ft	1,764,900,000	High number of reservoir heterogeneities due to fluvial channel sands encased in floodplain muds.
5750 ft	8,030,700,000	Contains numerous shale breaks and permeability barriers. Several genetic subunits in the 5750-ft sand result in a complex internal structure.
6150 ft	1,979,500,000	Virtually none: barrier-island sheet sand.
<u>Total pore volume, alternate sands:</u>		
	11,775,100,000 bbl	
<u>Total pore volume, all sands:</u>		
	19,880,800,000 bbl	

Calculated pore volumes for each of three primary and three alternate sands are summarized in table 8. Values listed in this table are optimum, calculated with the assumption that the number of interbedded shale stringers is minimal and that no major pore-filling cements are present in the sands. Certainly these two factors must still be taken into account when calculating a lower, more accurate amount of net pore volume. However, Miocene sands in this region are not deeply buried and are weakly cemented and poorly consolidated. Additionally, most of the shale stringers in these sands tend to occur on the updip and downdip margins of the system in which they were deposited, which in the study area are mostly confined to regions peripheral to Northeast Hitchcock and Alta Loma fields.

The effects of cementation due to diagenesis and permeability variations arising from the distribution of heterogeneous depositional facies will be assessed by analysis of whole-core and sidewall-core samples taken from the first brine-disposal well in Northeast Hitchcock field as the co-production project progresses. Not only will basic parameters such as sand permeability and porosity be evaluated, but also fluid-rock compatibility tests, stimulation fluid studies, and water sensitivity tests will be conducted in order to judge how effectively the original pore fluids may be displaced by the injected brines, and what effect the injected brines will have on the rock matrix.

CONCLUSIONS

Three lower Miocene sands, the 3,780 ft, 4,240 ft, and the 5,460 ft, should be capable of receiving 7,500 bbl of brine per day from a three-well disposal site centered around the Phillips Thompson No. 1 well in Northeast Hitchcock field in Galveston County, Texas. These sands, each generally 70 to 90 ft (21.3 to 27.4 m) thick in the

fault block containing Northeast Hitchcock field and adjacent Alta Loma field, are highly continuous as a consequence of having been deposited in barrier-island, shoreface, and wave-reworked delta-front environments.

In further support of selection of these sands for disposal of large volumes of brine, other lower Miocene sands in the neighboring Hastings West field in Brazoria County, which are correlative and analogous to the 3,780-ft, 4,240-ft, and 5,460-ft sands, are capable of receiving up to 9,500 bbl of brine per day per well. In Northeast Hitchcock field alone, a volume of approximately 2,000,000,000 bbl is available for brine disposal into the three primary proposed sands. The estimated future disposal of only 36,000,000 bbl of brine in the lifetime of the Northeast Hitchcock co-production project constitutes only 2 percent of the total available pore space.

Other factors that may detract from the optimum calculated pore volume available for brine disposal in the three primary and three alternate proposed disposal sands in Northeast Hitchcock field are heterogeneities caused by the presence of thin, laterally discontinuous shale stringers and cementation caused by diagenesis. Future analysis of whole-core and sidewall-core samples taken from the initial brine-disposal well in the Northeast Hitchcock field should result in a more accurate determination of reservoir discontinuities affecting the brine-injection capacity of the proposed disposal sands.

COMPATIBILITY OF FRIO 'A' AND MIOCENE FORMATION WATERS, NORTHEAST HITCHCOCK FIELD, GALVESTON COUNTY

by M. P. R. Light

Five Miocene formation-water analyses from Galveston County (table 10) (Kreitler and Richter, 1986) were averaged and compared with two Frio 'A' formation-water analyses (table 11) from the co-production Delee No. 1 well in the Northeast Hitchcock field, Galveston County, Texas. The Frio 'A' water analyses were conducted at the Bureau of Economic Geology. Two Miocene disposal depths were assumed, one at 4.050 ft (1.235 m) (118.4°F, 48°C) and the other at 5.850 ft (1.783 m) (146.3°F, 63.5°C) for computation purposes.

The equilibrium distribution of inorganic aqueous species in Frio 'A' and Miocene fluids and the different combinations of these waters at surface (separator) and formation temperature and pH values were estimated from chemical analyses (tables 12 and 13). The Bureau of Economic Geology's SOLMNEQ computer program (Kharaka and Barnes, 1973) was used to perform 40 equilibrium computations with these average analyses. A detailed discussion on the use of the SOLMNEQ program and uncertainties related to data acquisition, analyses, and computation is given in the "Compatibility of Hackberry and Miocene formation waters, Port Arthur Field, Texas" section of this report and will not be discussed further here.

Silica and carbonates appear to be oversaturated in Frio 'A' waters at formation (215°F, 101.7°C) and separator (180°F, 82.2°C) temperatures for pH values greater than 6 (fig. 72). Frio 'A' waters are in equilibrium with calcite at formation temperature (215°F, 101.7°C) when the pH is about 5.75, or 1.76 units less than the measured pH. Silica, carbonates, and barite are all oversaturated at temperatures lower than the Frio 'A' formation temperature at the measured pH (7.51) (fig. 73). Calcite also remains oversaturated at Miocene formation temperatures at the mean pH measured in Miocene formation water (6.92) (fig. 74).

Table 10. Analyses of Miocene formation waters from Galveston County
(Kreitler and Richter, 1986).

Sample No.	680103	691216	N.R.	741106	N.R.
Latitude	7°29.352	7°29.433	7°29.350	7°29.353	7°29.375
Longitude	94.866	94.967	94.884	94.886	94.923
Depth	4,018 ft	6,195 ft	7,500 ft	5,800 ft	7,000 ft
pH	6.9	6.8	7.0	7.1	6.8
T.D.S.	116,832	130,908	141,500	124,000	133,300
Na	40,330	46,689	50,000	43,200	46,689
Ca	3,400	3,040	3,300	3,100	3,040
Mg	986	952	1,100	910	952
Cl	71,000	80,100	87,000	77,100	80,100
HCO ₃	126	127	200	102	127
SO ₄	N.R.	N.R.	630	1	N.R.

Table 11. Analyses of Frio 'A' formation waters
 from the Delee No. 1 well
 Northeast Hitchcock field,
 Galveston County (BEG, 4/85, 9/85).

No.	86-157	86-158
Depth	9,100 ft	9,100 ft
pH	7.39	7.63
K	138	135
Na	16,400	16,400
Ca	495	490
Mg	78.2	78.3
Sr	33	33
Ba	14.4	8.0
Li	3.9	3.9
B	43	44
Cl	25,600	26,000
HCO ₃	730	780
SO ₄	29	31

All aqueous species expressed in mg/L.

Table 12. Temperature, pH, and concentration of aqueous species in combinations of Frio 'A' and Miocene waters, Northeast Hitchcock field.

	100% Frio	75% Frio	50% Frio	25% Frio	100% Miocene	Miocene Depth ft
Test	201	202	203	204	205	
Temp.	82.2°C	73.65°C	65.1°C	56.55°C	48°C	4050
pH	7.51	7.3625	7.215	7.0675	6.92	
Test	201	206	207	208	209	
Temp.	82.2°C	77.53°C	72.85°C	68.18°C	63.5°C	5850
pH	7.51	7.3625	7.215	7.0675	6.92	
Test	201	220	221	222	223	
Temp.	82.2°C	73.65°C	65.1°C	56.55°C	48°C	4050
pH	7.51	7.23	6.96	6.68	6.4	
Test	201	224	225	226	227	
Temp.	82.2°C	77.53°C	72.85°C	68.18°C	63.5°C	5850
pH	7.51	7.2	6.88	6.57	6.25	
Ca	492.5	1163.4	1834.25	2505.1	3176.0	
Mg	78.25	303.7	529.1	754.6	980.0	
Na	16400.0	23645.4	30890.8	38136.2	45381.6	
Cl	25800.0	39115.0	52430.0	65745.0	79060.0	
HCO ₃	755.0	600.4	445.7	291.1	136.4	

Table 13. Assumed temperatures of Miocene waters at varying pH.

Test	Temp.	pH	Test	Temp.	pH
213	48°C	4	216	63.5°C	4
214	48°C	5	217	63.5°C	5
215	48°C	6	218	63.5°C	6

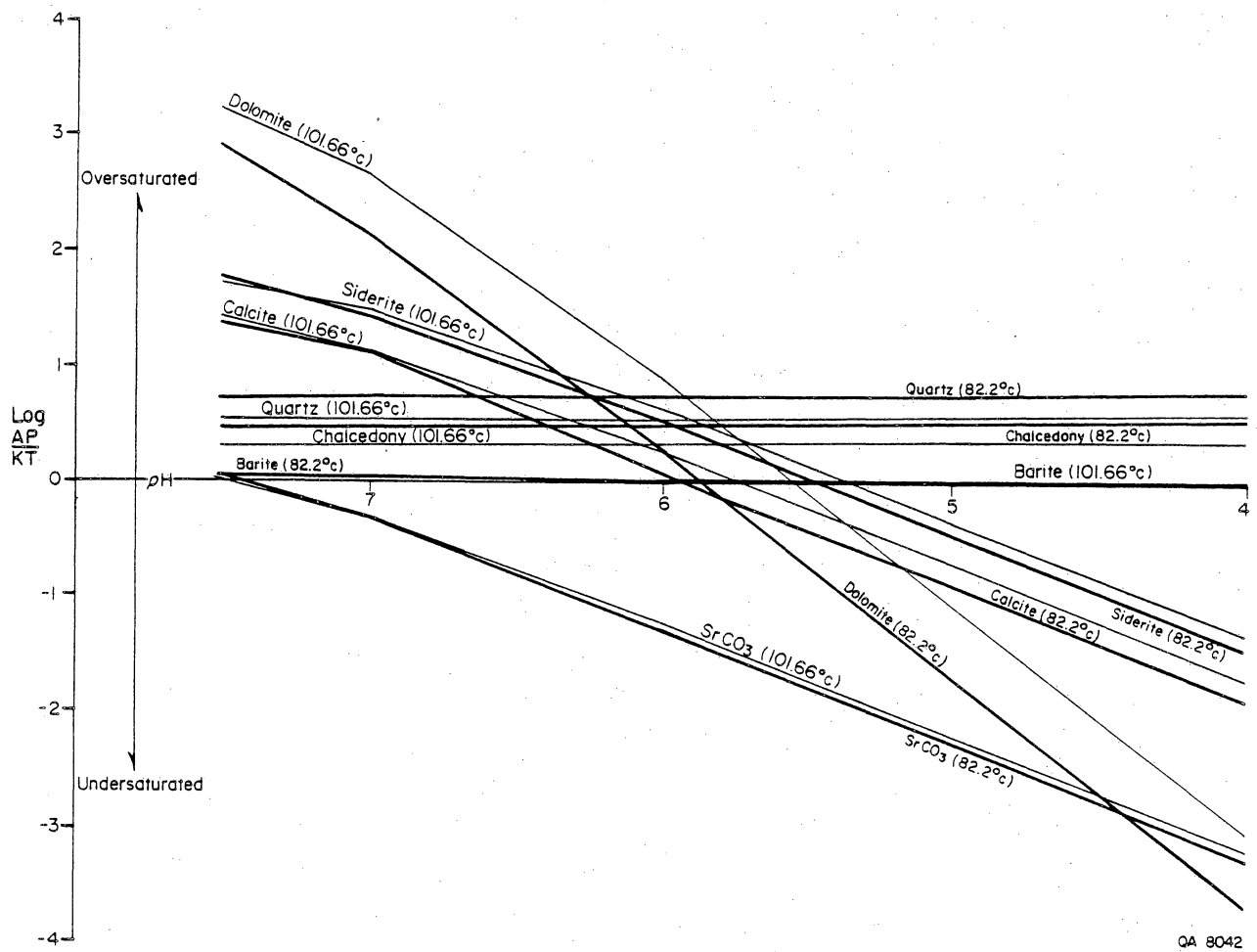
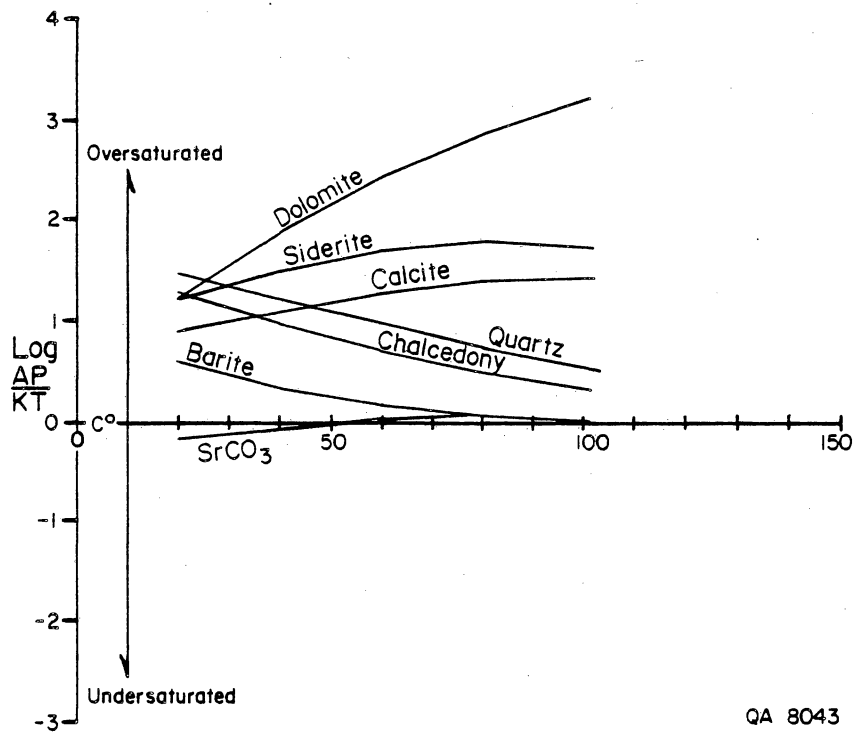


Figure 72. Saturation indices of silica and carbonates in Frio 'A' formation waters Delee No. 1 well, versus pH at formation temperature (215°F, 101.7°C) and separator temperature (180°F, 82.2°C).



QA 8043

Figure 73. Saturation indices of silica and carbonates in Frio 'A' formation waters Delee No. 1 well, versus temperature at measured pH (7.51).

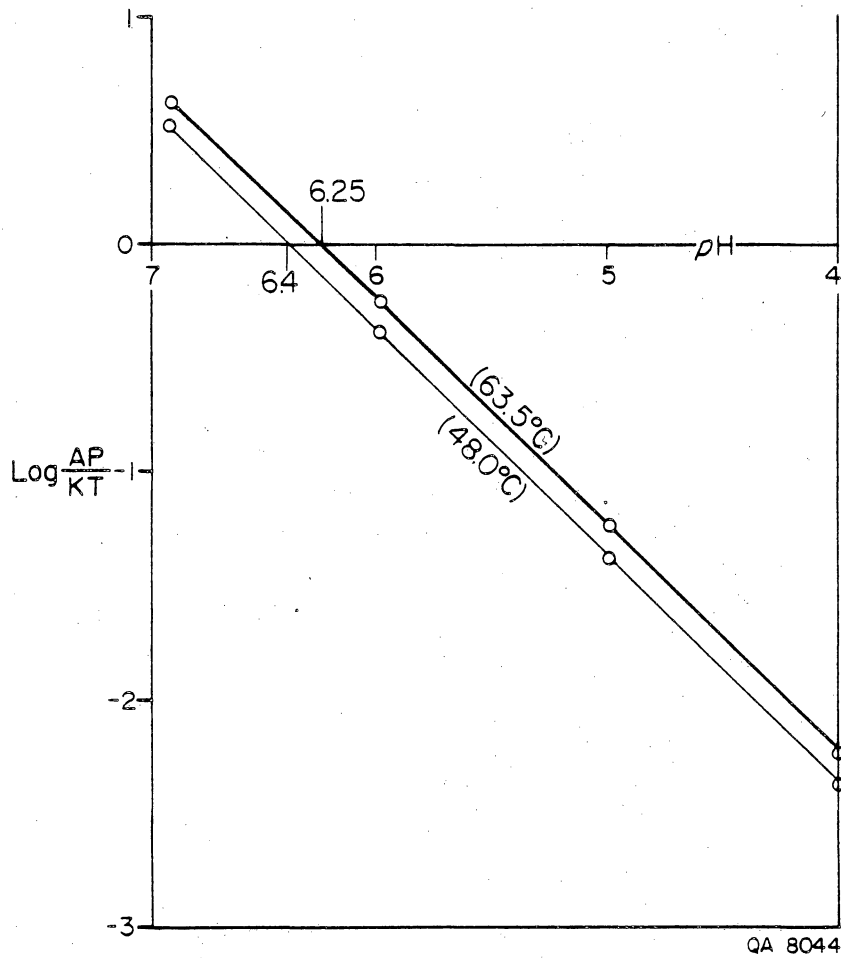


Figure 74. Saturation indices of calcite versus pH at Miocene formation temperatures of 118.4°F (48°C) and 146.3°F (63.5°C).

Carbonates remain oversaturated in nearly all mixtures of Frio 'A' formation waters with Miocene fluids at estimated formation temperatures (figs. 75 and 76). Because the SI indices are generally larger than 1 (Tomson and O'Day, 1987), inhibitors will need to be injected into the produced fluids to prevent scaling both in surface equipment and in the Miocene disposal formation.

ACKNOWLEDGMENTS

Funding for this research was provided by the Gas Research Institute under contract no. 5084-212-0924.

ICP spectrometer analyses of Frio 'A' waters were done at the Mineral Studies Laboratory by Steven W. Tweedy under the direction of David W. Koppelaar. The manuscript was reviewed by S. P. Dutton. Illustrations were drafted under the direction of Richard L. Dillon. Word processing was by Dottie Johnson under the direction of Lucille C. Harrell. Editing was by Mary Ellen Johansen.

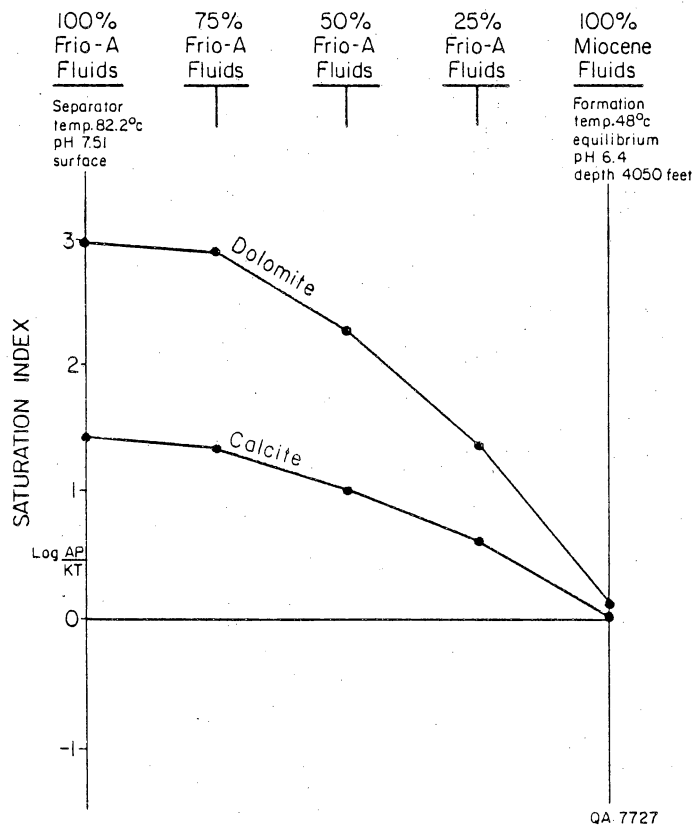


Figure 75. Saturation indices of various mixes of Frio 'A' and Miocene waters at a Miocene formation temperature of 118.4°F (48°C) and measured pH of 6.4.

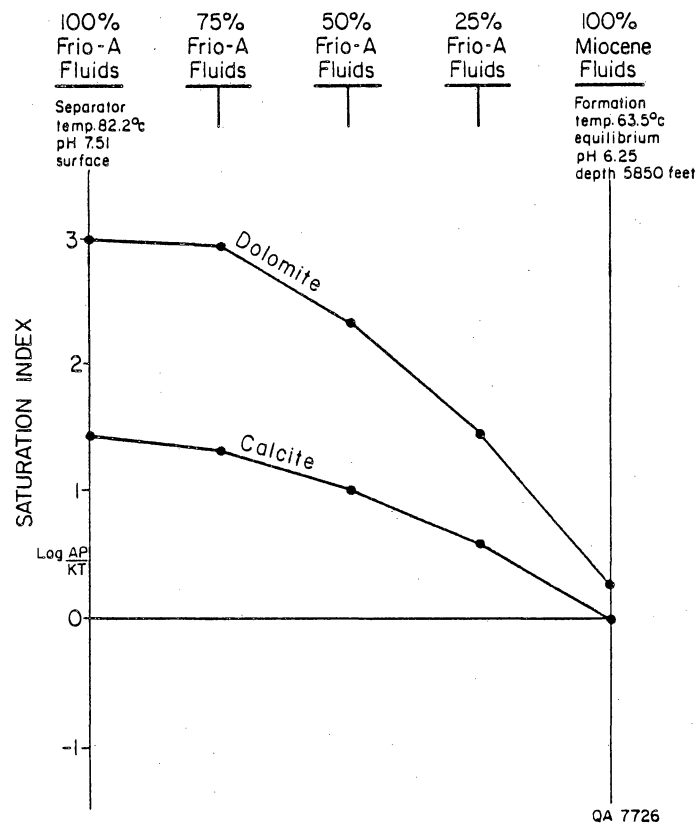


Figure 76. Saturation indices of various mixes of Frio 'A' and Miocene waters at a Miocene formation temperature of 146.3°F (63.5°C) and measured pH of 6.25.

REFERENCES

- Allen, J. R. L., and Banks, N. L., 1972. An interpretation and analysis of recumbent folded deformed cross-bedding: *Sedimentology*, v. 19, p. 257-283.
- Anderson, L. L., Peterson, K. P., and Parisi, W. A., 1984. Enhanced production from a slightly geopressured water-drive gas condensate field: Proceedings of the SPE/DOE/GRI Unconventional Gas Recovery Symposium, Pittsburgh, Pennsylvania, p. 334-341.
- Andrews, P. B., 1970. Facies and genesis of a hurricane-washover fan, St. Joseph Island, Central Texas Coast: The University of Texas at Austin, Bureau of Economic Geology Report of Investigations No. 67, 147 p.
- Barnes, I., and Clarke, F. E., 1969. Chemical properties of ground water and their encrustation effects on wells: U.S. Geological Survey Professional Paper 498-D, 58 p.
- Bassett, R. L., 1976. The geochemistry of boron in thermal waters, Stanford University, Ph.D. dissertation, p. 305.
- _____ 1980. A critical evaluation of thermodynamic data for boron ions, ion pairs, complexes, and polyions in aqueous solution at 298.1K and 1 bar: *Geochimica Cosmochimica Acta*, v. 44, p. 1151-1160.
- Blatt, H., Middleton, G., and Murray, R., 1980. Origin of sedimentary rocks: Englewood Cliffs, Prentice-Hall, 782 p.

Boles, J. R., and Franks, S. G., 1979. Clay diagenesis in Wilcox sandstones of southwest Texas, implications of smectite diagenesis on sandstone cementation: *Journal of Sedimentary Petrology* v. 49, no. 1, p. 55-70.

Burst, J. F., 1969. Diagenesis of Gulf Coast clayey sediments and its possible relationship to petroleum migration: *American Association of Petroleum Geologists Bulletin*, v. 53, p. 73-93.

Chamberlain, C. K., 1978. Recognition of trace fossils in cores, in Basan P. B., ed., *Trace fossil concepts: Society of Economic Paleontologists and Mineralogists Short Course No. 5*, p. 119-139.

Chave, K. E., 1960. Evidence on history of sea water from chemistry of deep subsurface waters of ancient basins: *American Association of Petroleum Geologists Bulletin*, v. 44, p. 357-370.

Coleman, J. M., and Prior, D. B., 1980. Deltaic sand bodies, a 1980 short course: *American Association of Petroleum Geologists Continuing Education Course Note Series 15*, 171 p.

Collins, G. A., 1970. Geochemistry of petroleum associated waters from Louisiana: U.S. Department of the Interior, Bureau of Mines Report of Investigations No. 7326, 31 p.

Correns, C. W., 1956. The geochemistry of the Halogens, in Ahrens, L. H., and others, eds., *Physics and chemistry of the Earth*: New York, Pergamon, p. 181-233.

Crimes, T. P., 1975. The stratigraphical significance of trace fossils, in Frey, R. W., ed., The study of trace fossils: New York, Springer-Verlag, p. 109-130.

Dorjes, J., and Hertweck, G., 1975. Recent biocoenoses and ichnocoenoses in shallow-water marine environments, in Frey, R. W., ed., The study of trace fossils: New York, Springer-Verlag, p. 459-491.

Doyle, J. D., 1979. Depositional patterns of Miocene facies, middle Texas coastal plain: The University of Texas at Austin, Bureau of Economic Geology Report of Investigations No. 99, 28 p.

Embry, A. F., III, Reinson, G. E., Schluger, P. R., 1974. Shallow marine sandstones: a brief review, in Shawa, M. S., ed., Use of sedimentary structures for recognition of clastic environments: Canadian Society of Petroleum Geologists, p. 53-66.

Ewing, T. E., and Reed, R. S., 1984. Depositional systems and structural controls of Hackberry sandstone reservoirs in southeast Texas: The University of Texas at Austin, Bureau of Economic Geology Geological Circular 84-7, 48 p.

Fisher, R. S., and Ozment, R. W., 1984. SOLMNEQ user's guide supplement: The University of Texas at Austin, Bureau of Economic Geology, 11 p.

Fisher, W. L., and Finley, R. J., 1986. Future trends in Texas oil and gas: presentation to Texas House Committee on Energy, January 23, 1986, 23 p.,

reprinted in part as Texas still has big hydrocarbon resource base: Oil and Gas Journal, v. 84, no. 22, p. 57-69.

Folk, R. L., 1974, Petrology of sedimentary rocks: Austin, Texas, Hemphill, 182 p.

Foscolos, A. E., Powell, T. G., and Gunter, P. R., 1976, The use of clay minerals, inorganic and organic geochemical indicators for evaluating the degree of diagenesis and oil generating potential of the shales: Geochimica et Cosmochimica Acta, v. 40, p. 953-960.

Freed, R. L., 1980, Shale mineralogy and burial diagenesis in four geopressed wells, Hidalgo and Brazoria Counties Texas, in Loucks R. G., Richman, D. L., and Milliken, K. L., eds, Factors controlling reservoir quality in Tertiary sandstones and their significance to geopressed-geothermal production: U.S. Department of Energy, Division of Geothermal Energy, contract no. DOE/ET/27111-1, p. 111-172.

Frey, R. W., 1978, Behavioral and ecological implications of trace fossils, in Basan, P. B., ed., Trace fossil concepts: Society of Economic Paleontologists and Mineralogists Short Course No. 5, p. 43-66.

Galloway, W. E., and Cheng, E. S., 1985, Reservoir facies architecture in a microtidal barrier system--Frio Formation, Texas Gulf Coast: The University of Texas at Austin, Bureau of Economic Geology Report of Investigations No. 144, 36 p.

Galloway, W. E., Hobday, D. K., and Magara, K., 1982. Frio Formation of the Texas Gulf Coast Basin: depositional systems, structural framework, and hydrocarbon origin, migration, distribution, and exploration potential: The University of Texas at Austin, Bureau of Economic Geology Report of Investigations No. 122, 78 p.

Galloway, W. E., Jirik, L. A., Morton, R. A., and DuBar, J. R., 1986. Lower Miocene (Fleming) depositional episode of the Texas Coastal Plain and continental shelf: structural framework, facies, and hydrocarbon resources: The University of Texas at Austin, Bureau of Economic Geology Report of Investigations No. 150, 50 p.

Ginsburg, R. N., 1953. Beachrock in south Florida: *Journal of Sedimentary Petrology*, v. 23, p. 89-92.

Gold, P. B., 1984. Diagenesis of Middle and Upper Miocene sandstones, Louisiana Gulf Coast: The University of Texas at Austin, Master's Thesis, 160 p.

_____ 1987. Textures and geochemistry of authigenic albite from Miocene sandstones, Louisiana Gulf Coast: *Journal of Sedimentary Petrology*, v. 57, no. 2, p. 353-362.

Goldhaber, M. B., Reynolds, R. L., and Rye, R. O., 1978. Origin of South Texas roll-type uranium deposit, 2. Petrology and sulfur isotope studies: *Economic Geologist*, v. 78, p. 1043-1063.

Goldhaber, M. B., Reynolds, R. L., Rye, R. O. and Grauch, R. I., 1979, Petrology and isotope geochemistry of calcite in a South Texas roll-type uranium deposit: U. S. Geological Survey Open-File Report 79-828, 21 p.

Gregory, A. R., Lin, Z. S., Reed, R. S., Morton, R. A., Ewing, T. E., 1984, Enhanced gas recovery from watered-out reservoirs--Port Arthur field, Jefferson County, Texas: The University of Texas at Austin, Bureau of Economic Geology Report of Investigations No. 142, 58 p.

Gregory, A. R., Lin, Z. S., Reed, R. S., Morton, R. A., and Rogers, L. A., 1983, Watered-out gas reservoirs profitable via enhanced recovery: Oil and Gas Journal, March 14, p. 55-60.

Guevara, E. H., in press, Geological characterization of submarine fan reservoirs of the Spraberry-Driver unit, Midland Basin, Texas: The University of Texas at Austin, Bureau of Economic Geology Report of Investigations.

Hayes, M. O., 1980, General morphology and sediment patterns in tidal inlets, in Bouma, A. H., and others, eds., Shallow marine processes and products: Sedimentary Geology, v. 26, no. 1-3, p. 139-156.

Howard, J. D., 1972, Trace fossils as criteria for recognising shorelines in the stratigraphic record, in Rigby, J. K., and Hamblin, W. K., eds., Recognition of ancient sedimentary environments: Society of Economic Paleontologists and Mineralogists Special Publication, v. 16, no. 215-225.

_____ 1975. The sedimentological significance of trace fossils, in Frey, R. W., ed.,
The study of trace fossils. New York. Springer-Verlag. p. 131-146.

Hunt, J. M., 1979. Petroleum geochemistry and geology: San Francisco. W. H.
Freeman. 617 p.

Kaiser, W. R., and Richmann, D. L., 1981. Predicting diagenetic history and reservoir
quality in the Frio Formation of Brazoria County, Texas, and Pleasant Bayou test
wells, in Proceedings, Fifth Conference on Geopressured Geothermal Energy: The
University of Texas at Austin. p. 67-74.

Kharaka, Y. K., and Barnes, I., 1973. SOLMNEQ: solution-mineral equilibrium
computations: U.S. Geological Survey Water Resources Publication No. 73-002,
81 p.

Kharaka, Y. K., Callender, E., and Carothers, W. W., 1977a. Geochemistry of
geopressured-geothermal waters from the Texas Gulf Coast, in Meriwether, J. R.,
ed., Third Geopressured-Geothermal Energy Conference, University of Southwestern
Louisiana, Lafayette, v. 1, G-121 - G-165.

Kharaka, Y. K., Callender, E., and Wallace, R. H., 1977b. Geochemistry of
geopressured geothermal waters from the Frio Clay in the Gulf Coast Region of
Texas: *Geology*, v. 5, p. 241-244.

Kharaka, Y. K., Carothers, W. M., and Law, L. M., 1985, Origin of gaseous hydrocarbons in geopressed geothermal waters (abs.): Abstracts, Sixth U.S. Gulf Coast Geopressed-Geothermal Energy Conference, February 4-6, Austin, Texas, p. 16.

Kharaka, Y. K., Lico, M. S., Wright, V. A., and Carothers, W. W., 1979, Geochemistry of formation waters from Pleasant Bayou No. 2 well and adjacent areas in coastal Texas: Proceedings, Fourth U. S. Gulf Coast Geopressed-Geothermal Energy Conference, v. 1, p. 168-193.

Komar, P. D., 1976, Beach processes and sedimentation: Englewood Cliffs, Prentice-Hall, 429 p.

Kreitler, C. W., and Richter, B. C., 1986, Hydrochemical characterization of saline aquifers of the Texas Gulf Coast used for disposal of industrial waste: The University of Texas at Austin, Bureau of Economic Geology, report prepared for the U. S. Environmental Protection Agency under contract no. R-812785-01-0, 34 p.

Land, L. S., Milliken, K. L., and McBride, E. F., 1987, Diagenetic evolution of Cenozoic sandstones, Gulf of Mexico sedimentary basin: *Sedimentary Geology*, v. 50, no. 1-3, p. 195-225.

Light, M. P. R., 1985, Structure, facies, continuity and internal properties of the Frio 'A' sandstone, N. E. Hitchcock field, Galveston County, Texas, in Dorfman, M. H., and Morton, R. A., Proceedings, Sixth U. S. Gulf Coast Geopressed-Geothermal Energy Conference: New York, Pergamon, p. 229-238.

Light, M. P. R., and D'Attilio, W., 1985. Structure, facies, and internal properties of the Frio 'A' reservoir, Hitchcock N. E. field, Galveston County, Texas, in Finley, R. J., Morton, R. A., Dorfman, M. H., and Sepehrnoori, K., Coordination of geological and engineering research on support of Gulf Coast co-production program: The University of Texas at Austin, Bureau of Economic Geology, prepared for the Gas Research Institute under contract no. 5084-212-0924, p. 1-51.

Light, M. P. R., Posey, H. H., Kyle, R. J., and Price, P. E., in press, Integrated hydrothermal model for the Texas Gulf Coast Basin: origins of geopressed brines and lead-zinc, barium, uranium, hydrocarbon, and cap-rock deposits, in Lerche, I., and O'Brien, J., eds., Dynamical geology of salt and related structures: New York, Academic Press.

Loucks, R. G., Richman, D. L., and Milliken, K. L., 1981, Factors controlling reservoir quality in Tertiary sandstones and their significance to geopressed geothermal production: The University of Texas at Austin, Bureau of Economic Geology Report of Investigations No. 111, 41 p.

Mason, B., 1966, Principles of geochemistry: New York, John Wiley, 329 p.

Milliken, K. L., Land, L. S., and Loucks, R. G., 1981, History of burial diagenesis determined from isotopic geochemistry, Frio Formation, Brazoria County, Texas: American Association of Petroleum Geologists Bulletin, v. 65, no. 8, p. 1397-1413.

Moore, R. C., Lalicker, C. G., and Fischer, A. G., 1952. Invertebrate fossils: New York, McGraw Hill, 766 p.

Morton, J. P., 1983. Age of clay diagenesis in the Oligocene Frio Formation, Texas Gulf Coast: The University of Texas at Austin, Ph.D. dissertation, 33 p.

Morton, R. A., 1981. Pleasant Bayou No. 2--a review of rationale, ongoing research and preliminary test results: Proceedings, Fifth Conference on Geopressed Geothermal Energy, The University of Texas at Austin, p. 55-57.

Morton, R. A., Ewing, T. E., and Tyler, N., 1983. Continuity and internal properties of Gulf Coast sandstones and their implications for geopressed fluid production: The University of Texas at Austin, Bureau of Economic Geology Report of Investigations No. 132, 70 p.

Morton, R. A., Garrett, C. M., Jr., Posey, J. S., 1983. Variations in chemical compositions of Tertiary formation waters, Texas Gulf Coast, in Morton, R. A., Ewing T. E., Kaiser, W. R., and Finley, R. J., Consolidation of geologic studies of geopressed-geothermal resources in Texas: The University of Texas at Austin, Bureau of Economic Geology, prepared for the U.S. Department of Energy under contract no. DE-AC08-79ET27111, p. 66-136.

Morton, R. A., Jirik, L. A., and Foote, R. Q., 1985. Depositional history, facies analysis, and production characteristics of hydrocarbon-bearing sediments, offshore

Texas: The University of Texas at Austin. Bureau of Economic Geology
Geological Circular 85-2. 31 p.

Pettijohn, F. J. and Potter, P. E., 1964. Atlas and glossary of primary sedimentary
structures: Berlin, Springer-Verlag, 370 p.

Pittman, E. D., 1979. Porosity, diagenesis, and productive capability of sandstone
reservoirs: Society of Economic Paleontologists and Mineralogists Special
Publication 26, p. 159-173.

Powell, T. G., Foscolos, A. E., Gunther, P. R., and Snowdon, L. R., 1978. Diagenesis
of organic matter and fine clay minerals: a comparative study: *Geochimica et
Cosmochimica Acta*, v. 42, p. 1181-1197.

Rainwater, E. H., 1964. Regional stratigraphy of the Gulf Coast Miocene: *Gulf Coast
Association of Geological Societies Transactions*, v. 14, p. 81-124.

Rainwater, E. H., and Thatcher, L. L., 1960. Methods for collection and analysis of
water samples: U.S. Geological Survey Water-Supply Paper No. 1454, 301 p.

Rankin, W. G., 1936. Lower Mississippi river delta, reports on the geology of
Plaquemines and St. Bernard Parishes: State of Louisiana, Department of
Conservation, Louisiana Geological Survey, Geological Bulletin No. 8, 454 p.

Rhoads, D. C., 1975. The paleoecologic and environmental significance of trace fossils, in Frey, R. W., ed., The study of trace fossils: New York, Springer-Verlag, p. 147-160.

Rimstidt, J. D., and Barnes, H. L., 1978. Experiments for rapid assessment of the scaling properties of geothermal fluids: Geothermal Research Council Transactions, v. 2, p. 567-569.

Schwartz, R. Z., 1975. Nature and genesis of some storm washover deposits: U.S. Army Coastal Engineering Research Center, Technical Memoir No. 61, 61 p.

Seal, W. L., and Gilreath, J. A., 1975. Vermillion Block 16 Field--a study of irregular gas reservoir performance related to non-uniform sand deposition: Gulf Coast Association of Geological Societies Transactions, v. 25, p. 63-79.

Seilacher, A., 1967. Bathymetry of trace fossils: Marine Geology, v. 5, p. 413-429.

_____ 1978. Use of trace fossils in recognising depositional environments, in Basan, P. B., ed., Trace fossil concepts: Society of Economic Paleontologists and Mineralogists Short Course No. 5, p. 167-181.

Selley, R. C., 1970. Ancient sedimentary environments and their subsurface diagnosis: London, Chapman and Hall, 287 p.

- _____ 1979. Concepts and methods of subsurface facies analysis: American Association of Petroleum Geologists Continuing Education Course Note Series No. 9, 82 p.
- Spencer, C. W., 1976. Hydrodynamic-energy classifications for interpretation of cores of cretaceous sandstones deposited in wave-dominated environments (abs.), in Wyoming Geological Association 28th Annual Field Conference Symposium, Geology and energy resources of the Powder River basin, Symposium Abstracts, p. 3-4.
- Tomson, M., 1983, Rice University future plans, in Minutes of the informal meeting of the Overview Group, Houston, Texas, June 9: report prepared for the U.S. Department of Energy, Division of Geothermal Energy, GeoEnergy Corporation, Las Vegas, p. 132-146.
- Tomson, M., and O'Day, P., 1987, Gas Research Institute project review, brine chemistry: Rice University, Department of Environmental Science and Engineering, 22 p.
- Tyler, N., and Ambrose, W. A., 1985, Facies architecture and production characteristics of strandplain reservoirs in the Frio Formation, Texas: The University of Texas at Austin, Bureau of Economic Geology Report of Investigations No. 146, 42 p
- Tyler, N., Galloway, W. E., Garrett, C. M., Jr., and Ewing, T. E., 1984, Oil accumulation, production characteristics, and targets for additional oil recovery in major oil reservoirs of Texas: The University of Texas, Bureau of Economic Geology Geological Circular 84-2, 31 p.

Tyler, N., and Gholston, J. C., in press. Heterogeneous deep-sea fan reservoirs, Shackelford and Preston waterflood units, Spraberry Trend, West Texas: The University of Texas at Austin, Bureau of Economic Geology Report of Investigations.

Tyler, N., and Hahn, J. H., 1982. Elements of high constructive deltaic sedimentation, Lower Frio Formation, Brazoria County, Texas: Transactions of the Gulf Coast Association of Geological Societies 32nd Annual Meeting, Houston, Texas, p. 527-540.

White, D. E., 1965. Saline waters of sedimentary rocks, in Young, A., and Galley, J. E., eds., Fluids in the subsurface environments: American Association of Petroleum Geologists Memoirs No. 4, p. 342-366.

Williams, H., Turner, F. J., and Gilbert, C. M., 1954. Petrography and introduction to the study of rocks in thin sections: San Francisco, W. H. Freeman, 416 p.

Winkler, H. G. F., 1976. Petrogenesis of metamorphic rocks, (4th ed.): New York, Springer-Verlag, 334 p.